



AEROSPACE INFORMATION REPORT	AIR1168™/3	REV. B
	Issued 1990-09 Reaffirmed 2011-06 Revised 2019-09 Stabilized 2025-03 Superseding AIR1168/3A	
SAE Aerospace Applied Thermodynamics Manual Aerothermodynamic Systems Engineering and Design		

RATIONALE

This document has been determined to contain basic and stable technology which is not dynamic in nature.

STABILIZED NOTICE

This document has been declared "STABILIZED" by SAE AC-9 Aircraft Environmental Systems Committee and will no longer be subjected to periodic reviews for currency. Users are responsible for verifying references and continued suitability of technical requirements. Newer technology may exist.

SAENORM.COM : Click to view the full PDF of AIR1168-3B

SAE Executive Standards Committee Rules provide that: "This report is published by SAE to advance the state of technical and engineering sciences. The use of this report is entirely voluntary, and its applicability and suitability for any particular use, including any patent infringement arising therefrom, is the sole responsibility of the user."

SAE reviews each technical report at least every five years at which time it may be revised, reaffirmed, stabilized, or cancelled. SAE invites your written comments and suggestions.

Copyright © 2025 SAE International

All rights reserved. No part of this publication may be reproduced, stored in a retrieval system, transmitted, in any form or by any means, electronic, mechanical, photocopying, recording, or otherwise, or used for text and data mining, AI training, or similar technologies, without the prior written permission of SAE.

TO PLACE A DOCUMENT ORDER: Tel: 877-606-7323 (inside USA and Canada)
Tel: +1 724-776-4970 (outside USA)
Fax: 724-776-0790
Email: CustomerService@sae.org
http://www.sae.org

SAE WEB ADDRESS:

For more information on this standard, visit
<https://www.sae.org/standards/content/AIR1168/3B/>

PREFACE

This document is one of 14 Aerospace Information Reports (AIR) of the Third Edition of the SAE Aerospace Applied Thermodynamics Manual. The manual provides a reference source for thermodynamics, aerodynamics, fluid dynamics, heat transfer, and properties of materials for the aerospace industry. Procedures and equations commonly used for aerospace applications of these technologies are included.

In the Third Edition, no attempt was made to update material from the Second Edition nor were SI units added. However, all identified errata were corrected and incorporated and original figure numbering was retained, insofar as possible.

The SAE AC-9B Subcommittee originally created the SAE Aerospace Applied Thermodynamics Manual and, for the Third Edition, used a new format consisting of AIR1168/1 through AIR1168/10. AIR1168/11 through AIR1168/14 were created by the SAE SC-9 Committee.

The AIRs comprising the Third Edition are shown below. Applicable sections of the Second Edition are shown parenthetically in the third column.

AIR1168/1	Thermodynamics of Incompressible and Compressible Fluid Flow	(1A,1B)
AIR1168/2	Heat and Mass Transfer and Air-Water Mixtures	(1C,1D,1E)
AIR1168/3	Aerothermodynamic Systems Engineering and Design	(3A,3B,3C,3D)
AIR1168/4	Ice, Rain, Fog, and Frost Protection	(3F)
AIR1168/5	Aerothermodynamic Test Instrumentation and Measurement	(3G)
AIR1168/6	Characteristics of Equipment Components, Equipment Cooling System Design, and Temperature Control System Design	(3H,3J,3K)
AIR1168/7	Aerospace Pressurization System Design	(3E)
AIR1168/8	Aircraft Fuel Weight Penalty Due to Air Conditioning	(3I)

AIR1168/9	Thermophysical Properties of the Natural Environment, Gases, Liquids, and Solids	(2A,2B,2C,2D)
AIR1168/10	Thermophysical Characteristics of Working Fluids and Heat Transfer Fluids	(2E,2F)
AIR1168/11	Spacecraft Boost and Entry Heat Transfer	(4A,4B)
AIR1168/12	Spacecraft Thermal Balance	(4C)
AIR1168/13	Spacecraft Equipment Environmental Control	(4D)
AIR1168/14	Spacecraft Life Support Systems	(4E)

F.R. Weiner, formerly of Rockwell International and past chairman of the SAE AC-9B Subcommittee, is commended for his dedication and effort in preparing the errata lists that were used in creating the Third Edition.

SAENORM.COM : Click to view the full PDF of air1168_3b

TABLE OF CONTENTS

SECTION 3A - AIR CONDITIONING LOAD ANALYSIS	8
1. INTRODUCTION.....	8
1.1 Scope	8
1.2 Nomenclature.....	8
1.3 Common Abbreviations.....	10
2. PHYSIOLOGICAL REQUIREMENTS.....	11
2.1 Effective Temperature.....	11
3. STATEMENT OF HEATING AND COOLING LOAD EQUATIONS.....	12
3.1 Heat Transfer Between the Air and Skin.....	12
3.2 Heat Transfer Between the Skin and Occupied Areas	14
4. SKIN TEMPERATURE COMPUTATIONAL METHODS	22
4.1 Skin Temperature at Flight Conditions Less Than Mach 2.....	22
4.2 Skin Temperature at Flight Above Mach 2.....	23
4.3 Skin Temperature at Ground Static Conditions	24
5. COOLING LOADS DUE TO RADIATION THROUGH TRANSPARENT AREAS	25
6. HEATING AND COOLING LOADS DUE TO INTERNAL SOURCES	25
6.1 Sensible and Latent Heat Emission by Occupants.....	25
6.2 Electrical Load.....	27
7. PRACTICAL CONSIDERATIONS IN THE DETERMINATION OF OVERALL HEATING AND COOLING LOADS	27
7.1 Conditions that Establish Heating and Cooling Loads.....	28
7.2 Example of Cooling and Heating Load Calculation	28
8. EXAMPLE OF SKIN TEMPERATURE COMPUTATION AT HIGH MACH NUMBER.....	38
9. REFERENCES.....	40
SECTION 3B - REFRIGERATION SYSTEM DESIGN	41
1. INTRODUCTION.....	41
1.1 Scope	41
1.2 Nomenclature.....	41
1.3 Common Abbreviations.....	42
1.4 Definitions of Available Heat Sinks.....	44
2. AIR CYCLE SYSTEMS.....	45
2.1 Basic Considerations and Cycle Components.....	45
2.2 Analysis of Basic Air Cycle System	47
2.3 Air Cycle Systems (Open and Closed Circuits)	50
2.4 Combination Air Cycle and Expendable Coolant Systems	61
2.5 Comparison of Air Cycle Systems	61
2.6 Water Separator Applications	65
3. VAPOR CYCLE SYSTEMS	68
3.1 Basic Considerations and Cycle Components.....	68
3.2 Analysis of Basic Vapor Cycle System	69
3.3 Vapor Cycle Systems Variants	73
3.4 Expendable Refrigerant Vapor Cycle Systems.....	77
3.5 Comparison of Vapor Cycle Systems	78
4. COMBINED VAPOR CYCLE AND AIR CYCLE SYSTEMS	83
5. THERMOELECTRIC COOLING	84
5.1 General Discussion	84
5.2 Present Application	85
5.3 Fundamental Theory.....	85
5.4 Application.....	87
6. REFERENCES.....	91

SECTION 3C - HEATING SYSTEM DESIGN.....	92
1. INTRODUCTION.....	92
1.1 Scope.....	92
1.2 Common Abbreviations.....	92
2. HEATING METHODS.....	92
2.1 Bypass Systems.....	92
2.2 Electric Heaters.....	92
2.3 Radiant Panels.....	93
2.4 Combustion Heaters.....	93
2.5 Exhaust Heating.....	93
3. SUMMARY AND RECOMMENDATIONS.....	93
4. REFERENCES.....	94
SECTION 3D - AIR DISTRIBUTION SYSTEM DESIGN.....	95
1. INTRODUCTION.....	95
1.1 Scope.....	95
1.2 Nomenclature.....	95
1.3 Common Abbreviations.....	96
2. LOW PRESSURE SYSTEMS.....	97
2.1 Introduction.....	97
2.2 Physiological Requirements in Cabin Air Systems.....	98
2.3 Design Approach, Cabin Air Systems.....	99
2.4 Air Jet Behavior.....	100
2.5 Velocities Near Return Grilles.....	106
2.6 Flow Straighteners for Outlets.....	106
2.7 Air Flow Quantity.....	107
2.8 Outlet Locations.....	107
2.9 General Exhaust Locations.....	108
2.10 Duct Mixing: Airstreams of Different Temperature.....	108
2.11 Flight Station Air Distribution.....	109
2.12 Air Distribution in Fighter Cockpits.....	109
2.13 Equipment Ventilation for Heat Removal.....	110
3. HIGH PRESSURE SYSTEMS.....	112
3.1 Engine Bleed Systems.....	112
3.2 Distribution System Schematics.....	113
4. REFERENCES.....	116

LIST OF FIGURES

FIGURE 3A-1 - PSYCHROMETRIC CHART, PERSONS AT REST, NORMALLY CLOTHED, IN STILL AIR.....	12
FIGURE 3A-2 - SIMPLE COMPOSITE WALL.....	15
FIGURE 3A-3 - SIMPLE COMPOSITE WALL INCLUDING AN AIR SPACE.....	17
FIGURE 3A-4 - NUSSELT NUMBER VERSUS GRASHOF NUMBER FOR VERTICAL AND HORIZONTAL AIR SPACES. NOTE: $N_{PR} = 0.72$	19
FIGURE 3A-5 - EQUIVALENT HEAT TRANSFER COEFFICIENT FOR RADIATION.....	20
FIGURE 3A-6 - A SIMPLE FIN.....	21
FIGURE 3A-7 - FIN EFFECTIVENESS FACTOR.....	22
FIGURE 3A-8 - TEMPERATURE DISTRIBUTION ALONG A FIN.....	22
FIGURE 3A-9 - AVERAGE EQUILIBRIUM SKIN TEMPERATURE AT GROUND STATIC CONDITIONS.....	25
FIGURE 3A-10 - THE RELATIONSHIP BETWEEN RADIATION AND CONVECTION LOSS FROM THE HUMAN BODY AND DRY BULB TEMPERATURE FOR STILL AIR. (REF. ASHRAE GUIDE).....	26
FIGURE 3A-11 - EVAPORATIVE HEAT AND MOISTURE LOSS FROM THE HUMAN BODY IN RELATION TO DRY BULB TEMPERATURE FOR STILL AIR CONDITIONS. (REF. ASHRAE GUIDE).....	26
FIGURE 3A-12 - FLIGHT COMPARTMENT TO BE AIR CONDITIONED.....	29
FIGURE 3A-13 - CONSTRUCTION DETAILS: BETWEEN FUSELAGE FRAMES.....	29
FIGURE 3A-14 - CONSTRUCTION DETAILS: THROUGH FUSELAGE FRAMES.....	29
FIGURE 3A-15 - CONSTRUCTION DETAILS: BETWEEN FLOOR BEAMS.....	29
FIGURE 3A-16 - CONSTRUCTION DETAILS: THROUGH FLOOR BEAMS.....	29

FIGURE 3A-17 - CONSTRUCTION DETAILS: THROUGH PRESSURE BULKHEAD	29
FIGURE 3A-18 - CONSTRUCTION AND THERMAL DETAILS: WINDSHIELD	29
FIGURE 3B-1 - OUTSIDE AIR HEAT SINK VERSUS MACH NUMBER. --- STAGNATION CONDITIONS (TOTAL TEMPERATURE). — RAM AIR FULLY EXPANDED (TURBINE EFFICIENCY = 70%)	45
FIGURE 3B-2 - REVERSED CARNOT CYCLE	47
FIGURE 3B-3 - BASIC OPEN AIR CYCLE SYSTEM, (A) RAM AIR SUPPLY; (B) BLEED AIR SUPPLY; (C) RAM AIR SUPPLY WITH PRESSURIZATION COMPRESSOR	48
FIGURE 3B-4 - SIMPLE AIR CYCLE WITH BRAKING COMPRESSOR	49
FIGURE 3B-5 - COEFFICIENT OF PERFORMANCE OF IDEAL REVERSED JOULE CYCLE (FROM RAM TEMPERATURE LEVEL T_1 TO FREESTREAM T_0). $COP = T_0 / (T_1 - T_0) = 5 / M_0^2$	50
FIGURE 3B-6 - BOOTSTRAP COOLING SYSTEM	51
FIGURE 3B-7 - IDEAL BOOTSTRAP OPEN CIRCUIT SYSTEM (REVERSED BRAYTON CYCLE)	52
FIGURE 3B-8 - COMPARISON OF IDEAL BOOTSTRAP SYSTEM WITH IDEAL SIMPLE AIR CYCLE	54
FIGURE 3B-9 - ACTUAL BOOTSTRAP CYCLE ILLUSTRATING THE EFFECT OF CONNECTING DUCT PRESSURE LOSSES	54
FIGURE 3B-10 - BOOTSTRAP SYSTEM VARIANTS, (A) BOOTSTRAP SYSTEM WITH PRECOOLER AND UTILIZING FUEL AS THE HEAT SINK; (B) SYSTEM WITH PRECOOLER AND EXPENDABLE COOLANT HEAT SINK	55
FIGURE 3B-11 - IDEAL REGENERATIVE AIR CYCLE SYSTEM; COMPLETE UTILIZATION OF ENERGY IN CABIN EXHAUST AIR IS SHOWN	55
FIGURE 3B-12 - REVERSED FLOW BOOTSTRAP CYCLE	58
FIGURE 3B-13 - SIMPLE CYCLE SYSTEM	59
FIGURE 3B-14 - CLOSED AIR CYCLE REFRIGERATION SYSTEM	59
FIGURE 3B-15 - COMPARISON OF OPEN CIRCUIT AIR CYCLE SYSTEMS. (A) TROPOPAUSE REGION; (B) SEA LEVEL	62
FIGURE 3B-16 - REGENERATIVE AIR CYCLE SYSTEM COMPARISONS	63
FIGURE 3B-17 - COMPARISON OF OPEN CIRCUIT SYSTEM UTILIZED FOR EQUIPMENT COOLING. (A) TROPOPAUSE; (B) SEA LEVEL. FOR BOTH (A) AND (B), HEAT EXCHANGER $\eta_x = 80\%$ AND EQUIPMENT OUT-TEMPERATURE = 140°F	64
FIGURE 3B-18 - PSYCHROMETRIC DIAGRAM OF MECHANICAL WATER SEPARATION PROCESS	66
FIGURE 3B-19 - PSYCHROMETRIC DIAGRAM OF CHEMICAL MOISTURE REMOVAL PROCESS	66
FIGURE 3B-20 - COMPARISON OF DESICCANTS (ADSORBENTS)	67
FIGURE 3B-21 - TYPICAL PRESSURE-ENTHALPY (P-H) DIAGRAM. NOTE: $\Delta T = 0 =$ CONSTANT TEMPERATURE AND $\Delta S = 0 =$ CONSTANT ENTROPY	69
FIGURE 3B-22 - IDEAL REFRIGERATION CYCLE	69
FIGURE 3B-23 - BASIC VAPOR CYCLE SYSTEM, (A) T-S DIAGRAM; (B) P-H DIAGRAM; (C) BASIC SIMPLE CYCLE	70
FIGURE 3B-24 - COMPARISON OF ACTUAL VERSUS THEORETICAL VAPOR CYCLES. PRESSURE DROPS HAVE BEEN NEGLECTED	71
FIGURE 3B-25 - EVAPORATOR PERFORMANCE	71
FIGURE 3B-26 - CONDENSER PERFORMANCE	72
FIGURE 3B-27 - VAPOR CYCLE SHOWING PRESSURE LOSSES	73
FIGURE 3B-28 - MULTIPLE EVAPORATOR OPERATION	73
FIGURE 3B-29 - SUBCOOLER-SUPERHEATER CYCLE	74
FIGURE 3B-30 - SIMPLE COMPOUND CYCLE	75
FIGURE 3B-31 - TWO-STAGE SYSTEM WITH INTERCOOLER	75
FIGURE 3B-32 - COMPOUND CYCLE WITH INTERCOOLING	75
FIGURE 3B-33 - COMPOUND CYCLE WITH SUBCOOLER	75
FIGURE 3B-34 - COMPOUND CYCLE WITH SUPERHEATER	75
FIGURE 3B-35 - COMPOUND CYCLES WITH SUBCOOLER AND SUPERHEATER	75
FIGURE 3B-36 - CASCADE SYSTEM	76
FIGURE 3B-37 - VAPOR CYCLE PERFORMANCE CURVES, R-11, $T_c =$ CONDENSER TEMPERATURE, COMPRESSOR EFFICIENCY = 60%	78
FIGURE 3B-38 - COMPARISON OF RELATIVE COP'S FOR 13 DIFFERENT REFRIGERANTS	79
FIGURE 3B-39 - EFFECT OF SUPERHEAT GAINED IN PERFORMING USEFUL COOLING, (A) REFRIGERANT 12, $T_{EVAP} = 40^\circ\text{F}$; (B) REFRIGERANT 11, $T_{EVAP} = 40^\circ\text{F}$	81
FIGURE 3B-40 - COP OF CASCADE CYCLE FOR REFRIGERANT 12 IN BOTH STAGES	82

FIGURE 3B-41 - REPRESENTATIVE COMBINED AIR CYCLE AND VAPOR CYCLE SYSTEMS. NOTE: ONE OR MORE VAPOR CYCLES IN SERIES (CASCADED) ARE REPRESENTED BY ONLY ONE CYCLE, FOR SIMPLICITY	83
FIGURE 3B-42 - SYSTEM COMPARISONS. NOTES: TURBOJET EFF = 83% (COMP); COMPRESSOR EFF = 60%; TURBINE EFF = 70%; $T_{CAB} = 510^{\circ}R$; HE EFFECTIVENESS = 80%; PRESSURE DROPS = 10% AIR SIDE HE, 5% CABIN SUPPLY LINE, AND 15% BLEED AIR LINE.....	84
FIGURE 3B-43 - PARAMETER VARIATIONS FOR COMBINED SYSTEM (TYPE IA): FIXED CONDENSER TEMPERATURE; FIXED MACH NUMBER AND ALTITUDE; FIXED CABIN-AIR COMPRESSION RATIO	84
FIGURE 3B-44 - BASIC THERMOELECTRIC COUPLE OR MODULE	86
FIGURE 3B-45 - OPTIMUM COP VERSUS TEMPERATURE DIFFERENCE FOR VARIOUS FIGURES OF MERIT. $T_H = 330 K$	88
FIGURE 3B-46 - COOLING CAPACITY IN WATTS AT $0^{\circ}F \Delta t$ (REF. 22).....	88
FIGURE 3B-47 - COOLING CAPACITY IN WATTS VERSUS Δt CORRECTION; APPLIES TO FIG. 3B-46 (REF. 22).....	88
FIGURE 3B-48 - VOLTAGE REQUIREMENTS AT $0^{\circ}F \Delta t$ (REF. 22)	88
FIGURE 3B-49 - VOLTAGE CORRECTION VERSUS Δt ; APPLIES TO FIG. 3B-48 (REF. 22).....	88
FIGURE 3B-50 - HEATING CAPACITY IN WATTS AT $0^{\circ}F \Delta t$ (REF. 22)	89
FIGURE 3B-51 - HEATING CAPACITY VERSUS Δt CORRECTION IN WATTS; APPLIES TO FIG. 3B-50 (REF. 22).....	89
FIGURE 3B-52 - THERMOELECTRIC SYSTEM (REF. 22).....	90
FIGURE 3D-1 - EFFECT OF TEMPERATURE, HUMIDITY, AND AIR MOTION (REF. 1).....	98
FIGURE 3D-2 - PHYSIOLOGICAL RESPONSE TO AIR MOTION; ROOM TEMPERATURE = $70^{\circ}F$; 90% OF SUBJECTS FEELING COMFORTABLE AFTER 1/2 HR. (FROM TABLE 1, REF. 11, P. 304.).....	99
FIGURE 3D-3 - AIR HEATED SURFACES.....	99
FIGURE 3D-4 - ELECTRICALLY HEATED SURFACES.....	99
FIGURE 3D-5 - RECIRCULATING SYSTEM SCHEMATIC	100
FIGURE 3D-6 - ASPIRATING OUTLET SCHEMATIC.....	100
FIGURE 3D-7 - ZONES IN JET EXPANSION	101
FIGURE 3D-8 - VELOCITY DECAY OF ISOTHERMAL FREE JETS, COMPRESSIBLE DECAY. $a' = a\sqrt{C_D}$, $D' = D\sqrt{C_D}$ (REF. 2).....	102
FIGURE 3D-9 - ENTRAINMENT RATIOS FOR FREE JETS, $a' = a\sqrt{C_D}$, $D' = D\sqrt{C_D}$ (REF. 2).....	103
FIGURE 3D-10 - VELOCITY DISTRIBUTION IN FREE JETS FROM CIRCULAR ORIFICES AND INFINITE SLOTS	103
FIGURE 3D-11 - OUTLET WITH MULTIPLE OPENINGS.....	104
FIGURE 3D-12 - VANED OUTLETS.....	104
FIGURE 3D-13 - PATH OF A HORIZONTALLY PROJECTED NONISOTHERMAL JET	104
FIGURE 3D-14 - VERTICAL NONISOTHERMAL JETS	105
FIGURE 3D-15 - VELOCITIES NEAR RETURN AND EXHAUST GRILLES, GRILLE = 4 IN. HIGH \times 7-1/2 IN. LONG; FLOW = 130 CFM, EQUIVALENT GRILLE DIAMETER $D = 6.19$ IN.	106
FIGURE 3D-16 - OUTLET DESIGN FOR UNIFORM VELOCITY	107
FIGURE 3D-17 - ACCELERATED MIXING IN DUCTS: (A) PERPENDICULAR ADMISSION; (B) COAXIAL ADMISSION.....	109
FIGURE 3D-18 - FLIGHT STATION AIR DISTRIBUTION SYSTEM.....	109
FIGURE 3D-19 - FIGHTER COCKPIT AIR DISTRIBUTION SYSTEM.....	110
FIGURE 3D-20 - FRONT VIEW OF ENCLOSURE WITH BAFFLES	111
FIGURE 3D-21 - SIDE VIEW OF ENCLOSURE WITH INLET AIR DISTRIBUTION.....	111
FIGURE 3D-22 - SIDE VIEW OF ENCLOSURE WITH DISTRIBUTED EXHAUST	111
FIGURE 3D-23 - SUCTION PLENUM SHELVES	111
FIGURE 3D-24 - COMPACT FORCED AIR DISTRIBUTION	111
FIGURE 3D-25 - TENSION SYSTEM	113
FIGURE 3D-26 - SUPPORTS FOR FLEXIBLE BELLOWS	113
FIGURE 3D-27 - BELLOWS WITH LINER.....	113
FIGURE 3D-28 - SWIVEL DUCT JOINT	113
FIGURE 3D-29 - SLIDING EXPANSION JOINT	113
FIGURE 3D-30 - TURBINE ENGINE BLEED SYSTEM SCHEMATIC	114
FIGURE 3D-31 - SYMMETRICAL TURBOCOMPRESSOR SYSTEM	115
FIGURE 3D-32 - FIGHTER BLEED AIR SYSTEM SCHEMATIC	116

LIST OF TABLES

TABLE 3A-1 - LOAD VALUES AT SEA LEVEL AND 20,000 FT.....	30
TABLE 3A-2 - VALUES FOR TEMPERATURE AND HEAT TRANSFER COEFFICIENT.....	33
TABLE 3A-3 - RESULTS OF ANALYSIS.....	35
TABLE 3A-4 - PASSENGER HEAT GENERATION.....	36
TABLE 3A-5 - AVERAGE VALUES OF HEAT TRANSFER COEFFICIENT.....	37
TABLE 3A-6 - SUMMATION OF UA VALUES.....	37
TABLE 3A-7 - HEATING LOAD AT 20,000 FT.....	38
TABLE 3A-8 - HEATING AND COOLING LOADS AT SEA LEVEL AND 20,000 FT ALTITUDE.....	38
TABLE 3B-1 - PERFORMANCE OF VAPOR CYCLE SYSTEMS.....	82
TABLE 3B-2 - SYSTEM SUMMARY.....	83
TABLE 3B-3 - SUMMARY OF SYSTEM COP VALUES.....	85

SAENORM.COM : Click to view the full PDF of air1168_3b

SECTION 3A - AIR CONDITIONING LOAD ANALYSIS**1. INTRODUCTION****1.1 Scope**

This section presents methods and examples of computing the steady-state heating and cooling loads of aircraft compartments. In a steady-state process the flows of heat throughout the system are stabilized and thus do not change with time. In an aircraft compartment, several elements compose the steady-state air conditioning load. Transfer of heat occurs between these sources and sinks by the combined processes of convection, radiation, and conduction in the following manner:

1. Convection between the boundary layer and the outer airplane skin.
2. Radiation between the external skin and the external environment.
3. Solar radiation through transparent areas directly on flight personnel and equipment and on the cabin interior surfaces.
4. Conduction through the cabin walls and structural members.
5. Convection between the interior cabin surface and the cabin air.
6. Convection between cabin air and flight personnel or equipment.
7. Convection and radiation from internal sources of heat such as electrical equipment.

The subsequent paragraphs discuss methods of determining each of the heat transfer rates listed above, as well as the physiological considerations involved in the selection of proper cabin conditions that are to be maintained.

1.2 Nomenclature

A = Area, ft², in.²

a = Insulation thickness, ft

c = Velocity of sound, ft/sec

c_p = Specific heat capacity at constant pressure, Btu/lb-°F

E = Electrical equipment power consumption, watts

e_w = Skin emissivity, dimensionless

f = Friction factor, dimensionless

F_a = Configuration factor, dimensionless

F_e = Emissivity factor, dimensionless

$F_{v-skin/soil}$ = Fuselage view factor of the reflective ground, dimensionless

G_s = Total solar radiation (irradiation), Btu/hr-ft²

g = Gravitational acceleration, ft/sec²

h'_c = Equivalent conductance due to conduction and convection, Btu/hr-ft²-°F

h_i = Film conductance, Btu/hr-ft²-°F

- h_o = External surface conductance, Btu/hr-ft²-°F
- h'_o = External surface conductance based on enthalpy, Btu/hr-ft²-°F
- h_r = Equivalent conductance due to radiation, Btu/hr-ft²-°F
- i^* = Reference enthalpy, Btu/lb
- i_o = Enthalpy corresponding to free stream temperature, or enthalpy corresponding to temperature at edge of boundary layer, Btu/lb
- i_r = Enthalpy corresponding to recovery temperature, Btu/lb
- i_w = Enthalpy corresponding to skin temperature, Btu/lb
- k = Thermal conductivity of air, Btu-ft/hr-ft²-°F
- k_i = Thermal conductivity of insulation, Btu-ft/hr-ft²-°F
- m = Mass, lb
- M = Mach number, V_o/c , dimensionless
- N_{Gr} = Grashof number, $x^3(\rho)^2 g\beta\Delta T/\mu^2$, dimensionless
- N_{Nu} = Nusselt number, $h'_c x / k$, dimensionless
- N_{Pr} = Prandtl number, $\mu c_p / k$ dimensionless
- N_{Re} = Reynolds No., $V_o x \rho / \mu$, dimensionless
- P = Pressure, lbf/ft²
- P_o = Ambient pressure, lbf/ft²
- q_c = Rate of heat flow, Btu/hr
- q_{cb} = Total heat flow from cabin, Btu/hr
- q_s = Total solar heat load transmitted through transparent areas, Btu/hr
- r = Recovery factor, dimensionless
- rf = Soil reflectance, dimensionless
- t = Temperature, °F
- ΔT = Difference in temperatures, °R
- T_c = Cabin temperature, °R
- T_k = Cargo compartment temperature, °R
- T_{max} = Maximum allowable temperature of electrical equipment compartment, °R
- T_r = Recovery temperature, °R
- T_o = Outside ambient temperature, °R

T_{st}	= Local ambient static temperature or static temperature at edge of boundary layer, °R
T_u	= Effective temperature of outer space, °R
T_w	= Outer skin (wall) temperature, °R
U	= Overall conductance Btu/hr-ft ² -°F
V_o	= Free stream velocity or velocity at edge of boundary layer, ft/sec
W	= Amount of cabin air required to cool electrical equipment, lb/hr
x	= Thickness or length, ft
Z	= Compressibility factor, dimensionless
α_s	= Solar absorptance, dimensionless
β	= Volumetric thermal expansion coefficient, dimensionless
ρ	= Density, lb/ft ³
τ	= Overall solar transmissivity of transparent area, dimensionless
γ	= Specific heat ratio, c_p/c_v , dimensionless
η	= Efficiency or effectiveness, dimensionless
μ	= Absolute viscosity, lb/ft-sec
σ	= Stefan-Boltzmann constant, 0.171×10^{-8} Btu/hr-ft ² -°R ⁴

1.3 Common Abbreviations

ARDC	— Air Research and Development Command
ASME	— American Society of Mechanical Engineers
ASHRAE	— American Society of Heating, Refrigeration and Air Conditioning Engineers
Btu	— British thermal unit
Eq.(Eqs.)	— Equation(s)
°F	— Degrees Fahrenheit
Fig.(Figs.)	— Figure(s)
fpm, ft/min	— Feet per minute
fps, ft/sec	— Feet per second
ft	— Feet
hr	— Hour
in.	— Inch
lb	— Pound mass

lbf	— Pound force
lbf/ft ²	— Pounds force per square foot
lb/hr	— Pounds mass per hour
min	— Minute
mph	— Miles per hour
no.	— Number
%	— Percent
Par.(Pars.)	— Paragraph(s)
°R	— Degrees Rankine
Ref.	— Reference
sec	— Second
WADC	— Wright Air Development Center (U.S. Air Force)

2. PHYSIOLOGICAL REQUIREMENTS

The maintenance of a comfortable and safe environment for human occupancy involves the simultaneous control of the temperature, moisture content, movement, purity, and absolute pressure of the air in occupied areas. In many applications, consideration of cost and weight make it impractical to control all factors that maintain ideal conditions, but in all cases sufficient control must be maintained to provide for the safety of the occupants and to ensure that the mission of the aircraft can be accomplished. As this section is concerned with the calculation of air conditioning thermal loads, only the temperature and humidity requirements will be considered here. For a more detailed discussion of physiological requirements, refer to Refs. 2 and 4.

The conditions required for comfort in an occupied area depend to a large extent on the individual. Conditions that are comfortable for one person may be decidedly uncomfortable for another. However, certain conditions have been determined to be comfortable for a large number of persons. The combinations of temperature, humidity, and air movement that cause comfort or discomfort have been tabulated and are expressed as "effective temperature."

2.1 Effective Temperature

The effective temperature is an experimentally determined index of the degree of warmth experienced by individuals on exposure to different combinations of temperature, humidity, and air movement. The numerical value of the effective temperature for a given set of conditions is the temperature of saturated, slowly moving (15-25 ft/min) air that results in the same feeling of warmth. The effective temperature cannot be measured directly, but must be obtained from charts (such as Fig. 3A-1) for various conditions of temperature, humidity, and air movement.

Lines of constant effective temperature show conditions that will produce equal sensations of warmth, but not necessarily equal sensations of comfort. Some degree of discomfort will be experienced at very high or very low relative humidity, high air velocity, or extreme temperatures, regardless of the effective temperature.

In summer the most popular effective temperature appears to be 71°F, and in winter, 68°F. However, the effective temperature index must be used with discretion since it is an experimentally determined index, based on tests of United States inhabitants who are normally clothed. Also, the tests that established the index were performed with convective type heating systems where radiation was not a factor. The summer index applies to persons completely adapted to artificial air conditions, which require from 1-1/2 to 3 hr exposures.

3. STATEMENT OF HEATING AND COOLING LOAD EQUATIONS

3.1 Heat Transfer Between the Air and Skin

The heat transfer between the air and the airplane skin is determined by an equation of the form

$$q_c = h_o A (T_2 - T_1) \quad (3A-1)$$

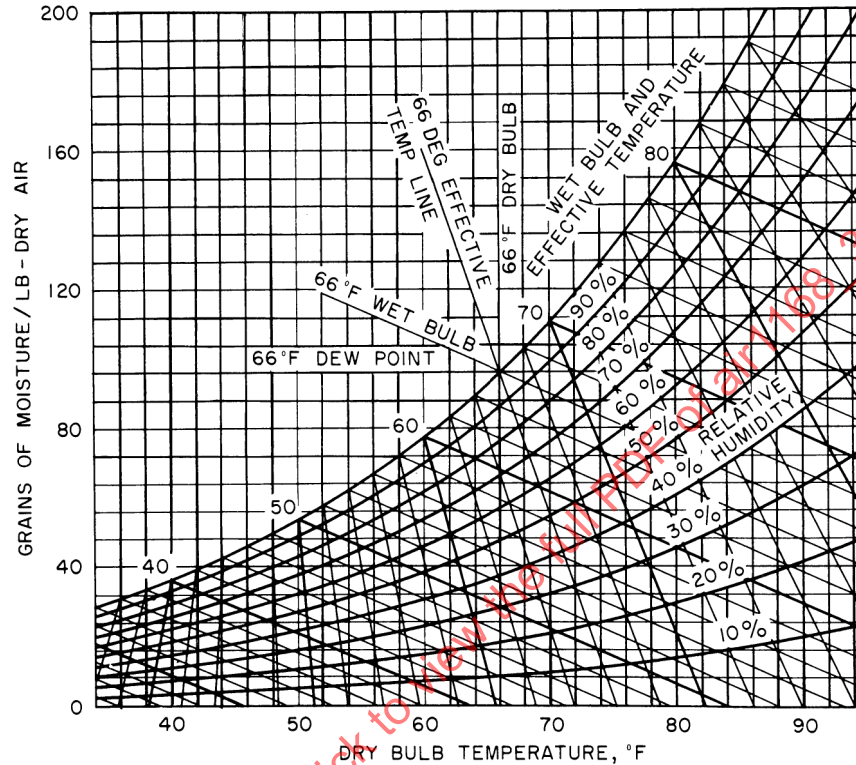


Figure 3A-1 - Psychrometric Chart, Persons at Rest, Normally Clothed, in Still Air

3.1.1 Ground Static Conditions

At ground static conditions, Eq. 3A-1 becomes:

$$q_c = h_o A (T_o - T_w) \quad (3A-2)$$

For this case, h_o may be evaluated in the same manner as the internal coefficient h_i discussed in Par. 3.2.2. The value of h_o may be obtained from Eq. 3A-25 at the design velocity. The outside wind velocity for design purpose is usually taken as 22 ft/sec unless it is known to be different for a particular application. For a velocity of 22 ft/sec, h_o has the value 8.9 Btu/hr-ft²-°F.

The evaluation of the skin temperature, T_w , necessary to solve Eq. 3A-2, is a tedious process, but as will be shown in Par. 3.2.1, it can be omitted by determining an overall coefficient of heat transfer from outside to inside. If it is necessary or desirable to determine the skin temperature, a heat balance at the skin must be formed as described in Par. 4.3.

3.1.2 Flight Condition

For flight conditions, Eq. 3A-1 takes the form

$$q_c = h_o A(T_r - T_w) \quad (3A-3)$$

$$\text{where } T_r = T_o \left[1 + r \left(\frac{\gamma - 1}{2} \right) M^2 \right] \quad (3A-4)$$

The recovery factor, r , has the value $\sqrt{N_{Pr}}$ for laminar flow and $\sqrt[3]{N_{Pr}}$ for turbulent flow. The determination of surface conductance for use in Eq. 3A-3 is more involved than for the ground static case and is the subject of the next paragraph.

3.1.2.1 Determination of Surface Conductance for the Flight Condition

In recent years (circa 1955-1965) much work has been done in the field of high velocity heat transfer, with most of it directed to the problem of aerodynamic heating. From this work, several methods of determining the film coefficient were evolved. The method given here is described in detail by Eckert in Ref. 5 and is known as the reference temperature method.

When the property values in the equations that describe the flow and heat transfer are evaluated at the reference temperature, the variation of the friction factor with Mach number and T_w/T_o vanishes. The equations required to evaluate the reference temperature and the surface conductance are as follows:

$$T^* = 0.5(T_o + T_w) + 0.22r \left[\frac{\gamma - 1}{2} \right] M^2 T_o \quad (3A-5)$$

$$\rho^* = \frac{P}{RT^*} \quad (3A-6)$$

$$N_{Re}^* = \frac{V_o \rho^* x}{\mu^*} \quad (3A-7)$$

$$\frac{f^*}{2} = \frac{0.332}{(N_{Re}^*)^{0.5}} \text{ (laminar flow)} \quad (3A-8)$$

$$\frac{f^*}{2} = \frac{0.0296}{(N_{Re}^*)^{0.2}} \text{ (turbulent flow)} \quad (3A-9)$$

$$Dh_o = \frac{\rho^* c_p (f^* / 2)}{(N_{Pr}^*)^{0.667}} (3600) V_o \quad (3A-10)$$

where T^* = Reference local static temperature, °R

x = Distance from origin of boundary layer, ft

In the preceding equations the asterisk superscript denotes the reference temperature and property values evaluated at the reference temperature. The equations are solved for a given flight condition as follows:

1. Assume a skin temperature T_w and solve Eq. 3A-5 for the reference temperature.
2. Solve the remaining equations, evaluating the fluid properties at the reference temperature. The resulting h_o , from Eq. 3A-10, is the surface conductance corresponding to the assumed skin temperature T_w .
3. Utilizing Eq. 3A-2 and the procedure described in Par. 4.2, determine by an iterative procedure the equilibrium skin temperature.

Note: See Par. 8 for a sample calculation.

Dissociation Effects — At air temperatures above about 3000°R, air begins to dissociate, and the specific heat increases rapidly, since dissociation energy as well as thermal energy is being absorbed. When this happens, temperature is no longer a correct measure of the energy content of the air, and it must be replaced by a corresponding enthalpy. Also, when dissociation occurs, the gas constant R changes.

This change is accounted for by introducing a compressibility factor, Z , which must be used in computations involving the gas constant. To allow for dissociation effects, certain of the equations in Pars. 3.1.2 and 3.1.2.1 must be modified as follows:

$$i^* = 0.5(i_w + i_o) + 0.22 \left(\frac{\gamma - 1}{2} \right) M^2 i_o r \quad (3A-11)$$

$$\rho^* = \frac{P}{RT^* Z} \quad (3A-12)$$

$$h'_o = \frac{\rho^* V_o (f^* / 2) c_p^*}{(N_{Pr}^*)^{0.667}} (3600) \quad (3A-13)$$

$$q_c = h'_o (i_r - i_w) \quad (3A-14)$$

The method of solution of Eqs. 3A-11 to Eq. 3A-14 combined with the unaffected equations of Par. 3.1.2.1 is essentially the same as when using the reference temperature method directly. An outer skin temperature is assumed and a corresponding i_w is determined. Eq. 3A-11 is then solved for i^* . A T^* corresponding to i^* is determined and the remaining equations evaluated, using fluid properties corresponding to T^* . An iterative procedure is then used to determine the equilibrium skin temperature.

3.2 Heat Transfer Between the Skin and Occupied Areas

The heat transfer between the skin and occupied areas occurs mainly by conduction, but the situation is complicated by the following factors:

1. The cabin wall usually consists of several layers of different material.
2. The construction throughout the structure is not the same; therefore, many parallel heat flow paths exist.
3. There may be dead air spaces that affect heat flow through a combination of conduction, free convection, and radiation.
4. The structural members, bulkheads, and floors usually act as fins to dissipate heat.
5. Heat transfer at the inner cabin walls is usually by convection.
6. Heat transfer may occur to or from adjacent nonconditioned compartments where the temperature is unknown or difficult to determine.

In order to simplify the calculations, it is assumed that heat flows in parallel paths and is one-dimensional; that is, the heat flows along radial lines with no circumferential or longitudinal pattern. For a discussion of methods that consider two- or three-dimensional heat transfer, refer to Ref. 6.

3.2.1 Combined Heat Transfer Through Composite Walls

The heat transfer equation for a simple composite wall as shown in Fig. 3A-2 can be written as

$$q = h_o A (T_o - T_w) \quad (3A-15)$$

$$q = \frac{k_1}{x_1} A (T_w - T_a) \quad (3A-16)$$

$$q = \frac{k_2}{x_2} A (T_a - T_b) \quad (3A-17)$$

$$q = \frac{k_3}{x_3} A (T_b - T_i) \quad (3A-18)$$

$$q = h_i A (T_i - T_c) \quad (3A-19)$$

For a steady-state process, the heat transfer is equal through each section of the wall; therefore, adding Eqs. 3A-15 to 3A-19 and solving for q gives

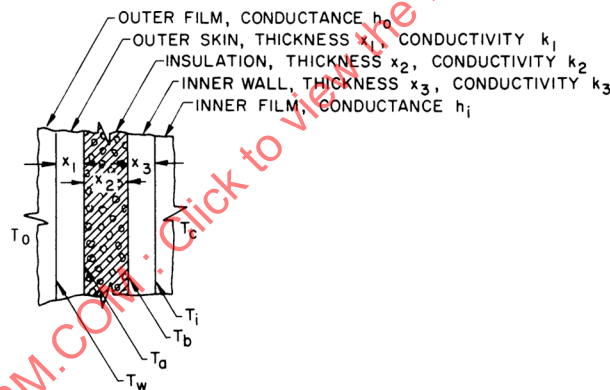


Figure 3A-2 - Simple Composite Wall

$$q = UA(T_o - T_c) \quad (3A-20)$$

where U , the overall conductance of the wall in Btu/hr-ft²-°F is given by

$$U = \frac{1}{\frac{1}{h_o} + \frac{x_1}{k_1} + \frac{x_2}{k_2} + \frac{x_3}{k_3} + \frac{1}{h_i}} \quad (3A-21)$$

or

$$U = \frac{1}{(1/h_o) + \left[\sum (x/k) \right] + (1/h_i)} \quad (3A-22)$$

3.2.1.1 Overall Conductance for Ground Static Heating

The maximum ground static heating load ordinarily occurs at night when solar radiation to the skin is not a factor. For this case, Eqs. 3A-20 and 3A-22 are valid as stated, with the overall conductance U based on total resistance from outside to inside.

The outside and inside film coefficients, h_o and h_i , can be evaluated from Eq. 3A-25 at the design velocity, ordinarily assumed to be 22 ft/sec for the outside and 3.3 ft/sec for the inside. The thermal conductivity values can be obtained from the tables in AIR1168/9.

3.2.1.2 Overall Conductance for Ground Static Cooling

The maximum ground static cooling load occurs during the day when solar radiation to the skin is a factor. For this case, Eqs. 3A-20 (see Fig. 3A-2) and 3A-22 take the form

$$q = UA(T_w - T_c) \quad (3A-23)$$

$$U = \frac{1}{\left[\sum (x/k) \right] + (1/h_i)} \quad (3A-24)$$

The difference is that, owing to solar radiation, the skin temperature may be higher than ambient temperature, thus requiring a heat balance at the skin to determine skin temperature, as shown in Par. 4.3. The overall conductance and heat transfer are determined from equations that apply from the outer skin to the cabin.

3.2.1.3 Overall Conductance for Flight Below Mach 2

In flight, at subsonic and low supersonic Mach numbers, the conductance of the outer film, h_o , is large in comparison with the conductance of the rest of the wall, and the effects of radiation to and from the skin are usually insignificant. Therefore, the skin temperature can be considered equal to the recovery temperature and can be determined as shown in Par. 4.1. The overall wall conductance and heat transfer can be determined using Eqs. 3A-23 and 3A-24.

3.2.1.4 Overall Conductance for Flight Exceeding Mach 2

In flight, at Mach numbers exceeding Mach 2, aerodynamic heating becomes significant and the skin temperature becomes hot enough to radiate considerable heat away from the skin to the atmosphere. The skin temperature is ordinarily lower than the recovery temperature and may be evaluated by the method shown in Par. 4.2. The overall conductance and heat transfer can be determined from Eqs. 3A-23 and 3A-24.

3.2.2 Internal Coefficient of Heat Transfer

Heat transfer between the inner walls and the air in the compartments occurs by forced convection due to cabin ventilating air or by free convection in unventilated spaces. Very little work has been done to determine accurate values of heat transfer coefficients under conditions directly applicable to aircraft cabins. However, experiments that have been conducted for commercial application provide an indication of values to be expected in aircraft applications.

An equation that fits a curve given in Ref. 2 for the surface film coefficient is

$$h_i = 2.0 + 0.314V_o \quad (3A-25)$$

The values from Eq. 3A-25 are actually reported for stucco from Ref. 2, but since these are the largest values reported, it is recommended that this equation be used unless better data are available. Generally, air velocities in an occupied compartment will be in the range 0 – 3.3 ft/sec. Therefore, h_i will have the range 2.0 – 3.04 Btu/hr-ft²-°F under ordinary conditions. It should also be noted that Eq. 3A-25 may be used to determine the outside surface conductance, h_o , for ground static conditions.

3.2.3 Heat Transfer Across an Enclosed Airspace

Often a composite wall includes an airspace between the outer skin and inner wall, as illustrated in Fig. 3A-3. The heat transfer across such an airspace occurs by a combination of conduction, radiation, and convection. It is convenient to lump the convective and conductive heat transfer together as an equivalent conductance and to consider heat transfer by radiation separately as an equivalent conductance due to radiation. The resulting equation for heat transfer across an airspace is (see Fig. 3A-3)

$$q = h'_c A(T_2 - T_3) + h_r A(T_2 - T_3) \quad (3A-26)$$

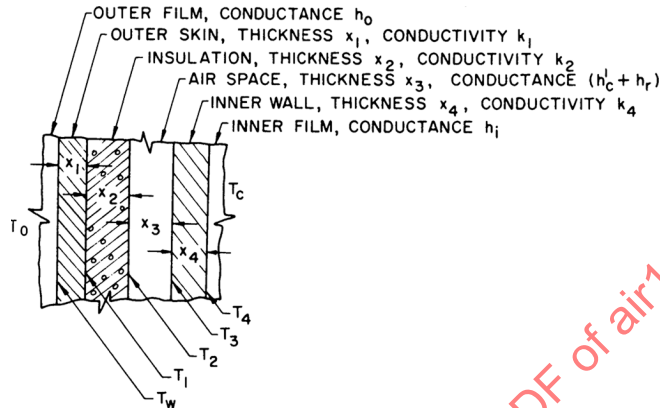


Figure 3A-3 - Simple Composite Wall Including an Air Space

To solve Eq. 3A-26, the surface temperatures T_2 and T_3 must be known. Also, as shown in Pars. 3.2.3.1 and 3.2.3.2, temperatures T_2 and T_3 are required to evaluate h'_c and h_r . This means that an iterative procedure is required to obtain an exact solution. A suggested procedure is as follows:

1. Estimate an equivalent conductance for the air space.
2. Compute the overall conductance of the wall from

$$U_{wc} = \frac{1}{\sum \left(\frac{x}{k} \right) + \left(\frac{1}{h'_c + h_r} \right) + \frac{1}{h_i}} \quad (3A-27)$$

(See Fig. 3A-3.)

3. Compute the surface temperatures T_2 and T_3 from

$$U_{wc}(T_w - T_c) = U_{w2}(T_w - T_2) \quad (3A-28)$$

$$U_{wc}(T_w - T_c) = U_{3c}(T_3 - T_c) \quad (3A-29)$$

where U_{wc} = Overall conductance of wall (wall-to-cabin), Btu/hr-ft²-°F

U_{w2} = Overall conductance from outer wall to inner surface of air space, Btu/hr-ft²-°F

$$U_{w2} = \frac{1}{(x_1/k_1) + (x_2/k_2)} \quad (3A-30)$$

U_{3c} = Overall conductance from inner surface of air space to cabin, Btu/hr-ft²-°F

$$U_{3c} = \frac{1}{(x_4/k_4) + (1/h_i)} \quad (3A-31)$$

4. Compute the equivalent conductance of the air space by the methods of Pars. 3.2.3.1 and 3.2.3.2.
5. With the computed conductance of the air space, return to step 2 and compute the overall conductance of the wall. For the desired accuracy, repeat this procedure until two successive values of the overall conductance agree.

3.2.3.1 Equivalent Conductance of an Air Space Due to Conduction and Convection

The equivalent conductance of an air space may be determined as a function of the Grashof number, Prandtl number, Nusselt number, and the length/width ratio of the air space, by using the following equations:

1. Vertical air spaces (walls enclosing air spaces are vertical):

$$\frac{h'_c x}{k} = 1 \text{ for } N_{Gr} \leq 2000 \quad (3A-32)$$

$$\frac{h'_c x}{k} = \frac{0.20}{(L/x)^{1/9}} (N_{Gr} N_{Pr})^{0.25} \text{ for } 2 \times 10^4 \leq N_{Gr} \leq 2.1 \times 10^5 \quad (3A-33)$$

$$\frac{h'_c x}{k} = \frac{0.071}{(L/x)^{1/9}} (N_{Gr} N_{Pr})^{0.333} \text{ for } 2.1 \times 10^5 \leq N_{Gr} \leq 1.1 \times 10^7 \quad (3A-34)$$

2. Horizontal air spaces (walls enclosing air spaces are horizontal):

$$\frac{h'_c x}{k} = 0.21 (N_{Gr} N_{Pr})^{0.25} \text{ for } 10^4 \leq N_{Gr} \leq 3.2 \times 10^5 \quad (3A-35)$$

$$\frac{h'_c x}{k} = 0.075 (N_{Gr} N_{Pr})^{0.333} \text{ for } 3.2 \times 10^5 \leq N_{Gr} \leq 10^7 \quad (3A-36)$$

where ΔT = Difference in surface temperatures, °R (used in N_{Gr})

L = Height of air space, ft

x = Width of air space, ft

3. Inclined air spaces - For air spaces inclined at an angle from the horizontal, it is satisfactory to interpolate between the values for horizontal and vertical air spaces.

The preceding equations are plotted for vertical and horizontal air spaces in Fig. 3A-4.

3.2.3.2 Equivalent Conductance of an Air Space Due to Radiation

Radiant heat exchange is proportional to the difference of the fourth power of the absolute temperature of the surfaces emitting and receiving the radiant energy:

$$q = \sigma A F_a F_e (T_2^4 - T_3^4) \quad (3A-37)$$

(see Fig. 3A-3) where

F_e = Emissivity factor, a function of the emissivities and the configuration of the surfaces, dimensionless

F_a = Configuration factor, a function of the configuration of the surfaces, dimensionless

Since the heat transfer due to convection and conduction is proportional to the difference of the first power of the temperature, it is convenient to determine an equivalent conductance due to radiation that can be used with the first power of the temperature. This can be done by setting the second term of Eq. 3A-26 equal to Eq. 3A-37 and solving for h_r (see Fig. 3A-3):

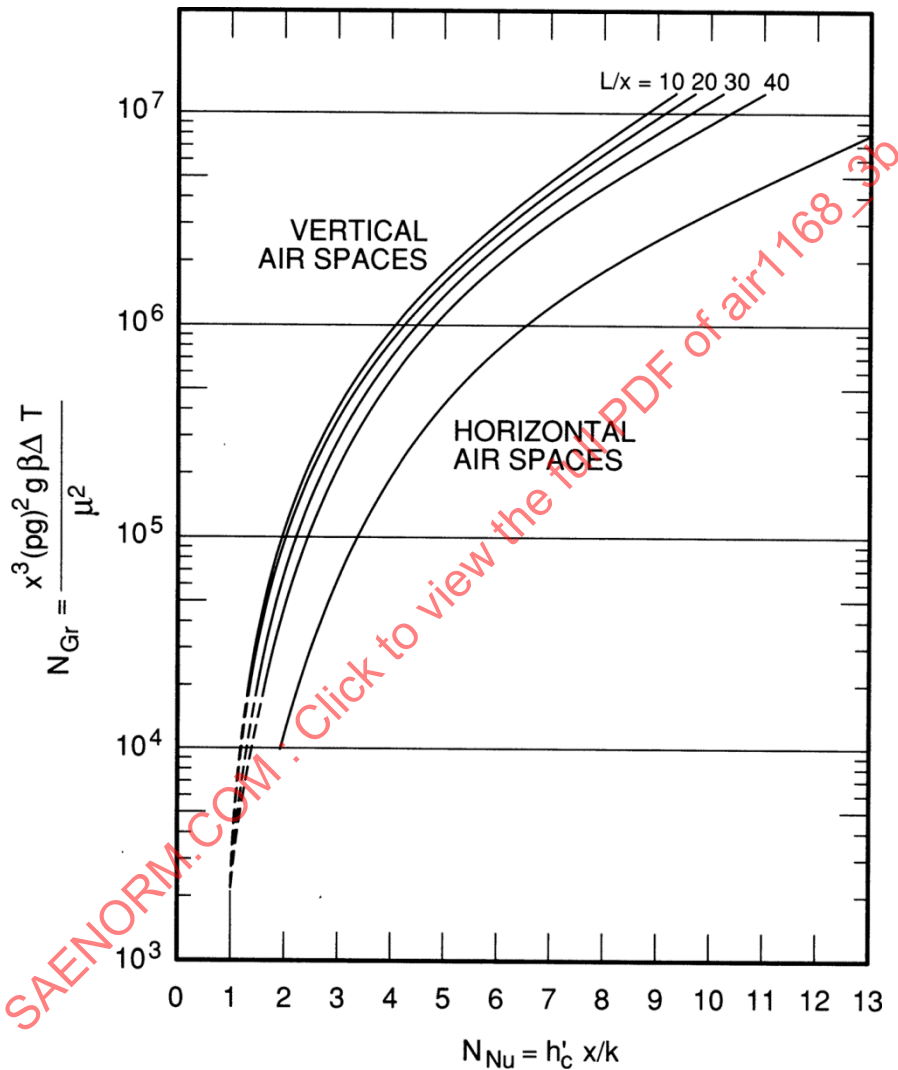


Figure 3A-4 - Nusselt Number versus Grashof Number for Vertical and Horizontal Air Spaces. Note: $N_{Pr} = 0.72$

$$h_r = \frac{\sigma F_a F_e (T_2^4 - T_3^4)}{(T_2 - T_3)} \quad (3A-38)$$

Values of h_r are plotted in Fig. 3A-5 for various values of surface temperature and for $F_a F_e = 1$. For other values of $F_a F_e$, the h_r obtained from Fig. 3A-5 must be multiplied by the correct $F_a F_e$. The configuration and emissivity factors for infinite parallel planes give a good approximation to those for dead air spaces. The configuration factor is 1, and the emissivity factor is:

$$F_e = \frac{1}{(1/e_2) + (1/e_3) - 1} \quad (3A-39)$$

(see Fig. 3A-3) where e_2 and e_3 are the emissivities of walls enclosing the air space.

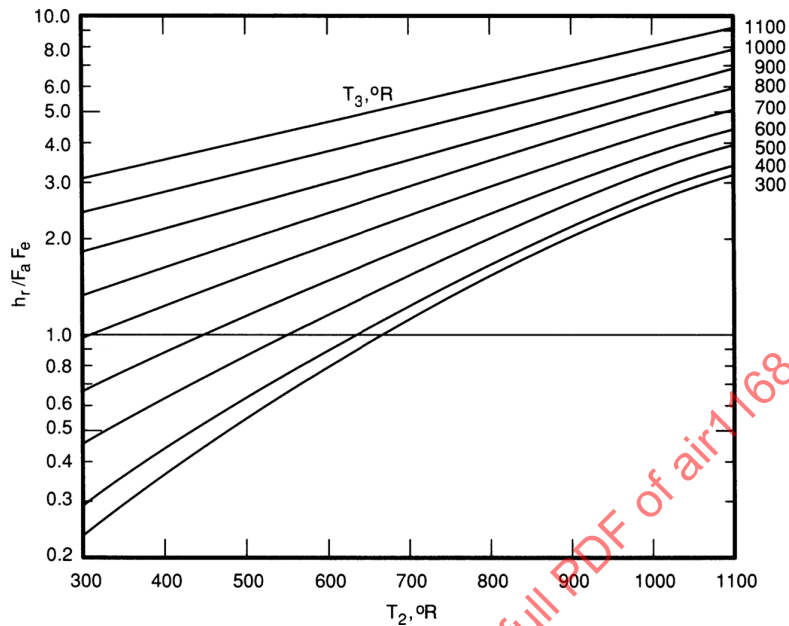


Figure 3A-5 - Equivalent Heat Transfer Coefficient for Radiation

3.2.4 Fin Effect of Structural Members

Structural members that are attached to the aircraft skin and protrude into the cabin interior, such as fuselage frames, can be considered as fins.

For the purpose of this analysis, it is assumed that the base of the frame is in contact with the skin and therefore is at skin temperature. The heat transfer from a plain fin in contact with the skin, as shown in Fig. 3A-6, can be determined using Eq. 3A-40:

$$q = C u_c L \frac{\tanh m_f L}{m_f L} (T_w - T_c) \quad (3A-40)$$

where C = Perimeter of fin

$$= 2(b + \delta), \text{ ft (see Fig. 3A-6)}$$

L = Projection of fin into cabin, ft

$$m_f = \sqrt{u_c C / kA}, \text{ ft}^{-1}$$

u_c = Unit conductance of surface of fin, including insulation, Btu/hr-ft², given by $1/[(1/h_i) + (a/k_i)]$

and where, for u_c and m_f , respectively,

A = Conduction cross – sectional area of fin

$$= b\delta, \text{ ft}^2$$

a = Insulation thickness, ft

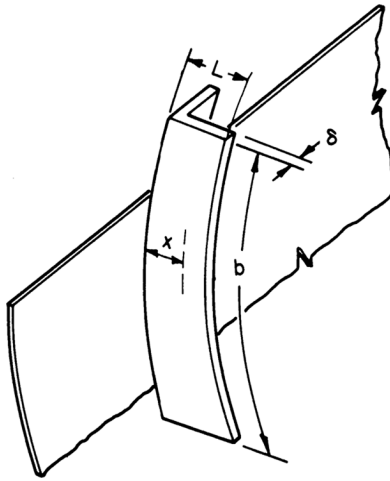


Figure 3A-6 - A Simple Fin

Eq. 3A-40 can be written as

$$q = Cu_c L \eta_f (T_w - T_c) \quad (3A-41)$$

where $\eta_f = \frac{\tanh m_f L}{m_f L} = \text{Fin effectiveness, dimensionless}$

Fig. 3A-7 plots η_f as a function of $m_f L$.

Another factor to be considered, especially for noninsulated fins, is the temperature distribution along the fin. It is undesirable from a comfort standpoint to have very cold or very hot surfaces in occupied areas. The temperature distribution along a fin, shown in Fig. 3A-6, is solved by

$$\frac{T_x - T_c}{T_w - T_c} = \frac{\cosh m_f (L - x)}{\cosh m_f L} \quad (3A-42)$$

where T_x is the temperature of the surface of the fin at a distance x from the wall. Eq. 3A-42 is plotted in Fig. 3A-8 for various values of x/L and $m_f L$.

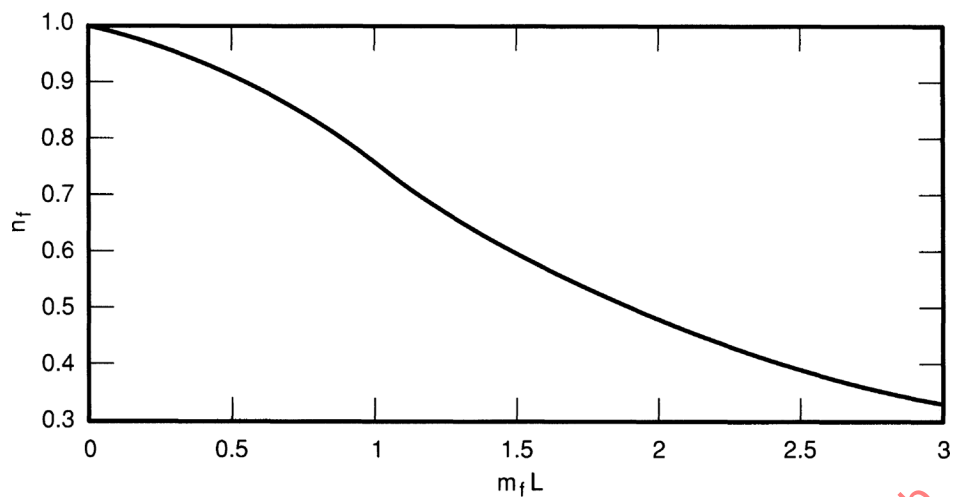


Figure 3A-7 - Fin Effectiveness Factor

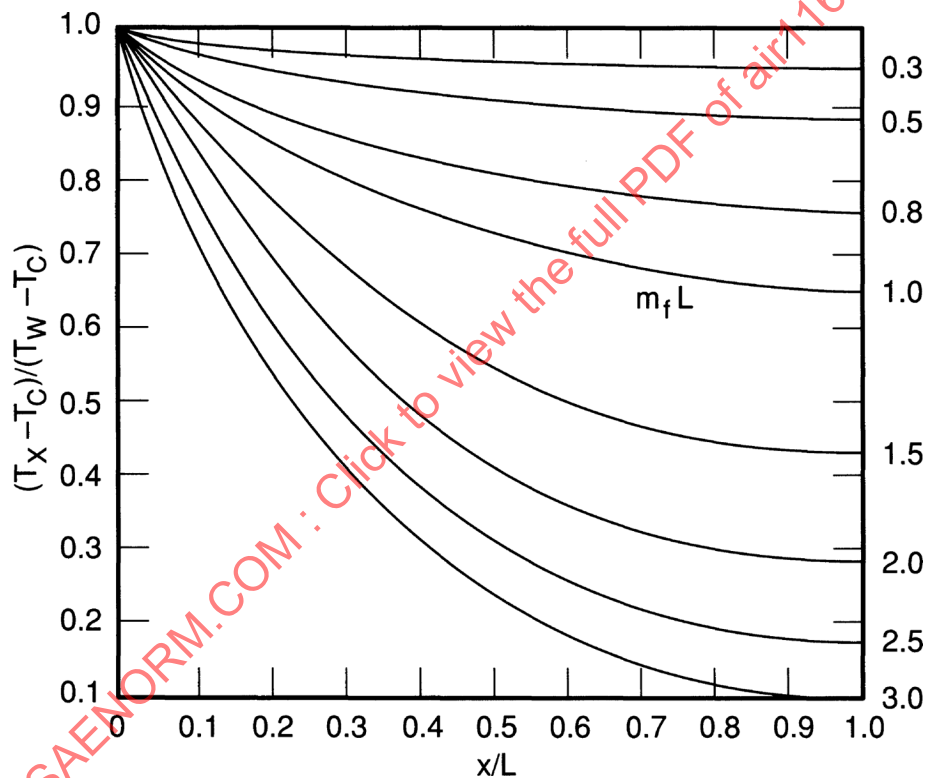


Figure 3A-8 - Temperature Distribution Along a Fin

4. SKIN TEMPERATURE COMPUTATIONAL METHODS

4.1 Skin Temperature at Flight Conditions Less Than Mach 2

In the flight range below Mach 2, it is satisfactory to assume that the skin temperature is equal to the recovery temperature:

$$T_w = T_r = T_o \left[1 + r \left(\frac{\gamma - 1}{2} \right) M^2 \right] \quad (3A-43)$$

When this assumption for skin temperature is used, the outside film conductance, h_o , is not to be included in the computation of the overall conductance, U , of the wall.

4.2 Skin Temperature at Flight Above Mach 2

At approximately Mach 2 the skin temperature becomes high enough for radiation from the skin to become significant. To determine accurately the skin temperature under these conditions, a heat balance at the skin must be written as follows:

$$h_o(T_r - T_w) = -\alpha G_s \frac{A_p}{A} - \alpha G_s (rf) F_{v-skin-soil} + U(T_w - T_c) + \frac{1}{2} \sigma F_e F_a (T_w^4 - T_u^4) + \frac{1}{2} \sigma F_e F_a (T_w^4 - T_e^4) \quad (3A-44)$$

where $h_o(T_r - T_w)$	= Heat transferred to the skin by aerodynamic heating, Btu/hr-ft ²
$\alpha G_s (A_p/A)$	= Heat gained by solar irradiation, Btu/hr-ft ²
$\alpha G_s (rf) (F_{v-skin/soil})$	= Heat gained by solar irradiation reflected from ground (Albedo), Btu/hr-ft ²
$U(T_w - T_c)$	= Heat lost by skin through cabin walls to cabin interior, Btu/hr-ft ²
$(1/2) \sigma F_e F_a (T_w^4 - T_e^4)$	= Heat radiated from lower half of airplane skin to earth's surface, Btu/hr-ft ²
$(1/2) \sigma F_e F_a (T_w^4 - T_u^4)$	= Heat radiated from upper half of airplane skin to atmosphere, Btu/hr-ft ²
α_s	= Solar absorptance, dimensionless
A_p/A	= Ratio of projected area of fuselage to the total area, dimensionless
T_e	= Mean temperature of earth's surface, °R
F_e	= Emissivity factor, dimensionless
F_a	= Configuration factor, dimensionless
rf	= Soil reflectance, dimensionless
$F_{v-skin/soil}$	= Fuselage view factor of the reflective ground, dimensionless

At high altitudes, the solar irradiation intensity is approximately 430 Btu/hr-ft² (from Ref. 7 or other sources). For a body of revolution, the value of A_p/A is $1/\pi$. The configuration factor for fuselage shapes is 1 and the emissivity factor is equal to the emissivity of the skin, e_w . The effective temperature of space is assumed to be 0°R and of the earth's surface to be 510°R. (At lower altitudes, T_{sky} values available on line should be used.) The albedo becomes insignificant at altitude. α_s is assumed to be 0.25 for white paint on aluminum. (See AIR1168/12 for additional values.) By substituting these numerical values into Eq. 3A-44 it can be seen that

$$h_o(T_r - T_w) = -0.25 \frac{430}{\pi} + U(T_w - T_c) + 0.173 e_w \left(\frac{T_w}{100} \right)^4 - 58.52 e_w \quad (3A-45)$$

The equilibrium skin temperature can be determined from Eq. 3A-45 in conjunction with the methods outlined in Par. 3.1.2 by an iterative procedure. Such a procedure is as follows:

1. Compute the overall wall conductance, U .
2. Determine the emissivity, e_w , of the skin and select the desired cabin temperature, T_c .
3. Assume a wall temperature, T_w .
4. Solve Eq. 3A-45 for the convective heat transfer rate, $h_o(T_r - T_w)$.

5. For the known flight conditions and the assumed wall temperature, compute, using the methods described in Pars. 3.1.2 and 3.1.2.1, the convective heat transfer rate from Eq. 3A-3.
6. If the skin temperature assumed in step 3 is correct, the convective heat transfer rate computed in steps 4 and 5 will be equal. If not, assume a new skin temperature and repeat the process.

4.3 Skin Temperature at Ground Static Conditions

For ground static conditions, the heat balance at the skin is identical to that determined by using Eq. 3A-44, but some of the numerical quantities used to establish Eq. 3A-45 are different for the sea level case. The solar irradiation intensity at sea level can be taken as 360 Btu/hr-ft², and the effective temperature of outer space is assumed to be 410°R.

Note: Typical values of the effective temperature of outer space (also known as T_{sky}) and ground temperature are assumed. There are many derivations of these temperatures available on line that may be available for specific applications.

Albedo is given as $\alpha G_s(rf)(F_{v-skin/soil})$. rf is the soil reflectance and assuming light concrete ground is 0.8. $F_{v-skin/soil}$ is the fuselage view factor of the reflective ground is assumed to be 0.5 for a view factor between a cylinder and a plane.

Substitution of the numerical values used to establish Eq. 3A-45 with the above changes gives:

$$h_o(T_o - T_w) = -0.25 \frac{360}{\pi} - 0.25[-360 \times 0.8 \times 0.5] + U(T_w - T_c) + 0.173e_w \left(\frac{T_w}{100}\right)^4 - 82.96e_w \quad (3A-46)$$

Solving Eq. 3A-46 for T_w gives:

$$T_w = \frac{T_o h_o + (90/\pi) + 36 + UT_c}{U + h_o} + \frac{82.96e_w - 0.173e_w(T_w/100)^4}{U + h_o} \quad (3A-47)$$

Eq. 3A-47 can be written as

$$T_w = B - CT_w^4 \quad (3A-48)$$

where

$$B = \frac{T_o h_o + (90/\pi) + 36 + UT_c + 82.96e_w}{U + h_o}, \text{ } ^\circ R$$

$$C = \frac{0.173 \times 10^{-8} e_w}{U + h_o}, \text{ } ^\circ R^{-3}$$

Values of T_w for various values of B and C are given in Fig. 3A-9.

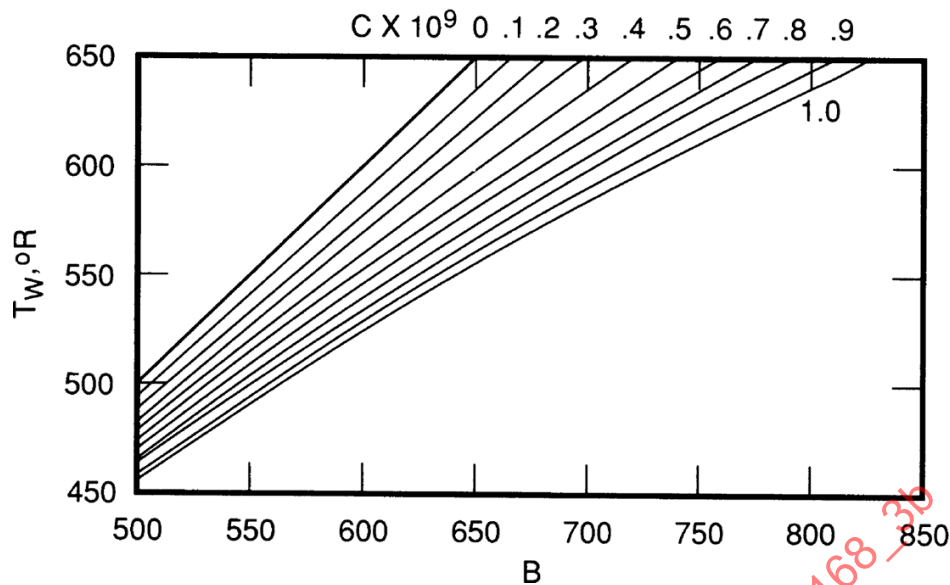


Figure 3A-9 - Average Equilibrium Skin Temperature at Ground Static Conditions

5. COOLING LOADS DUE TO RADIATION THROUGH TRANSPARENT AREAS

Solar radiation is transmitted directly through transparent areas to the cabin interior. The reradiated energy from the interior surfaces does not pass through the transparent areas because they are nearly opaque to these longer wavelengths. The solar radiant heat transmitted through transparent areas is

$$q_s = \tau G_s A_p \quad (3A-49)$$

where A_p = Projected area of transparent surface normal to sun's rays, ft²

Often a window or canopy is constructed of several layers of material in series. Sometimes these layers consist of different materials and sometimes there is an air space between the layers. In any case, the overall transmissivity is the product of the transmissivities of the individual layers:

$$q_s = (\tau_1 \cdot \tau_2 \dots \tau_n) G_s A_p \quad (3A-50)$$

6. HEATING AND COOLING LOADS DUE TO INTERNAL SOURCES

6.1 Sensible and Latent Heat Emission by Occupants

In densely occupied areas, such as the cabin of transports, the heat produced by the occupants can be a substantial factor in the total cooling load. Fig. 3A-10 shows the sensible heat production of human beings at various activity levels versus dry bulb temperature, and Fig. 3A-11 shows the latent heat production for the same conditions. The total heat production is the sum of the two. The latent heat emission is in the form of evaporated moisture (perspiration) and has no effect on the dry bulb temperature of the space.

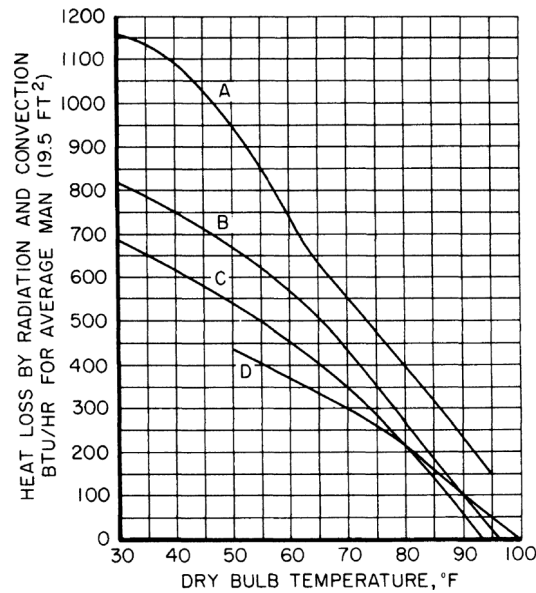


Figure 3A-10 - The Relationship between Radiation and Convection Loss from the Human Body and Dry Bulb Temperature for Still Air. (Ref. ASHRAE Guide)

For a system that uses 100% fresh air (no recirculation), the latent heat production of the occupants does not enter into the calculation of the cooling load, but does enter into a calculation of the relative humidity of the cabin. If some of the cabin air is recirculated, the latent heat production must be included in a moisture balance for the cabin and cooling equipment. Some of the moisture released by the occupants will be condensed in the cooling equipment, and this heat of condensation is a part of the total cooling load.

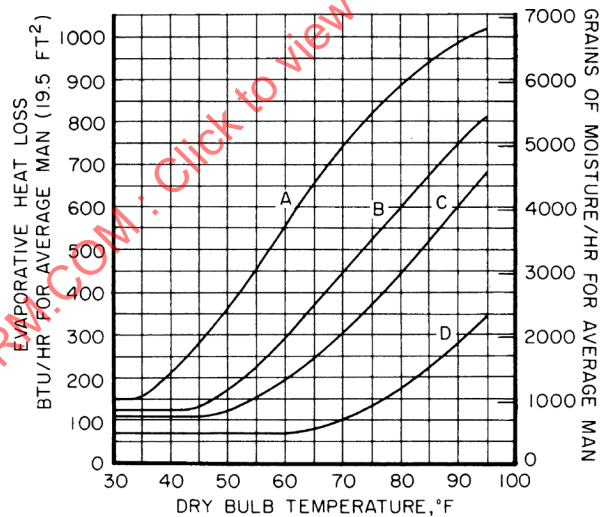


Figure 3A-11 - Evaporative Heat and Moisture Loss from The Human Body in Relation to Dry Bulb Temperature for Still Air Conditions. (Ref. ASHRAE Guide)

Fig. 3A-10 shows:

1. Curve A, persons working, metabolic rate 1310 Btu/hr.
2. Curve B, persons working, metabolic rate 850 Btu/hr.
3. Curve C, persons working, metabolic rate 660 Btu/hr.
4. Curve D, persons seated at rest, metabolic rate 400 Btu/hr.

Fig. 3A-11 shows:

1. Curve A, persons working, metabolic rate 1310 Btu/hr.
2. Curve B, persons working, metabolic rate 850 Btu/hr.
3. Curve C, persons working, metabolic rate 660 Btu/hr.
4. Curve D, persons seated at rest, metabolic rate 400 Btu/hr.

6.2 Electrical Load

The wattage rating of electrical equipment installed in modern aircraft is large. A conservative, but not unrealistic, estimate of the cooling load introduced by the electrical equipment can be obtained by assuming that the electrical equipment converts all of its energy to heat and that all of the heat is released to the cabin:

$$q_e = 3.415E \quad (3A-51)$$

where q_e = Electrical load, Btu/hr

E = Power input to electrical equipment, watts

Usually all or a portion of the cabin air is exhausted overboard at cabin temperature. Also, the electrical equipment usually can operate in an ambient atmosphere warmer than the cabin. If it is possible to enclose the electrical equipment in a compartment isolated from the cabin and to pass a portion of the cabin air through this compartment before exhausting it overboard, the contribution of the electrical load to the cabin cooling load can be reduced. The amount of cabin air required to completely absorb the electrical load is

$$W = \frac{q_e}{0.24(T_{max} - T_c)} \quad (3A-52)$$

where W = Amount of cabin air required to cool electrical equipment, lb/hr

The contribution of the electrical equipment to the cabin cooling load in this case is the transmission heat gain through the equipment compartment walls to the cabin. If the amount of cabin air required by Eq. 3A-52 is not available, the cabin air must be supplemented by additional air, or the cabin air must be cooled before passing it through the equipment compartment.

7. PRACTICAL CONSIDERATIONS IN THE DETERMINATION OF OVERALL HEATING AND COOLING LOADS

An exact analysis of aircraft cooling and heating loads would result in equations and methods of solution that would be impractical to handle except by large digital and analog computers. The prediction of skin temperature alone has been the subject of dozens of technical papers and possibly by as many computer programs.

The temperature distribution in the structure as a result of aerodynamic heating is more complicated than the methods of predicting skin temperature. Usually, in high performance aircraft and missiles, the cooling problem is transient and never reaches a true steady-state condition. Therefore, it must be recognized that the methods presented here have been simplified considerably to reduce the problem to one that can be handled by a hand calculator. This is not to suggest that the methods presented here are of limited value or that a computer must be used to obtain acceptable results.

For subsonic and low supersonic applications, the methods presented here usually are adequate. For missile or high supersonic applications, the methods presented can serve as a preliminary or "first approximation" to the final answer. Usually some preliminary design calculations must be made to estimate system weight and envelope before the design becomes firm enough to conduct a more exact analysis.

7.1 Conditions that Establish Heating and Cooling Loads

Since aircraft operate over a wide range of altitudes, speeds, and ambient conditions, it is necessary to compute the loads for several conditions to establish a complete envelope. The usual procedure is to compute the loads for several altitudes at the maximum and minimum speeds of the aircraft and at the maximum and minimum temperatures expected.

7.1.1 Maximum Flight Condition Requiring Heating

The maximum flight condition requiring heating may be defined as follows:

1. Minimum airplane speed.
2. Cold day.
3. Minimum electrical load.
4. Zero solar load.
5. Minimum crew and passenger load.
6. Minimum temperatures in adjoining compartments.
7. Maximum passenger compartment temperature required for the condition under consideration.

7.1.2 Maximum Flight Condition Requiring Cooling

The maximum flight condition requiring cooling can be defined as follows:

1. Maximum airplane speed.
2. Hot day.
3. Maximum electrical load.
4. Maximum passenger and crew load.
5. Maximum solar load.
6. Maximum temperature in adjoining compartments.
7. Minimum passenger compartment temperature required at the condition under consideration.

7.2 Example of Cooling and Heating Load Calculation

7.2.1 Flight Compartment Details

The flight deck of a hypothetical aircraft to be air conditioned is shown in Fig. 3A-12. The flight compartment is located in the forward section of the upper fuselage and accommodates a total of 12 persons. The fuselage construction in the area of the flight compartment consists of a skin with frames located approximately every 18 in. in station planes. The floor beams run laterally across the fuselage, attaching to the frames. The nominal insulation thickness is 5 in. on the fuselage walls and 3 in. under the floor and attached to the aft bulkhead.

Typical construction details are shown in Figs. 3A-13 through 3A-18. The areas have been computed from detail drawings not shown here for reasons of simplification and space limitations.

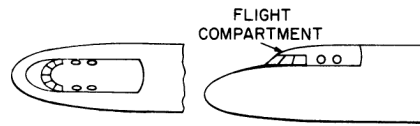


Figure 3A-12 - Flight Compartment to be Air Conditioned

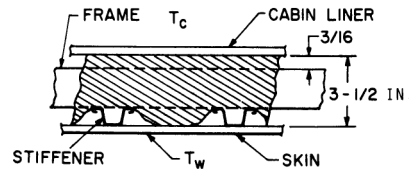


Figure 3A-13 - Construction Details: between Fuselage Frames

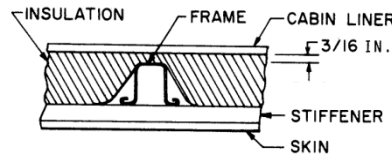


Figure 3A-14 - Construction Details: through Fuselage Frames

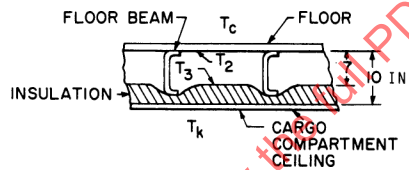


Figure 3A-15 - Construction Details: between Floor Beams

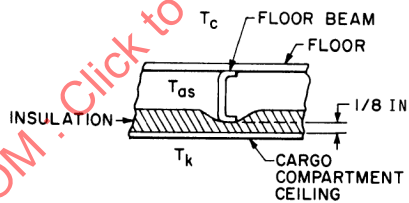


Figure 3A-16 - Construction Details: through Floor Beams

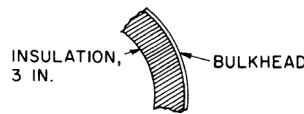


Figure 3A-17 - Construction Details: through Pressure Bulkhead

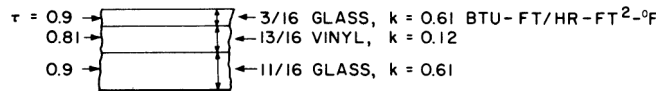


Figure 3A-18 - Construction and Thermal Details: Windshield

7.2.2 Flight and Ambient Conditions

The loads will be computed at the sea level static condition and at the 20,000 ft flight condition (see Table 3A-1). In a complete analysis, the loads would be computed at several altitudes as noted in Par. 7.1.

7.2.3 Determination of Overall Heat Transfer Coefficients

The values of conductivity, emissivity, and other physical properties used to compute overall values of heat transfer coefficients may be obtained from AIR1168/9. However, when the loads were computed, that AIR was not available, so values were obtained from various sources and may not agree with values included in AIR 1168/9.

7.2.3.1 Between Fuselage Frames

This construction is detailed in Fig. 3A-13. The 5 in. blanket is compressed to a maximum of 3.5 in. with an average of 3.25 in. (0.271 ft), considering the stiffeners. The inside coefficient, h_i , is computed from Eq. 3A-25 at an assumed inside velocity of 3.3 ft/sec:

$$h_i = 2.0 + 0.314V_o = 3.04 \text{ Btu/hr-ft}^2\text{-}^\circ\text{F}$$

The resistance to heat flow of the metal cabin liner and outer skin in flight can be neglected in comparison with the resistance of the film and insulation. The overall conductance may be computed from Eq. 3A-24:

Table 3A-1 - Load Values at Sea Level and 20,000 Ft

Case	Condition	Altitude Ft	T_o , °R (1)	Mach No.	T_r , °R (2)	T_w , °R (2)
A	Heating	20,000	407.7	0.28	412.4	412.4
B	Heating	0	400	0	---	(3)
C	Cooling	20,000	488.3	0.89	558.5	558.5
D	Cooling	0	560	0	---	580.0 (4)

NOTES:

1. T_o = Ambient static temperature, assumed to be Standard less 40°F for heating and Standard plus 40°F for cooling except sea level heating, which is -60°F.
2. T_r = Recovery temperature = T_w = skin temperature computed from Eq. 3A-43 with $r = 0.90$.
3. For sea level heating conditions, skin temperature is not required (Par. 3.2.1.1).
4. Skin temperature for ground static cooling computed by methods of Par. 4.3. (See Par. 7.2.6.)
5. k assumed to be .0185 typical of a glass fiber insulation. Specification sheet of insulation to be used should be consulted. Note that "k" will vary with density, so that compressed insulation will have a different value than the same insulation that is not compressed.

$$\begin{aligned}
 U &= \frac{1}{(x/k) + (1/h_i)} \\
 &= \frac{1}{(0.271/0.0185) + (1/3.04)} \\
 &= 0.067 \text{ Btu/hr-ft}^2\text{-}^\circ\text{F}
 \end{aligned}$$

7.2.3.2 Through Fuselage Frames

Details are shown in Fig. 3A-14. The insulation is compressed to 3/16 in. (0.0156 ft) over the frame. The frame is assumed to be at the skin temperature T_w :

$$\begin{aligned}
 U &= \frac{1}{(0.0156/0.0185) + (1/3.04)} \\
 &= 0.853 \text{ Btu/hr-ft}^2\text{-}^\circ\text{F}
 \end{aligned}$$

7.2.3.3 Between Floor Beams

Fig. 3A-15 represents details of this construction.

$$U_{ck} = \frac{1}{\frac{1}{h_i} + \frac{x}{k} + \frac{1}{h'_c + h_r} + \frac{1}{h_i}} \quad (3A-53)$$

Since there is a dead air space between the floor and the cargo compartment ceiling, the conductance is a function of the surface temperature of the air space and may be computed by the methods described in Par. 3.2.3.

For the 20,000 ft heating case (case A) the cabin is maintained at 70°F and the cargo compartment at 45°F. Assume $h'_c + h_r = 0.32$. Then

$$U_{ck} = \frac{1}{\frac{1}{3.04} + \frac{0.25}{0.0183} + \frac{1}{0.32} + \frac{1}{3.04}} \\ = 0.0575 \text{ Btu/hr-ft}^2\text{-}^\circ\text{F}$$

$$U_{c2} = \frac{1}{(1/h_i)} = 3.04 \text{ Btu/hr-ft}^2\text{-}^\circ\text{F}, \text{ ignoring floor resistance}$$

$$U_{k3} = \frac{1}{\frac{1}{3.04} + \frac{0.25}{0.0183}} \\ = 0.0717 \text{ Btu/hr-ft}^2\text{-}^\circ\text{F}$$

(ignoring frame fin effect which is accounted for in Par. 7.2.3.4).

The surface temperatures may be computed from Eqs. 3A-28 and 3A-29.

$$T_2 = T_c - \frac{U_{ck}}{U_{c2}} (T_c - T_k) \\ = 530 - \frac{0.0575}{3.04} (530 - 505) \\ = 529.5^\circ\text{R}$$

$$\begin{aligned}
 T_3 &= T_k + \frac{U_{ck}}{U_{k3}}(T_c - T_k) \\
 &= 505 + \frac{0.0575}{0.0717}(530 - 505) \\
 &= 525^\circ\text{R}
 \end{aligned}$$

$$T_{av} = 527.25^\circ\text{R}$$

$$\Delta T = (T_2 - T_3) = 4.5^\circ\text{R}$$

$\rho = .0765 \text{ lb/ft}^3$ (for cabin air density, a sea level cabin is assumed here)

$$\begin{aligned}
 N_{Gr} &= \frac{x^3 \rho^2 g \beta \Delta T}{\mu^2} \\
 &= \frac{(0.583)^3 (0.0765)^2 (32.2) \left(\frac{1}{527.25} \right) (4.5)}{(12.2 \times 10^{-6})^2} \\
 &= 2,141,000
 \end{aligned}$$

$$\frac{h'_c x}{k} = 8.7 \text{ (for horizontal air spaces; from Fig. 3A-4)}$$

$$\begin{aligned}
 h'_c &= \frac{(0.0147)(8.7)}{0.583} \\
 &= 0.219 \text{ Btu/hr-ft}^2\text{-}^\circ\text{F}
 \end{aligned}$$

The radiation coefficient, h_r , is obtained from Fig. 3A-5 as a function of the surface temperatures and $F_a F_e$:

$$\frac{h_r}{F_a F_e} = 1 \text{ for } T_2 = 529.5^\circ\text{R} \text{ and } T_3 = 525^\circ\text{R}$$

For this case, $F_a = 1$, $e_2 = 0.10$, $e_3 = 0.8$, and

$$\begin{aligned}
 F_e &= \frac{1}{(1/e_2) + (1/e_3) - 1} \\
 &= \frac{1}{(1/0.10) + (1/0.8) - 1} \\
 &= 0.098
 \end{aligned}$$

$$\begin{aligned}
 \text{Then } h_r &= (1)F_a F_e = (1)(1)(0.098) \\
 &= 0.098 \text{ Btu/hr-ft}^2\text{-}^\circ\text{F}
 \end{aligned}$$

$$\begin{aligned}
 h'_c + h_r &= 0.219 + 0.098 \\
 &= 0.3165 \text{ Btu/hr-ft}^2\text{-}^\circ\text{F}
 \end{aligned}$$

This is close enough to the assumed value of 0.32; therefore, the overall conductance is

$$U_{ck} = 0.0575 \text{ Btu/hr-ft}^2\text{-}^\circ\text{F}$$

For the 20,000 ft cooling case (case C), the cabin is maintained at 70°F and the cargo compartment is assumed to be at the skin temperature of 98.5°F. The difference in cabin and cargo compartment temperature is 28.5°F for this case, compared with 25°F for the heating case. Therefore the values of h'_c , h_r , and the overall conductance are the same for each case. For the sea level heating case (case B), the cabin is maintained at 70°F and the cargo compartment is assumed to be at the outside ambient temperature of -60°F. Computations for this case show that

$$h'_c + h_r = 0.474 \text{ Btu/hr-ft}^2\text{-}^\circ\text{F}$$

$$\text{and } U_{ck} = 0.061 \text{ Btu/hr-ft}^2\text{-}^\circ\text{F}$$

Note that an increase of $(h'_c + h_r)$ of 48% results in an increase of U_{ck} of only 6%. Therefore, the larger value of $U_{ck} = 0.061$ will be used in all calculations.

7.2.3.4 Through the Floor Beams

For construction details, see Fig. 3A-16. Heat transfer through the floor beams is complex, since the beam ends are attached to the outer skin and are therefore at approximately skin temperature. Heat is transferred through the beam ends to or from the cargo compartment and the cabin.

In the following analysis, the beam extends to the centerline of the airplane and is considered as a fin with one end at skin temperature. Weighted averages are used to determine the equivalent temperature at which heat transfer takes place, the conductance of the fin surface, and the percentage of heat transferred from the cabin.

Table 3A-2 shows the average temperature and heat transfer coefficients to use in the fin equation.

In addition to values of Table 3A-2, other considerations are

- (1) Cabin temperature $t_c = 70^\circ\text{F}$, or $T_c = 530^\circ\text{R}$ (case A)
- (2) Cargo compartment temperature $t_k = 45^\circ\text{F}$, or $T_k = 505^\circ\text{R}$
- (3) Skin temperature $t_w = -47.6^\circ\text{F}$

The weighted average temperature t_{eff} and the conductance h_{eff} to use in the fin equation are

$$t_{eff} = \frac{UA t}{UA} = \frac{1018}{18.69} = 54.6^\circ\text{F}$$

$$h_{eff} = \frac{UA t}{At} = \frac{1018}{513.9} = 2 \text{ Btu/hr-ft}^2\text{-}^\circ\text{F}$$

Table 3A-2 - Values for Temperature and Heat Transfer Coefficient

	Area (1) ft ²	U	t(4) °F	UA t	UA	At
Beam Top	0.468	3.04	70	100	1.42	32.8
Beam Bottom	0.468	0.86 (2)	45	18	0.40	21.1
Beam Sides	8.430	2.00 (3)	53.3 (5)	900	16.87	460
Total				1018	18.69	513.9

NOTES:

(1) Areas obtained from detail drawings.

$$(2) U = \frac{1}{(1/3.04) + (0.0104/0.012)} = 0.86 \text{ Btu/hr-ft}^2\text{-}^\circ\text{F}$$

(3) $h = 2.0 + 0.314V_o = 2.0$ (Eq. 3A-25 at zero velocity).

(4) Temperature to which heat transfer takes place.

(5) Initially assumed and checked during analysis.

From Eq. 3A-41 (modified), the total heat transfer from the beam end is

$$q_t = Ch_{eff}L\eta_f(t_w - t_{eff})$$

where

$$\eta_f = \frac{\tanh m_f L}{m_f L}$$

and

$$m_f = \left[\frac{h_{eff}C}{kA} \right]^{1/2}$$

Substituting the following information obtained from detail drawings:

$C =$ Perimeter of fin, ft = 2.16

$L =$ Projection of fin into cabin, ft = 4.5

$A =$ Conduction cross-sectional area, ft² = 0.00812

Using $k = 70$ Btu-ft/hr-ft²-°F,

$$m_f L = (2.79)(4.5) = 12.52$$

$$\eta_f = \frac{\tanh 12.52}{12.52} = \frac{1}{12.52} = 0.0798$$

$$q_t = (2.16)(2)(4.5)(0.0798)(t_w - t_{eff})$$

$$= 1.55(t_w - t_{eff})$$

To check the initial assumption of 53.3°F for the temperature of the airspace, assume that the heat transferred from the air space to the beam came initially from the cabin, since the insulation limits heat transfer between the cargo compartment and the air space. Assume also that the ratio of heat flow from the air space to the total heat flow is the ratio of the UA_t value of the sides of the beam to the total UA_t value (see values in Table 3A-2).

$$\frac{q_{as}}{q_t} = \frac{900}{1018} = 0.884$$

$$q_{as} = (0.884)(1.55)(-47.6 - 54.6)$$

$$q_{as} = -142 \text{ Btu/hr-beamend}$$

Since this heat must first pass through the floor to the air space, the required air space temperature to transfer the heat may be computed. The area between the beams is 6.75 ft².

$$\begin{aligned}
 U_{\text{floor}} &= \frac{1}{(1/3.04) + (1/2)} \\
 &= 1.204 \text{ Btu/hr-ft}^2\text{-}^\circ\text{F} \\
 UA &= (1.204)(6.75) = 8.15 \\
 q_{\text{as}} &= UA(t_c - t_{\text{as}}) \\
 \text{or } t_{\text{as}} &= 70 - \frac{142}{8.15} = 52.6^\circ\text{F}
 \end{aligned}$$

which is close enough to the assumed temperature of 53.3 °F.

The total heat flow from the cabin, including that through the top of the beam, may be determined from the UA ratio:

$$\begin{aligned}
 \frac{q_{\text{cb}}}{q_t} &= \frac{1000}{1018} = 0.982 \\
 q_{\text{cb}} &= (0.983)(1.55)(-47.6 - 54.6) \\
 &= -157.3 \text{ Btu/hr-beam end}
 \end{aligned}$$

Since there are 44 beam ends, the total heat flow from the cabin is

$$\text{Total } q_{\text{cb}} = 44(-157.3) = -6922 \text{ Btu/hr}$$

A similar analysis for all design points considered in this example problem gives the results summarized in Table 3A-3.

Table 3A-3 - Results of Analysis

Case	Condition	Altitude, ft	q , Btu/hr
A	Heating	20,000	-6922
B	Heating	0	-7709
C	Cooling	20,000	1633
D	Cooling	0	2838

7.2.3.5 Through the Pressure Bulkhead

For the bulkhead shown in Fig. 3A-17, the following equation is used:

$$\begin{aligned}
 U &= \frac{1}{(1/h_i) + (x/k) + (1/h_i)} \\
 &= \frac{1}{\frac{1}{3.04} + \frac{0.25}{0.0183} + \frac{1}{3.04}} = 0.07 \text{ Btu/hr-ft}^2\text{-}^\circ\text{F}
 \end{aligned}$$

7.2.3.6 Through the Windshield

Fig. 3A-18 gives the data applicable to the windshield computation:

$$\begin{aligned}
 U &= \frac{1}{(1/h_i) + \sum (x/k)} \\
 &= \frac{1}{\frac{1}{3.04} + \frac{0.0729}{0.61} + \frac{0.0673}{0.12}} \\
 &= 0.99 \text{ Btu/hr-ft}^2\text{-}^\circ\text{F}
 \end{aligned}$$

7.2.4 Solar Heat Transmission Through the Windshield

The solar heat transmission is included only in the cooling load calculations. It is assumed that a maximum of one-half the glass area is normal to the sun's rays at one time. Overall solar transmissivity values for the windshield are shown in Fig. 3A-18. The heat gain may be computed from Eq. 3A-50.

$$\begin{aligned} \text{At 20,000 ft, } q_s &= (\tau_1)(\tau_2)(\tau_3)G_s A_p \\ &= (0.9)(0.81)(0.9)(430)(15) \\ &= 4240 \text{ Btu/hr} \end{aligned}$$

$$\begin{aligned} \text{At sea level, } q_s &= (0.9)(0.31)(0.9)(360)(15) \\ &= 3550 \text{ Btu/hr} \end{aligned}$$

7.2.5 Internal Heat Sources

7.2.5.1 Passenger Load

The sensible heat generation of the passengers is 300 Btu/hr-person, and the latent heat is 100 Btu/hr-person as obtained from Figs. 3A-10 and 3A-11 for curve *D*. For the cooling load calculation, it is assumed that 12 persons are in the compartment, and for the heating load calculation, it is assumed that 7 persons are present. Results are shown in Table 3A-4.

Table 3A-4 - Passenger Heat Generation

Condition	Sensible Heat, Btu/hr	Latent Heat, Btu/hr
Heating	2100	
Cooling	3600	1200

7.2.5.2 Equipment Load

Electrical equipment installed in the cabin consumes 1700 watts of power (defined as *E*, watts) that contribute directly to the cabin load. The remainder of the electrical equipment is installed in a separate rack with special cooling provisions. In computing the cooling load, it is assumed that 100% of the equipment is operating. In computing the heating load, it is assumed that 50% of the equipment is operating.

$$\begin{aligned} q_e &= 3.415 E \\ &= 3.415(1700) = 5800 \text{ Btu/hr(Cooling)} \\ &= 3.415(1700/2) = 2900 \text{ Btu/hr(Heating)} \end{aligned}$$

where q_e = Heat load due to electrical equipment, Btu/hr

7.2.6 Estimation of Skin Temperature for the Ground Static Cooling Case

The skin temperature for the ground static cooling case may be determined by the method shown in Par. 4.3. The weighted average value of the fuselage heat transfer coefficient will be used to determine an average skin temperature (see Table 3A-5).

$$U_{av} = \frac{89.7}{750} = 0.119 \text{ Btu/hr-ft}^2\text{-}^\circ\text{F}$$

For an assumed wind velocity, V_o , of 5 mph (7.4 fps), compute h_o from Eq. 3A-25:

Table 3A-5 - Average Values of Heat Transfer Coefficient

	<i>U</i>	<i>A</i>	<i>UA</i>
Through Fuselage Frames (Par. 7.2.3.2)	0.853	50	42.7
Between Fuselage Frames (Par. 7.2.3.1)	0.067	700	46.9
Total		750	89.6

$$h_o = 2.0 + 0.314(7.4) = 4.3 \text{ Btu/hr-ft}^2\text{-}^\circ\text{F}$$

From Fig. 3A-9, assuming $e_w = 0.1$, $T_c = 530^\circ\text{R}$, and $T_o = 500^\circ\text{R}$,

$$B = \frac{560(4.3) + (360/\pi) + 0.119(530) + 82.96(0.1)}{0.119 + 4.3} = 587^\circ\text{R}$$

$$C = \frac{0.173 \times 10^{-8}(0.1)}{0.119 + 4.3} = 0.039 \times 10^{-9} \text{ }^\circ\text{R}^{-3}$$

Substituting into Eq. 3A-48:

$$T_w = 580^\circ\text{R} \text{ or } t_w = 120^\circ\text{F}$$

7.2.7 Adjustment of Overall Heat Transfer Coefficients to Account for Outside Film Coefficient

At sea level, with the aircraft at zero velocity, and a wind present, the outside film coefficient must be considered because it has a significant effect on heat transfer. The method of accounting for this additional resistance is demonstrated below for the U value for heat flow through fuselage frames computed in Par. 7.2.3.2.

Assume a 15 mph (22 fps) velocity and compute h_o from Eq. 3A-25:

$$\begin{aligned} h_o &= 2.0 + 0.314(22) \\ &= 8.9 \text{ Btu/hr-ft}^2\text{-}^\circ\text{F} \\ U_{\text{overall}} &= \frac{1}{(1/U_{wc}) + (1/h_o)} \\ &= \frac{1}{(1/0.853) + (1/8.9)} \\ &= 0.778 \text{ Btu/hr-ft}^2\text{-}^\circ\text{F} \end{aligned}$$

The remaining heat transfer coefficients are adjusted in the same way.

7.2.8 Summary of Loads

Since several of the heat flow paths transfer heat across the same ΔT , the UA values may be added, as shown in Table 3A-6. The load for the 20,000 foot heating case is shown in Table 3A-7. A similar computation for the other three cases gives total loads as summarized in Table 3A-8.

Table 3A-6 - Summation of UA Values

Description	<i>U</i>	<i>A</i>	<i>UA</i>	ΔT
Between Fuselage Frames	0.067	700	46.9	$T_w - T_c$
Through Fuselage Frames	0.853	50	42.7	$T_w - T_c$
Through the Pressure Bulkhead	0.07	100	7.0	$T_w - T_c$
Through the Windshield	0.99	30	29.7	$T_w - T_c$
Total			126.3	$T_w - T_c$

¹For the ground static heating case, this total is 109 because of the added resistance of the outer film. Also for this case, the $\Delta T = (T_o - T_c)$, where T_o is ambient temperature.

Table 3A-7 - Heating Load at 20,000 Ft

	UA Btu/hr-°F	ΔT^1 °F	q Btu/hr
Transmission Loads			
(1) Fuselage, Pressure			
Bulkhead, Windshield	126.3	-117.6	-14,847
(2) Between Floor Beams	12.2	-25	-305
(3) Through Floor Beams			-6922
Solar Load			
Passenger Load			2,100
Equipment Load			<u>2,900</u>
Total			-17,074

$$^1(T_w - T_o) = 412.4 - 530 = -117.6^\circ\text{F}$$

$$(T_k - T_o) = 505 - 530 = -25^\circ\text{F}$$

Table 3A-8 - Heating and Cooling Loads at Sea Level and 20,000 Ft Altitude

Case	Condition	Altitude, ft	q , Btu/hr
A	Heating	20,000	-17,074
B	Heating	0	-19,784
C	Cooling	20,000	20,417
D	Cooling	0	21,653

8. EXAMPLE OF SKIN TEMPERATURE COMPUTATION AT HIGH MACH NUMBER

The method shown in Par. 4.2 is used to determine the skin temperature of an aircraft at the following flight condition:

- Altitude = 70,000 ft
- Ambient temperature, $T_o = 390^\circ\text{R}$
- Ambient pressure, $P_o = 92.63 \text{ lbf/ft}^2$
- Mach number, $M = 7$, dimensionless
- Overall wall conductance, $U = 0.10 \text{ Btu/hr-ft}^2\text{-}^\circ\text{F}$
- Emissivity of outer skin, $e_w = 0.80$, dimensionless
- Cabin temperature, $T_c = 530^\circ\text{R}$
- Distance from origin of boundary layer, $x = 10 \text{ ft}$

As a first approximation, assume that free stream conditions exist at the edge of the boundary layer. For a more accurate analysis, these latter conditions should be based on values calculated by considering the properties of the flow field behind the body shock wave system. Assume the skin temperature $T_w = 1970^\circ\text{R}$. Then, from Eq. 3A-45,

$$\begin{aligned}
 h_o(T_r - T_w) &= -0.25 \frac{430}{\pi} + U(T_w - T_c) + 0.173e_w \left(\frac{T_w}{100} \right)^4 - 58.52e_w \\
 &= -0.25 \frac{430}{\pi} + 0.10(1970 - 530) + 0.173(0.8)(19.7)^4 - 58.52(0.8) \\
 &= -34.2 + 144 + 20,800 - 46.8 \\
 &= 20,863 \text{ Btu/hr} \cdot \text{ft}^2
 \end{aligned}$$

Note that only the third term at the right side of the preceding equation is significant, and thus is usually the only term computed.

By the method shown in Par. 3.1.2.1, compute the convective heat flux to be compared with that computed from Eq. 3A-45:

$$\begin{aligned}
 T^* &= 0.5(T_w + T_o) + 0.22 \left(\frac{\gamma - 1}{2} \right) M^2 T_o r \\
 &= 0.5(1970 + 390) + 0.22(0.2)(7)^2(390)(0.9) \\
 &= 1935^\circ \text{R}
 \end{aligned} \tag{3A-54}$$

$$\begin{aligned}
 \rho^* &= \frac{P}{RT^*} \\
 &= \frac{92.63}{53.3(1935)} = 0.000898 \text{ lb/ft}^3
 \end{aligned} \tag{3A-55}$$

$$\begin{aligned}
 V_o &= cM = 49\sqrt{T_o}M \text{ (where } c = 49\sqrt{T} \text{ in general)} \\
 &= 49\sqrt{390}(7) = 6780 \text{ ft/sec}
 \end{aligned}$$

$$\begin{aligned}
 N_{Re}^* &= \frac{V_o \rho^* x}{\mu^*} \\
 &= \frac{(6780)(0.000898)(10)}{0.0000292} \\
 &= 2,085,000
 \end{aligned} \tag{3A-56}$$

$$\begin{aligned}
 \frac{f^*}{2} &= \frac{0.0296}{(N_{Re}^*)^{0.2}} \\
 &= \frac{0.0296}{(2,085,000)^{0.2}} = 0.00162
 \end{aligned} \tag{3A-57}$$

$$\begin{aligned}
 h_o &= \frac{\rho^* V_o c_p^* (f^*/2)}{(N_{Pr}^*)^{0.667}} (3600) \\
 &= \frac{(0.000898)(6780)(0.251)(0.00162)(3600)}{(0.715)^{0.667}} \\
 &= 11.18 \text{ Btu/hr} \cdot \text{ft}^2 \cdot ^\circ \text{F}
 \end{aligned} \tag{3A-58}$$

$$\begin{aligned} T_r &= T_o \left[1 + r \left(\frac{\gamma - 1}{2} \right) M^2 \right] \\ &= 390 [1 + (0.9)(0.2)(7)^2] \\ &= 3830^\circ\text{R} \end{aligned} \tag{3A-59}$$

$$\begin{aligned} q_c &= h_o A (T_r - T_w) \\ &= 11.18(1)(3830 - 1970) \text{ (for } A = 1 \text{ ft}^2\text{)} \\ &= 20,800 \text{ Btu/hr-ft}^2 \end{aligned} \tag{3A-60}$$

Since the convective heat flux computed from Eq. 3A-60 is equal to that computed from Eq. 3A-45, the assumed skin temperature of 1970°R is correct. If the heat flux values were not equal, it would be necessary to assume a different skin temperature and recalculate the heat flux until a balance was obtained.

9. REFERENCES

1. W. L. Torgeson, H. C. Johnson, and N. B. Wright, Jr., "Engineering Study of Air Conditioning Load Requirements for Aircraft Compartments," WADC Technical Report 55-254, June 1955.
2. "Heating, Ventilating, and Air Conditioning Guide," ASHRAE, 1951.
3. M. Jakob, Heat Transfer, Vol. I. John Wiley & Sons, Inc., 1949.
4. Handbook of Instructions for Aircraft Designers, ARDC Manual No. 80-1.
5. E. R. G. Eckert, "Survey on Heat Transfer at High Speeds," WADC Technical Report 54-70.
6. J. R. Woolf and L. R. Scott, "Influence of Through Metal on Heat Transfer Through Aircraft Structural Sandwich Panels," ASME Paper 56-SA-23.
7. Department of Defense Joint Services Specification Guide, JSSG-2009, Air Vehicle Subsystems.

SAENORM.COM : Click to view the full PDF of air1168-3b

SECTION 3B - REFRIGERATION SYSTEM DESIGN**1. INTRODUCTION****1.1 Scope**

The major air conditioning task for missiles and aircraft is solving the various cooling problems that arise from high speed flight; that is, the dissipation of heat that is generated within and external to the aircraft or missile. Of almost equal importance in most applications is the availability of ground cooling. Heat must be transferred from the heat sources to a heat sink, outside or within the aircraft. Since in most cases some type of heat pump is necessary, the mechanical energy into the pump that is converted into heat must also be dissipated into the heat sink.

It must be kept in mind that each aircraft or missile air conditioning application requires a system designed especially for the cooling loads and temperature levels peculiar to that aircraft or missile, and its mission.

1.1.1 Heat Sources

Heat sources may be grouped into two categories:

1. External Heat Sources - From aerodynamic heating and heat received through solar radiation, even though a major portion of this heat is prevented from being transferred into the aircraft interior by the use of thermal insulation.
2. Internal Heat Sources - From heat generated within the aircraft by electronic, electrical, and mechanical equipment, and people.

1.2 Nomenclature

COP = Coefficient of performance, dimensionless

c_p = Specific heat capacity, constant pressure, Btu/lb-°F

E = Electromotive force, volts (V)

g = Gravitational acceleration, ft/sec²

g_c = Gravitational constant, 32.2 lb-ft/lbf-sec²

Δh = Difference in enthalpy between 2 points, Btu/lb

h_{stag} = Specific enthalpy at stagnation temperature, Btu/lb

h_{stat} = Specific enthalpy at static temperature, Btu/lb

I = Current, amperes (A)

J = Mechanical equivalent of heat, 778 ft-lbf/Btu

k = Specific heat ratio, C_p/C_v , dimensionless

M_o = Mach number, dimensionless

P = Power, watts (W)

p = Pressure, lbf/in.²

Q = Heat energy, Btu

q	= Rate of heat transfer, Btu/min
R	= Universal gas constant, ft-lbf/lb-°R
T	= Temperature, °R
t	= Temperature, °F
Δt	= Temperature difference, °F
V	= Velocity, ft/sec
W	= Work, ft-lbf
w	= Mass flow rate, lb/min
η_c	= Compressor efficiency, dimensionless
η_t	= Turbine efficiency, dimensionless
η_x	= Heat exchanger effectiveness, dimensionless
η_{sep}	= Water separator efficiency, dimensionless
τ	= time, min

Subscript

a	= air
f	= fluid

1.3 Common Abbreviations

A	— Amperes
AC	— Alternating current
Aircraft Eng.	— Aircraft Engineering
approx	— Approximately
ASME	— American Society of Mechanical Engineers
Btu	— British thermal unit
cab	— Cabin
cfm, ft ³ /min	— Cubic feet per minute
comp.	— Compressor
cond	— Condenser
COP	— Coefficient of performance
DC	— Direct Current

eff	— Efficiency
el motor	— Electric motor
emf	— Electromotive force
Eq.	— Equation
evap	— Evaporator
°F	— Degrees Fahrenheit
Fig.(Figs.)	— Figure(s)
fpm, ft/min	— Feet per minute
fps, ft/sec	— Feet per second
ft	— Feet
ft ³ /min	— Cubic feet per minute
HE	— Heat exchanger
hp	— Horsepower
hr	— Hour
in.	— Inch
lb	— Pound mass
lbf	— Pound force
lbf/in. ²	— Pounds force per square inch
min	— Minute
min	— Minimum
mm	— Millimeter
mph, miles/hr	— Miles per hour.
NACA	— National Advisory Committee for Aeronautics
no.	— Number
%	— Percent
Par.(Pars.)	— Paragraph(s)
Press.	— Pressure
psi	— Pounds force per square inch
psia	— Pounds force per square inch absolute

psig	— Pounds force per square inch gage
R	— Electrical resistance
°R	— Degrees Rankine
Ref.	— Reference
Refrig.	— Refrigerant
sat	— Saturated
sec	— Second
sep	— Separator
std.	— Standard
temp.	— Temperature
turb	— Turbine
V	— Volts
W	— Watts
μ	— Micron (10^{-6} meter)
Δ	— Difference
Ω	— Ohms

1.4 Definitions of Available Heat Sinks

Available heat sinks for an aircraft or missile are:

Outside (Ambient) Air - This may be either ram air or bleed air from main engines. Any air taken aboard for use as a heat sink is at the stagnation (total) temperature. A plot of air heat sink temperatures versus Mach number is shown in Fig. 3B-1. An expansion turbine may be used to expand, and thus decrease, the temperature of ram air taken aboard (see Fig. 3B-1), however ram air expansion turbines are large and heavy. The necessity of rejecting heat at high temperature levels as aircraft speeds increase requires a more complex heat pump configuration.

Fuel - Utilization of the sensible heat or the latent heat of vaporization of fuel produces a low system penalty, since fuel is carried onboard for propulsive and auxiliary power purposes regardless of cooling applications. However, appreciable problems are associated with the use of fuel as a heat sink. Some of these are:

1. Fuel flow management and priority control of engines may not correspond with air conditioning requirements.
2. Fuel temperature limits of 250-300 °F are imposed to prevent fuel “gumming.”
3. Use of the fuel sink for other purposes, such as engine oil cooling, may preclude its use for air conditioning.
4. Coordination with the engine manufacturer will be necessary during the engine design stage at a time when specific cooling applications for the aircraft may not be known.
5. Fuel tanks must be insulated for high speed flights.

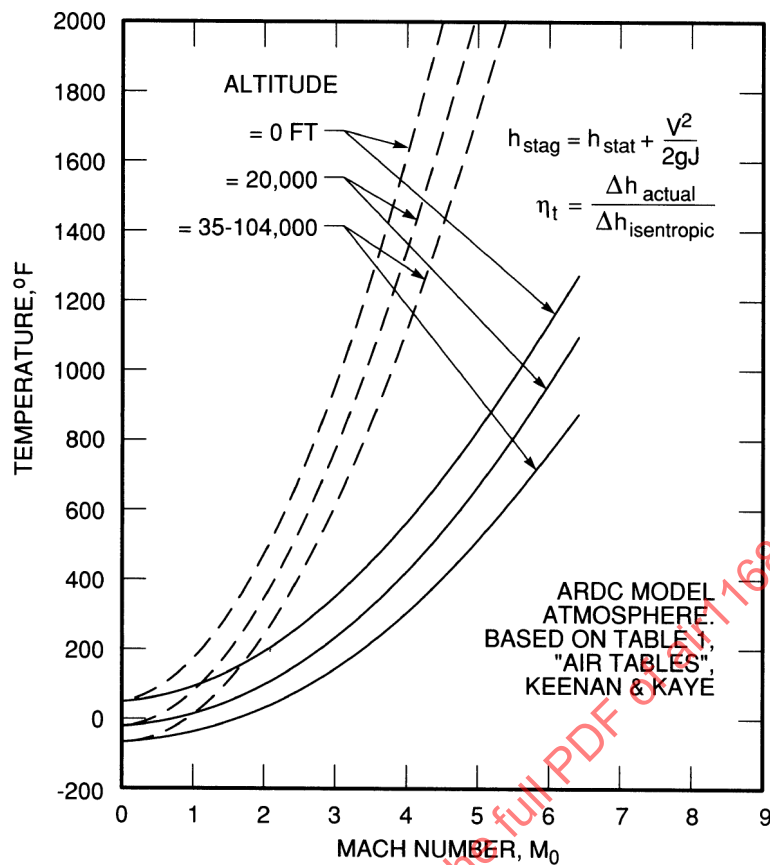


Figure 3B-1 - Outside Air Heat Sink versus Mach Number — Stagnation conditions (total temperature). — Ram air fully expanded (turbine efficiency = 70%)

Expendable Cooling Media - Any substance that may be carried in the aircraft purely for cooling purposes and is eventually discharged overboard. Both sensible heat and latent heat of vaporization are available as heat sinks. Typical expendable coolants: water (best on latent heat and storage volume bases); liquid hydrogen (best on weight basis). Additional advantages are low drag installations and applications to widely dispersed equipment items.

Heat Capacity of Aircraft Structure - Thermal lag cooling utilizing the heat capacity of airplane or missile structures, an application useful for only very short duration flights.

Radiation to Space - Cooling by radiation, utilizing the very low (approximately 50°R) temperature of outer space. This is applicable only at very high altitudes because, below approximately 150,000 ft, aerodynamic heating is much greater than radiation-to-space cooling can handle.

2. AIR CYCLE SYSTEMS

2.1 Basic Considerations and Cycle Components

There are two main types of cooling systems in use today that can be used individually or combined.

1. The air cycle system, which is based on the reduction of heat by the transformation of heat energy into work.
2. The vapor cycle system in which the heat of vaporization is lost by evaporating a liquid refrigerant.

Basically, the air cycle cooling system is supplied with air from an engine-driven compressor or from air bled from the main engine compressor. The air is expanded through an air turbine that drives a compressor or fan, thus converting heat energy into useful work.

For low speed flight, integrated cooling and pressurization requirements for cabin cooling can be met advantageously by air cycle systems. As a result, most propeller driven and many jet transports use air cycle systems for cooling and pressurization. In spite of generally high power requirements, air cycle equipment is used for cooling to take advantage of the source of pneumatic power from the cabin pressurization compressor. It is essential to employ the minimum air pressure ratio across the cooling turbine, consistent with the needs of cooling and pressurizing, in order to keep the horsepower absorbed by the engine-driven compressor at a minimum.

When engine bleed air is available from the main powerplant, air cycle refrigeration (with or without a supplemental water boiler) is often used because of the simplicity and the inherent compactness of air cycle equipment.

During high speed flight at high altitudes, maximum cooling requirements are coincident with maximum pressurization requirements. In addition, because of the high cooling loads, a cooling system having as high an efficiency as possible is required to minimize power consumption, making available a region of operation for other systems such as the vapor cycle system.

For any application involving a high heat load, the amount of air flow required for cooling is considerable, requiring large diameter ducts and a large ram air drag penalty. If bleed air from a jet engine is used, the high mass flow necessary would result in high fuel penalties. For these reasons the air cycle system has its limitations.

Another limitation of the air cycle system is that frosting in the downstream air ducts can occur if the turbine outlet temperature falls to the freezing point.

Two types of air cycles are possible:

1. Open Cycles - Those in which air is taken continuously from outside the airplane, processed through the cycle components, and then, after absorption of heat, is discharged from the aircraft. The final process where the air reverts to its initial static state often occurs after discharge to free-stream. Therefore the air is replaced continuously.
2. Closed Cycles - Those in which the air is recirculated through the components continuously, being reused much in the same manner as a refrigerant is reused in vapor cycle refrigeration systems.

2.1.1 Carnot Cycle (Standard for Comparison)

The ideal Carnot thermodynamic cycle may be compared with the basic air refrigeration cycles (Joule or reversed Brayton) in which the isothermal heating and cooling processes of the Carnot cycle are replaced by constant pressure processes. The ideal reversed Carnot cycle is the standard used for comparison with actual air cycle refrigeration systems, and is shown in Fig. 3B-2, where points are represented as

- (1) 1-2 = Isothermal expansion; heat absorbed from heat source.
- (2) 2-3 = Reversible adiabatic compression; work into cycle.
- (3) 3-4 = Isothermal compression; heat removed to heat sink.
- (4) 4-1 = Reversible adiabatic expansion; work out.

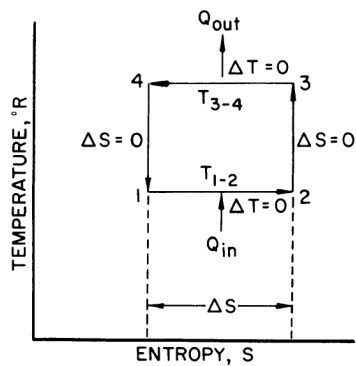


Figure 3B-2 - Reversed Carnot Cycle

The heat equivalent of net work done during a complete cycle is

$$\begin{aligned}
 W_{net} &= Q_{out} - Q_{in} \\
 &= (T_{3-4} - T_{1-2})\Delta S \\
 COP &= \frac{Q_{in}}{Q_{out} - Q_{in}} \\
 &= \frac{T_{1-2}}{T_{3-4} - T_{1-2}} \\
 &= \frac{JQ_{in}}{W_{net}} \quad (3B-1)
 \end{aligned}$$

2.2 Analysis of Basic Air Cycle System

The basic air cycle system (Joule or reversed Brayton cycle) consists of a source of pressurized air, a heat exchanger, and a high speed turbine that drives a fan used to boost the flow of coolant air through the heat exchanger. Three basic high pressure air sources are illustrated in Figs. 3B-3(a), 3B-3(b), and 3B-3(c): ram air supply, bleed air supply, and ram air supply with pressurization compressor, respectively.

Adequate air pressure is required to pressurize the cabin and ensure a pressure drop across the turbine sufficient to provide the amount of cooling required. It is necessary to provide a power absorber for the turbine work, and this is accomplished by augmenting the air flow through the heat exchanger by a fan. This arrangement provides a degree of cooling when the aircraft is on the ground, although it is necessary for the engines to be operated. The arrangements illustrated in Fig. 3B-3 are all open cycles.

In the temperature-entropy diagram of Fig. 3B-3, components (assuming ideal conditions) are represented as follows (cabin pressure is assumed to be at free-stream static):

- (1) 0-1: Ram scoop for induction of outside air (isentropic compression process).
- (2) 1-2: Heat exchanger for cooling incoming air (constant pressure cooling process). Heat sink coolant may be fuel, expendable coolant or ram air.
- (3) 2-3: Turbine for cooling air to a temperature sufficient to absorb heat input of cabin (isentropic expansion process).
- (4) 3-0: Aircraft cabin, heat removal from source (constant pressure heating process). An aircraft cabin is shown in this example, but any other heat source may replace the cabin; that is, electronic equipment, another heat exchanger, or similar source.

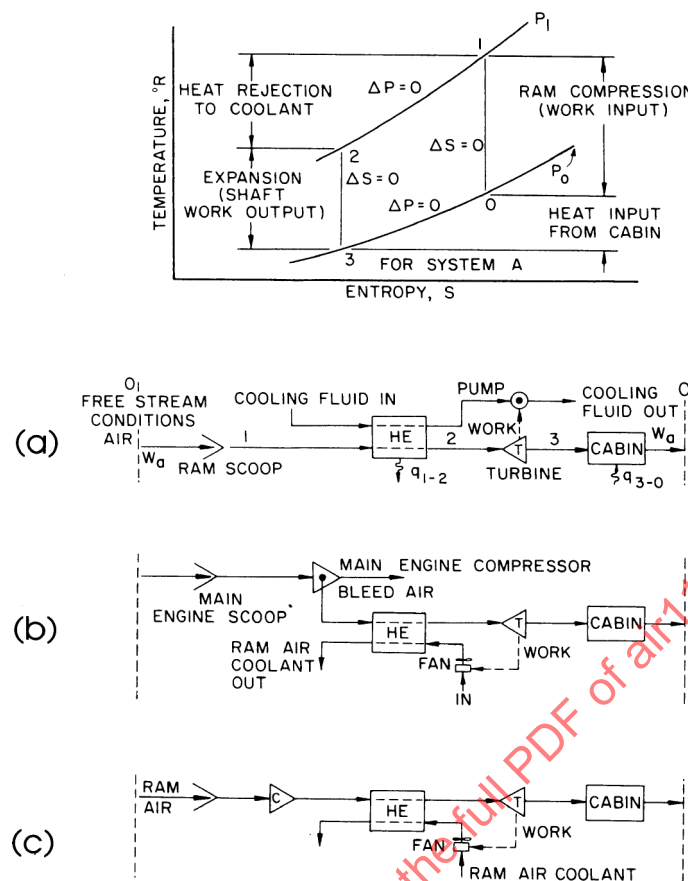


Figure 3B-3 - Basic Open Air Cycle System, (a) Ram air supply; (b) Bleed air supply; (c) Ram air supply with pressurization compressor

2.2.1 General Comments on Basic Air Cycle Systems

1. Cooling capacity is a direct function of the pressure ratio.
2. Cooling capacity above a maximum figure is little affected by an increase in the number of air-to-air heat exchangers (for a given heat sink), since a maximum value of overall heat exchanger effectiveness is reached that cannot be exceeded.
3. When a large amount of moisture is present in the air being cooled, moisture is condensed, and if the discharge temperature from the turbine is low enough, ice is formed. Condensed moisture in the air (fogged air) may also be introduced into the occupied areas of an aircraft. Thus, a moisture separator is usually required with an air cycle system to remove enough moisture to prevent fogging.
4. No matter where condensation of ambient humidity occurs in the cycle, the heat liberated is practically constant.
5. When air is dry, higher component efficiencies are possible, improving cooling capacity. If appreciable amounts of moisture exist, it is necessary to hold the turbine discharge temperatures above the freezing point, and maximum advantage cannot be taken of component efficiencies.
6. If the power absorber for the turbine is not doing useful work and is used only to load the turbine, turbine work ultimately becomes an additional internal heat source of the aircraft and thus ultimately decreases the overall coefficient of performance (COP).
7. In an actual cycle, when component efficiencies and duct losses are taken into account, the coefficient of performance falls off much faster with increasing Mach number when compared with the basic Joule cycle. For a given Mach number, the COP is also much below what would be expected from the ideal Joule cycle.

2.2.2 A Scheme for Utilization of Turbine Shaft Work

In Fig. 3B-4,

$$\text{Flow ratio} = \frac{w'_a}{w_a} \approx 2.0 \quad (3B-2)$$

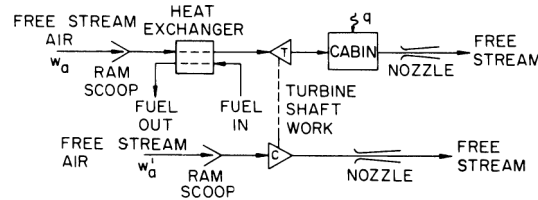


Figure 3B-4 - Simple Air Cycle with Braking Compressor

2.2.3 Summary of Equations

For Fig. 3B-3, equations are as follows:

Work of compression

$$\begin{aligned} &= \text{Kinetic energy input} \\ &= w_a c_p (T_1 - T_0) \tau \\ &= \frac{w_a V_0^2}{2g_c J} = \frac{W_{O-1} / \tau}{J} \end{aligned} \quad (3B-3)$$

Heat rejected to heat sink = q_{1-2}

$$\begin{aligned} &= w_a c_p (T_1 - T_2) \\ &= q_{3-O} + \frac{W_{\text{cycle}} / \tau}{J} \end{aligned} \quad (3B-4)$$

Turbine work output

$$\begin{aligned} &= \text{Work of isentropic expansion} \\ &= w_a c_p (T_2 - T_3) \tau \\ &= \frac{W_{2-3}}{J} \end{aligned} \quad (3B-5)$$

Heat absorbed from cabin (or heat source)

$$\begin{aligned} &= w_a c_p (T_0 - T_3) \\ &= q_{3-O} \end{aligned} \quad (3B-6)$$

$$\begin{aligned} \text{Net cycle work} &= \frac{W_{O-1}}{J} - \frac{W_{2-3}}{J} \\ &= \frac{W_{\text{cycle}}}{J} \end{aligned}$$

Coefficient of performance = COP

$$\begin{aligned}
 &= \frac{\text{Heat extracted}}{\text{Cycle work}} \\
 &= \frac{JQ_{3-0}}{W_{\text{cycle}}} = \frac{T_0}{T_1 - T_0} \\
 &= \frac{T_0}{T_0 \left(\frac{\gamma - 1}{2} \right) M_0^2} = \frac{5}{M_0^2}
 \end{aligned} \tag{3B-7}$$

where T_0 = Freestream static temperature, °R

T_1 = Ram total temperature, °R

A plot of COP versus Mach number is shown in Fig. 3B-5. Note: duct pressure and temperature losses have been neglected.

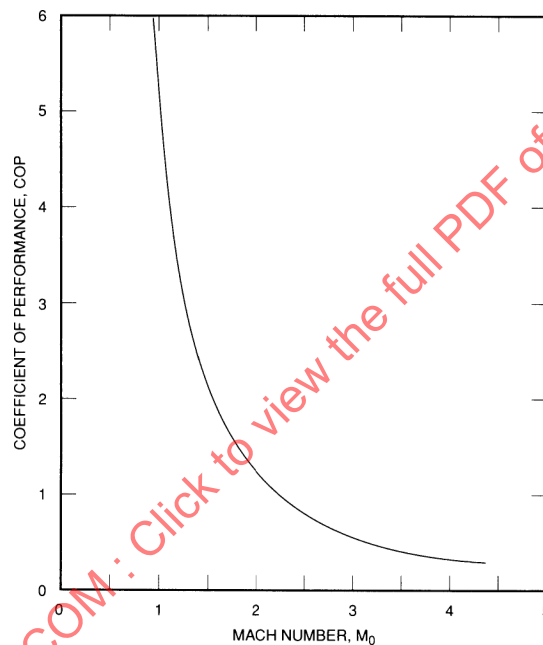


Figure 3B-5 - Coefficient of Performance of Ideal Reversed Joule Cycle (from ram temperature level T_1 to freestream T_0). $COP = T_0 / (T_1 - T_0) = 5 / M_0^2$

2.3 Air Cycle Systems (Open and Closed Circuits)

2.3.1 Bootstrap Cooling Systems

The bootstrap system is based on a cold air unit incorporating a turbine-driven compressor, and is normally used in aircraft where available air pressure levels are limited. Low pressure results in insufficient cooling when using the simple basic air cycle.

By causing the turbine to drive a compressor, which further increases the pressure of the air supplied to the cooling turbine, a higher pressure ratio is achieved with a correspondingly higher temperature drop across the turbine.

A simplified schematic is shown in Fig. 3B-6. Air from the engine-driven compressor, precooled by passing through a primary heat exchanger, is compressed and then passed through another air-to-air heat exchanger (called the secondary heat exchanger or the intercooler), and then enters the turbine where it is expanded to the required cabin pressure. Heat energy is converted into shaft work in the turbine and is used for driving the bootstrap compressor.

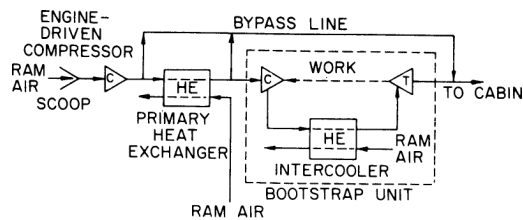


Figure 3B-6 - Bootstrap Cooling System

The primary and the secondary heat exchangers are cooled by ram air in this example, although fuel or other heat sinks could also be used. Air-to-air heat exchangers for bootstrap applications are normally designed with an effectiveness of at least 80%, thus requiring a coolant air flow approximately three times the cabin supply air flow. Bypass lines for temperature control and heating are also shown in Fig. 3B-6.

Applications may also be made to jet aircraft not fitted with engine-driven compressors, since very low bleed pressures are obtained from jet engine compressors operating at very high altitudes. This creates another area for possible bootstrap cooling system applications.

2.3.1.1 General Comments on Bootstrap Systems

Some characteristics are as follows:

1. Bootstrap systems have been used extensively for passenger and crew compartment and equipment cooling.
2. Bootstrap systems improve the performance of the simple cycle system by using the turbine output work for increased compression of the air upstream of the turbine.
3. The system is capable of producing the required amount of refrigeration with reasonable efficiency.
4. The efficiency of the system is increased by the addition of the primary heat exchanger (precooler), utilizing air, fuel, or expendable fluid heat sinks, and further improved by adding a regenerative heat exchanger in series with the precooler.
5. Very little capacity is available for ground cooling, since ram air is lacking for the heat exchangers. Also, main engine operation is required for cooling.
6. For altitude operation, the bootstrap system can provide rated cooling over a wide range of flight conditions.
7. Component matching and pressurization control are relatively easy.
8. The use of ram air in the secondary heat exchanger becomes inadequate at low supersonic speeds (approximately Mach 1.25); therefore, an auxiliary heat sink (fuel or expendable fluid) is required.
9. Since moderate flows are usually passed through the turbine unit, the turbine wheel diameter and nozzle throat areas are small and require high speed operation (approximately 60,000 to 100,000 rpm) in order to obtain the requisite temperature and pressure ratios. The combination of small size and high speed magnifies losses with corresponding low component efficiencies.

2.3.1.2 Summary of Equations for Basic Bootstrap Systems

Equations for Fig. 3B-7 include the following:

Work of compression = Work of expansion

$$\text{Thus } \frac{W_{comp}}{Jw_a c_p} = \frac{W_{turbine}}{Jw_a c_p} \tag{3B-8}$$

$$T_2 - T_1 = T_3 - T_4$$

Input energy of ram compression (per lb)

$$= c_p(T_1 - T_0) = \frac{V_0^2}{2Jg} \tag{3B-9}$$

$$\text{Net work of cycle } \frac{W_{net}}{J} = w_a c_p [(T_2 - T_3) - (T_0 - T_4)] \tau$$

Since turbine work $w_a c_p(T_3 - T_4) =$ Compressor work $w_a c_p(T_2 - T_1)$, the cycle net work is equal to ram compression input energy, or

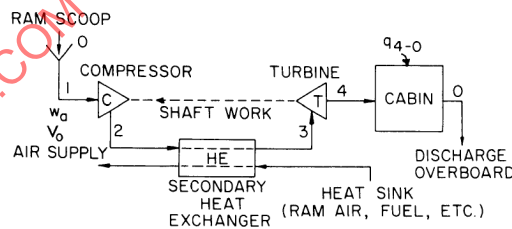
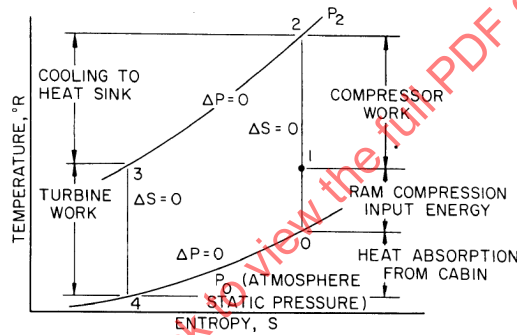


Figure 3B-7 - Ideal Bootstrap Open Circuit System (reversed Brayton cycle)

$$\frac{W_{net}}{J} / \tau = w_a c_p (T_1 - T_0) = \frac{w_a V_0^2}{2Jg_c} \tag{3B-10}$$

Heat absorbed from cabin

$$= q_{4-0}$$

$$= w_a c_p (T_0 - T_4) \tag{3B-11}$$

Heat rejected to heat sink

$$\begin{aligned}
 &= q_{4-0} + \frac{W_{net}}{J} \\
 &= w_a c_p (T_2 - T_3) \\
 &= w_a c_p (T_1 - T_4)
 \end{aligned}
 \tag{3B-12}$$

Coefficient of performance (COP)

$$\begin{aligned}
 COP &= \frac{JQ_{4-0}}{W_{net}} \\
 &= \frac{T_0 - T_4}{T_1 - T_0} \\
 &= 2Jg_c c_p \left(\frac{T_0 - T_4}{V_0^2} \right) \\
 &= \frac{5}{M_0^2} \left(1 - \frac{T_4}{T_0} \right)
 \end{aligned}
 \tag{3B-13}$$

since

$$\begin{aligned}
 T_1 - T_0 &= T_0 \left(\frac{\gamma - 1}{2} \right) M_0^2 \\
 &= \frac{T_0 M_0^2}{5} \text{ for } \gamma = 1.4
 \end{aligned}$$

A plot of COP versus Mach number is shown in Fig. 3B-8 with T_4/T_0 as the parameter.

2.3.1.3 Effect of Connecting Duct Pressure Losses

The comparison of an actual bootstrap system installation with the ideal adiabatic processes is shown in Fig. 3B-9. Note that connecting duct losses have a major effect on the performance of the system. Temperature losses were neglected.

2.3.1.4 Some Bootstrap System Variations

Although many possible bootstrap system variations are possible, two of the more practical are illustrated in Fig. 3B-10. These are:

1. Bootstrap System Utilizing Fuel as the Heat Sink - Because of possible contamination of air supply by the fuel and because of space and location requirements, an intermediate coolant loop between the supply air and the fuel heat sink may be required.
2. Bootstrap System with Precooler and Expendable Coolant Heat Sink - Expendable coolant could be eliminated by substitution of an expanded ram air heat sink, which may be available as a by-product of an auxiliary drive turbine.

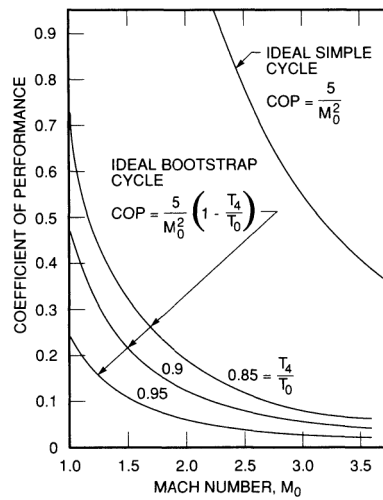


Figure 3B-8 - Comparison of Ideal Bootstrap System with Ideal Simple Air Cycle

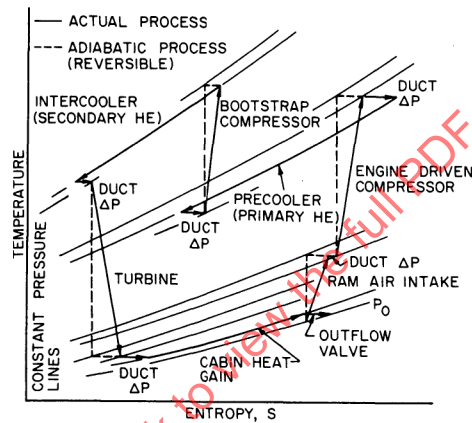


Figure 3B-9 - Actual Bootstrap Cycle Illustrating the Effect of Connecting Duct Pressure Losses

2.3.2 Regenerative Cycle Systems

For operation at Mach numbers greater than 1, the following factors may eliminate the use of either the simple system or the bootstrap system for a particular application:

1. Ram air for the heat exchangers causes a considerable drag penalty.
2. Increased ram air temperatures limits the use of ambient air as a heat sink.
3. At high altitudes, very little air is available for cooling purposes.

The problems raised by high speed and high altitudes may be alleviated greatly by the use of regenerative air cycle systems. This is illustrated in the simplified schematic, Fig. 3B-11, where air for pressurizing the cabin is bled from the jet engine compressor or obtained directly from a ram scoop, and then passed through an air-to-air heat exchanger.

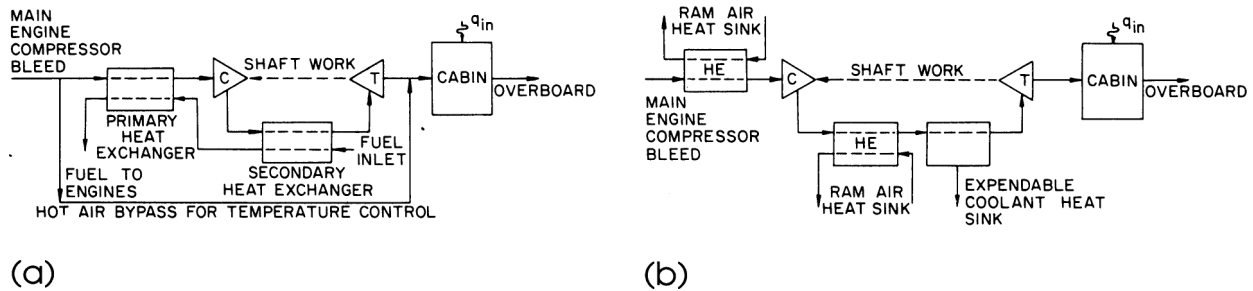


Figure 3B-10 - Bootstrap System Variants, (a) Bootstrap system with pre-cooler and utilizing fuel as the heat sink; (b) System with pre-cooler and expendable coolant heat sink

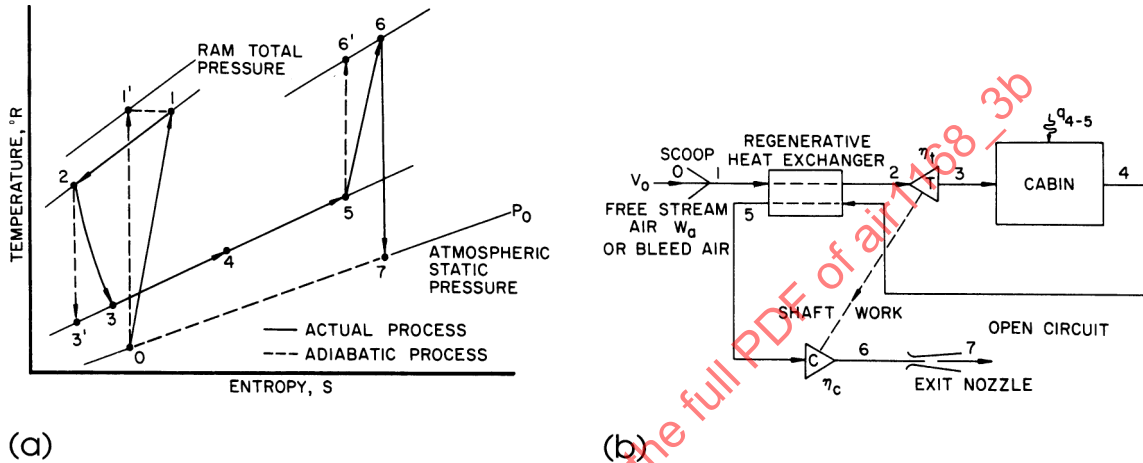


Figure 3B-11 - Ideal Regenerative Air Cycle System; complete utilization of energy in cabin exhaust air is shown

The air then passes through the turbine and into the cabin. Instead of discharging the air directly overboard, as is customary, it is first passed through the heat exchanger to provide the coolant air flow. The flow of cabin exhaust air is aided by either a compressor or a fan located downstream from the heat exchanger in the cabin exhaust air circuit and driven by the turbine.

Further use is made of the exhaust air by passing it through an exit nozzle to derive propulsive thrust. An important principle is to attempt to extract all available energy from the exhaust air before finally rejecting it overboard. This type of system is particularly applicable to small military aircraft.

2.3.2.1 General Comments on Regenerative Systems

1. The heat balance between turbine and compressor permits very little cabin leakage. Any appreciable leakage from the cabin causes a marked decrease in system performance.
2. The 1:1 flow ratio heat exchanger is bulky.
3. Component matching and pressure control are relatively complicated.
4. Regenerative systems produce colder turbine discharge temperatures than basic simple air cycle systems.

2.3.2.2 Summary of Equations and Calculation Procedure for Regenerative System

In Fig. 3B-11, the following assumptions are made:

1. Ram recovery, turbine, and compressor efficiencies are constant.
2. Duct pressure losses are neglected (except for ram intake scoop).
3. Duct heat losses are neglected.
4. Cabin pressure is given.
5. There is no cabin air leakage.
6. Mechanical efficiency between turbine and compressor is 100%.
7. Cabin cooling load remains constant.
8. There is isentropic expansion in exit jet nozzle.
9. Dynamic pressure in ducts is negligible (low air velocity).

The general equations are:

Net cycle work = Change in kinetic energy

$$= \frac{W_a}{g_c} \left(\frac{V_0^2}{2} - \frac{V_7^2}{2} \right) \quad (3B-14)$$

$$\text{COP} = \frac{JQ_{3-4}}{\text{Net cycle work}} \quad (3B-15)$$

Referring to Fig. 3B-11,

(1) 0-1: Compression in ram scoop

a. State point 0:

$$\begin{aligned} p_0 &= \text{Freestream static pressure} \\ T_0 &= \text{Freestream static pressure} \\ V_0 &= \frac{M_0}{\sqrt{kgRT_0}} \end{aligned} \quad (3B-16)$$

b. State point 1':

$$\begin{aligned} p_{1'} &= p_0 \left(\frac{T_{1'}}{T_0} \right)^{\gamma/(\gamma-1)} \\ T_{1'} &= T_0 \left(1 + \frac{\gamma-1}{2} M_0^2 \right) \\ V_{1'} &= 0 \end{aligned} \quad (3B-17)$$

c. State point 1:

$p_1 = (\eta p_1')$ where η = Inlet total pressure recovery

$$\begin{aligned} T_1 &= T_1 \\ V_1 &= 0 \end{aligned} \quad (3B-18)$$

(2) 1-2: Cooling in heat exchanger

State Point 2:

$$\begin{aligned} p_2 &= p_1 \\ V_2 &= 0 \\ \eta_x &= \frac{T_1 - T_2}{T_1 - T_4} \end{aligned} \quad (3B-19)$$

(3) 2-3: Expansion through turbine

State point 3:

$$\begin{aligned} p_3 &= \text{Given (cabin pressure)} \\ T_3 &= T_2 \left[1 - \eta_t \left(\frac{Y}{1+Y} \right) \right] \end{aligned} \quad (3B-20)$$

where

$$\begin{aligned} Y &= \left[\left(\frac{p_2}{p_3} \right)^{(\gamma-1)/\gamma} - 1 \right] \\ V_3 &= 0 \end{aligned}$$

(4) 3-4: Heat absorption (cabin or equipment being cooled)

State point 4:

$$\begin{aligned} p_4 &= p_3 \\ q_{3-4} &= w_a c_p (T_4 - T_3) \\ V_4 &= 0 \end{aligned} \quad (3B-21)$$

(5) 4-5: Heat absorption in regenerative heat exchanger

State point 5:

$$\begin{aligned} p_5 &= p_4 \\ T_5 &= T_4 + (T_1 - T_2) \\ V_5 &= 0 \end{aligned} \quad (3B-22)$$

(6) 5-6: Compression through compressor

State point 6:

$$\frac{p_6}{p_5} = \left[1 + \eta_c \left(\frac{T_6}{T_5} - 1 \right) \right]^{\gamma/(\gamma-1)}$$

$$T_6 - T_5 = T_2 - T_3$$

$$V_6 = 0$$
(3B-23)

(7) 6-7: Expansion through nozzle

State point 7:

$$p_7 = p_o$$

$$T_7 = T_6 \left(\frac{p_7}{p_6} \right)^{(\gamma-1)/\gamma}$$

$$V_7 = \sqrt{2Jg_c c_p (T_6 - T_7)}$$
(3B-24)

2.3.3 Open Circuit Air Cycle Systems for Equipment Cooling

Equipment cooling (that is, electronic cooling) is conducted at a temperature level higher than is possible with passenger or crew compartment cooling. Therefore it is usually possible to omit the precooling heat exchanger.

2.3.3.1 Reversed Flow Bootstrap System

This system is shown in Fig. 3B-12. Typical secondary fluids are (1) air passed through equipment, thus cooling by forced convection and (2) water-glycol liquid pumped through equipment.

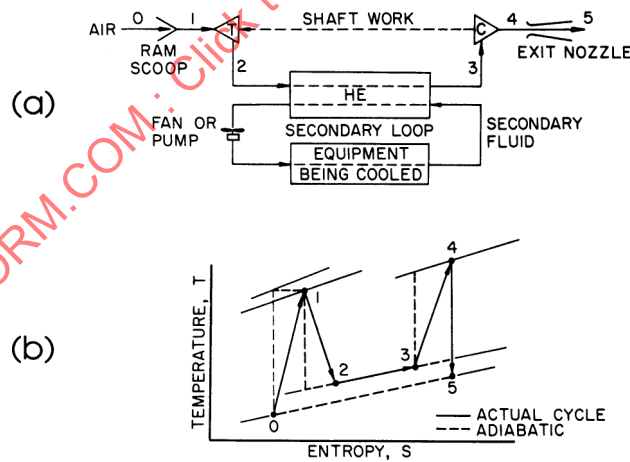


Figure 3B-12 - Reversed Flow Bootstrap Cycle

2.3.3.2 Equipment Being Cooled by Simple Cycle System

In Fig. 3B-13, the precooling heat exchanger is optional and may be used during low speed operating regime.

2.3.4 Closed Air Cycle Refrigeration System

The closed circuit air cycle system illustrated in Fig. 3B-14 consists of two heat transfer components coupled with a turbine and a compressor. The cycle is very similar to a vapor cycle system, with the expansion valve being replaced by the expansion turbine, and the working fluid being air instead of a refrigerant that changes phase.

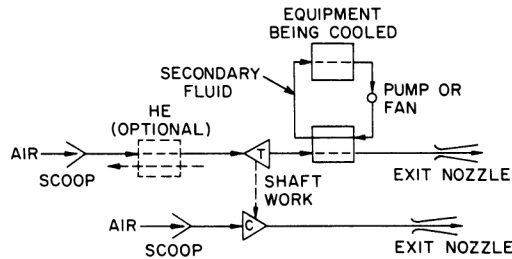


Figure 3B-13 - Simple Cycle System

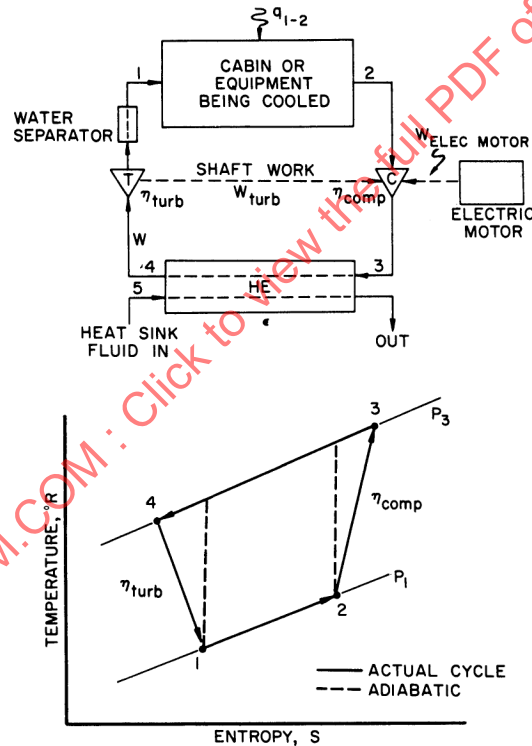


Figure 3B-14 - Closed Air Cycle Refrigeration System

For Mach numbers greater than 1, the closed air cycle is more efficient than the open cycle. It also has advantages of a low operating pressure ratio, ease of control, and an ability to eliminate moisture.

As shown in Par. 2.5, the coefficient of performance of the closed air cycle system for both crew and equipment cooling is lower than for the vapor cycle.

2.3.4.1 General Comments on Closed Air Cycle Systems

1. In closed air cycles, the matching between compressor and turbine is for equal pressure ratios rather than for equal shaft power, as it is for the open cycle. Therefore, augmented power (that is, an electric motor) is required for a closed cycle.
2. In a given system, cooling can be readily adjusted to requirements, with economy in power consumption, by varying the turbine outlet pressure.
3. The use of an electric motor drive simplifies ground cooling.

2.3.4.2 Summary of Equations

Refer to Fig. 3B-14:

$$\begin{aligned} \text{COP} &= \frac{T_2 - T_1}{(T_3 - T_4) - (T_2 - T_1)} \\ &= \frac{T_2 - T_1}{(T_3 - T_2) - (T_4 - T_1)} \end{aligned} \quad (3B-25)$$

Heat exchanger effectiveness

$$\begin{aligned} &= \eta_x \\ &= \frac{w_a c_p (T_3 - T_4)}{(w c_p)_{\min} (T_3 - T_5)} \end{aligned} \quad (3B-26)$$

Heat absorbed (cabin or equipment)

$$\begin{aligned} &= q_{1-2} \\ &= w_a c_p (T_2 - T_1) \end{aligned} \quad (3B-27)$$

Compressor work = W_{comp}

$$\begin{aligned} &= W_{\text{turb}} + W_{\text{el motor}} \\ &= w_a c_p (T_3 - T_2) \tau \end{aligned} \quad (3B-28)$$

$$\text{Turbine work} = w_a c_p (T_4 - T_1) \tau \quad (3B-29)$$

Augmenting electrical work

$$\begin{aligned} &= W_{\text{comp}} - W_{\text{turb}} \\ &= w_a c_p [(T_3 - T_2) - (T_4 - T_1)] \tau \end{aligned} \quad (3B-30)$$

Note: Heat exchanger pressure drop, and duct pressure and temperature drops have been neglected in these computations.

2.4 Combination Air Cycle and Expendable Coolant Systems

No new concepts are introduced by the use of an expendable coolant in any air cycle system. In the systems previously described, any of the heat exchangers that utilize ram air or fuel as the heat sink may be replaced by the expendable coolant heat sink. The use of an expendable coolant makes possible air cycle system operation independent of the flight atmosphere. In general, stored coolants permit greater flexibility of component location, simpler installation configurations, and lower drag penalties.

2.5 Comparison of Air Cycle Systems

2.5.1 General Rules for the Optimum Design of Air Cycle Refrigeration Systems

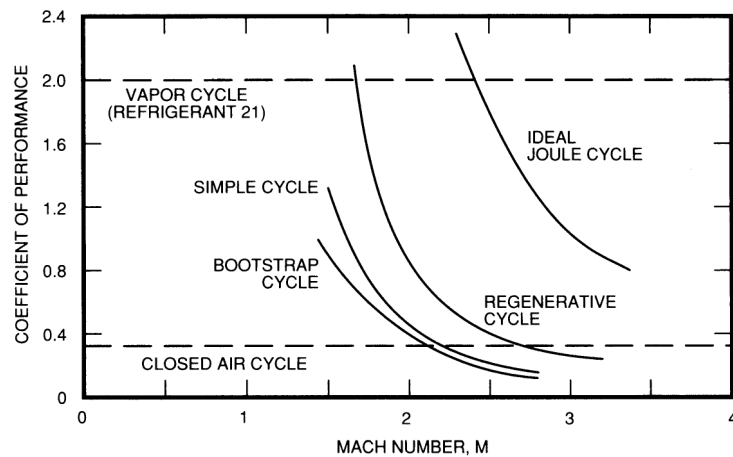
Before the various air cycle systems are compared, the following generalized rules are presented as a summary and guide for general air cycle system design:

1. When a turbine is used in the cabin cooling air line, it should always be located downstream of all other heat transfer components in the line.
2. A compressor is of no utility for cooling purposes unless it is followed by both a heat exchanger and a turbine in the same line or it serves to increase the pressure ratio of a turbine in the heat sink line while acting as a load for the turbine.
3. The use of a turbine in the heat sink line is theoretically more attractive the higher the flight altitude and the higher the Mach number.
4. In some systems, performance benefits are obtained when expanded bleed air is used as a heat sink to reduce the size of the components, which would result otherwise if expanded ram air were used.
5. The addition of an evaporator or a regenerative heat exchanger to any basic air cycle system will always result in improved thermodynamic performance. This advantage must be weighed against airplane penalty factors.
6. The use of expendable cooling media in conjunction with an air cycle system permits larger cooling capacities and lower temperature levels.

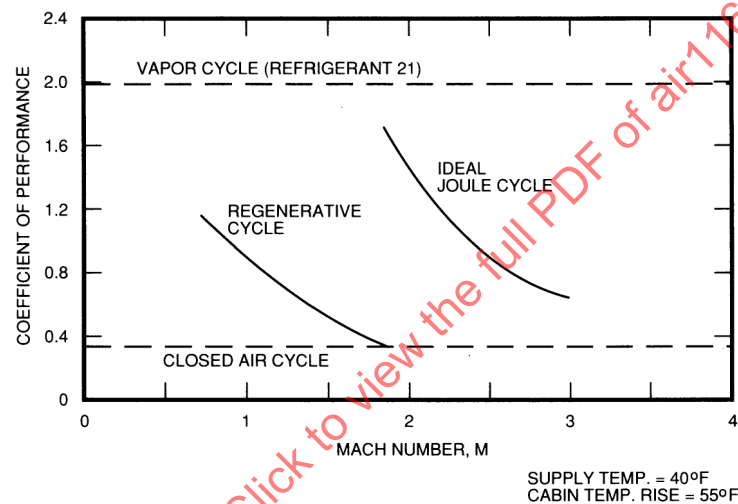
2.5.2 Comparison of Various Air Cycle Systems

A comparison of the thermodynamic performance of basic air cycle systems is presented in Fig. 3B-15. The following systems are compared:

1. Self-contained regenerative system (Fig. 3B-11).
2. Fuel heat sink bootstrap system (refer to system a, Fig. 3B-10).
3. Simple cycle, fuel precooler, and braking compressor (refer to Fig. 3B-4).



(a) TROPOPAUSE REGION



(b) SEA LEVEL

Figure 3B-15 - Comparison of Open Circuit Air Cycle Systems, (a) Tropopause region; (b) Sea level

In addition, the ideal Joule cycle, a closed air cycle system, and a vapor cycle system are shown for comparison. The significant feature to note is that all open air cycle systems decrease in performance as the Mach number increases, and in comparing the performance in the tropopause region with the higher ambient temperature conditions at sea level, the coefficient of performance also decreases as the ambient temperature increases.

The following assumptions were made:

1. Practical compressor and turbine efficiencies were taken into account.
2. System pressure drops and duct heat losses were neglected.
3. Initial compression was derived entirely from intake ram, corrected for shock and subsonic losses.
4. Leakage and pressurization control valve flow were neglected.

Further comparisons may be made, taking into account actual pressure losses in the ducting and heat exchangers. A comparison of the performance of the regenerative open circuit air cycle system in the tropopause region may be made with a regenerative system in which nominal heat exchanger and ducting pressure drops have been taken into account. As shown in Fig. 3B-16, the effect on the coefficient of performance of nominal pressure losses is very pronounced.

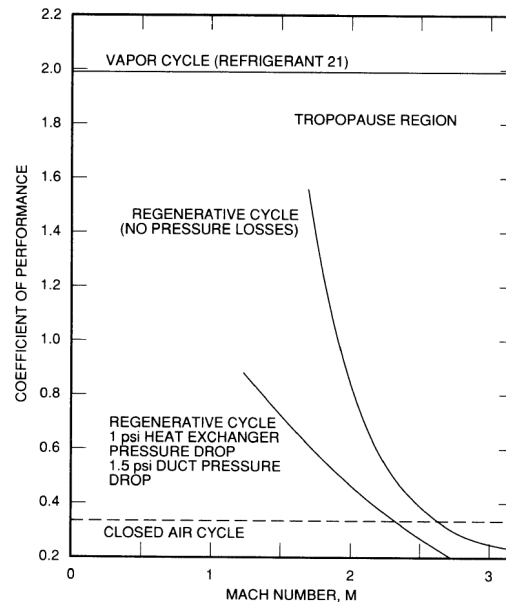


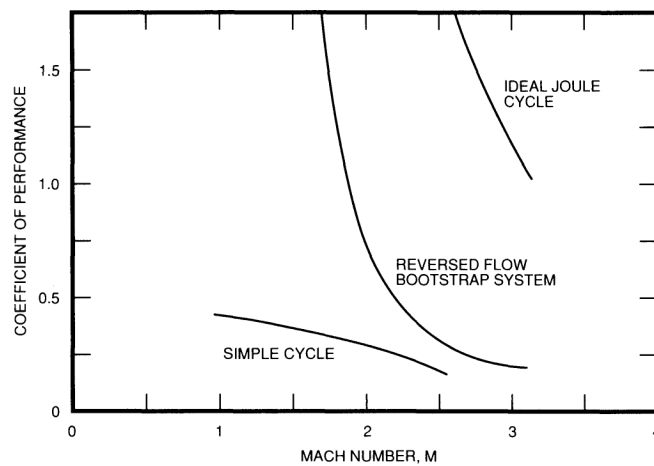
Figure 3B-16 - Regenerative Air Cycle System Comparisons

2.5.3 Comparison of Open Circuit Systems Utilized for Equipment Cooling

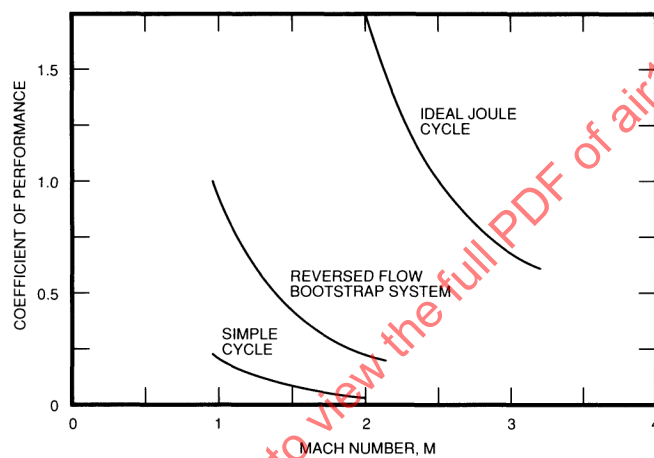
A comparison of the thermodynamic performance is presented in Fig. 3B-17. The following systems are compared:

1. Reversed flow bootstrap system (Par. 2.3.3.1).
2. Simple air cycle with braking compressor (Par. 2.3.3.2).
3. The ideal Joule cycle.

SAENORM.COM : Click to view the full PDF of air1168_3b



(a) TROPOPAUSE



(b) SEA LEVEL

Figure 3B-17 - Comparison of Open Circuit System Utilized for Equipment Cooling. (a) Tropopause; (b) Sea level. For both (a) and (b), heat exchanger $\eta_x = 80\%$ and equipment out-temperature = 140°F

As previously stated, system performance for the open circuit cycles decreases rapidly with increasing Mach number. Performance at altitude (tropopause region) is better than at sea level because of the lower ambient temperatures. Since a more efficient use of turbine shaft work is obtained from the reversed bootstrap cycle, its performance is appreciably better than the open circuit simple cycle.

The performance of the open air cycle systems presented in Fig. 3B-17 may be compared further with the following closed circuit systems operating under the same conditions:

1. Closed air cycle:

$$\text{COP} = 0.74$$

2. Vapor cycle system:

$$\text{Refrigerant 12, COP} = 5.3$$

$$\text{Refrigerant 21, COP} = 4.4$$

2.5.4 General Comments and Comparisons of Air Cycle Systems with Vapor Cycle Systems

1. Closed vapor cycle refrigeration systems possess much higher coefficients of performance than open or closed air cycle systems.
2. Air cycle systems tend to be lighter in weight.
3. High ratios of fresh air-to-recirculation air dictate air cycle cooling, whereas vapor cycle systems are generally best for low fresh air-to-recirculation air ratios.
4. Vapor cycles permit centralized refrigeration systems with intermediate transport media to various compartments or pieces of equipment being cooled.
5. Vapor cycles are recommended where full recirculation (no fresh air supply) is required and water or ram air heat sinks are available.
6. Vapor cycles possess large capacity ground cooling and pulldown capabilities.
7. Air cycle systems possess the fundamental advantage of direct supply of air for both cooling requirements and pressurization control.
8. Air cycle units are characterized by high specific output from compact units.
9. When requirements dictate a high fresh air supply quantity, an open circuit basic bootstrap system provides the most latitude both functionally and in cooling capacity over a wide speed range.

2.6 Water Separator Applications

The question of passenger comfort is one of prime importance and involves not only the problems of cooling and ventilation, but also humidity control both in flight at low altitudes and while on the ground. Consequently, sufficient capacity and means should be provided for removing the latent heat resulting from dehumidification, especially during ground operation in hot humid weather.

The situation changes for aircraft operating for long periods of time at high altitude. Because the moisture content of the atmosphere drops with altitude, so that at 40,000 ft the ambient atmosphere has a relative humidity of the order of 1-2%, it is necessary to make provisions for increasing the internal compartment humidity to over 30%, as dictated by comfort requirements.

In addition, it is also important to exercise humidity control to prevent condensation that can damage electronic equipment and appear on windows, windshields, and on thermal and acoustical insulation. Metal parts or other high thermal conductivity materials exposed to the cabin air should be isolated from the cold skin of low flying, low speed aircraft.

2.6.1 Dehumidification

The problem of removing water from the air supply is in two parts. The first requirement is to prevent fogging of transparent areas and excessive condensation inside the aircraft that tend to deteriorate electronic and electrical equipment, thermal insulation, and similar equipment. The second requirement is to prevent fog from coming into the cabin through the inlet grilles. The nature of the water particles (1 or 2 μ in size) in the air on the downstream side of the air cycle turbine makes it necessary to agglomerate the minute particles into larger droplets before they can be trapped and drained away. For operation with open air cycle systems, two types of water separators are commonly utilized, mechanical and kinetic.

2.6.1.1 Water Separator (Mechanical Separation)

Separator devices provide the means for reducing the moisture content in the air supply to prevent precipitation in the ducting and in the cabin when operating at altitudes at which the ambient air has an appreciable water content.

Water separators are normally located far enough downstream from the air cycle turbine to allow agglomeration of 1-2 μ particles to a size that allows the separator to function properly. Some tests indicate that 0.043 sec is required for droplet size to increase to the desired value.

Water separators can be made available in a range of sizes to handle various air flows. Advantages of water separators are that they are efficient without imposing an undue back pressure, simple in construction, and light weight. A relief valve is used to allow the air to bypass in the event the water separator becomes iced.

A simple water separator consists of a coalescer, internal relief valve, and collector tubes or plates. Air from the air cycle turbine, with its free water in the form of minute drops (fog), passes through the filtration element of the coalescer. Passing through the restricted passages causes the droplets to join together to form larger drops, which are blown on the collector tubes or plates in the downstream portion of the water separator. The collected water runs down the tubes or plates where it is drained from the unit. If the coalescer assembly becomes choked because of icing conditions, the relief valve opens, allowing the moist air to bypass the extractor and pass directly into the cabin system.

Fig. 3B-18 presents a psychrometric diagram of the mechanical moisture separation process. The efficiency of the separator (η_{sep}) is defined as the change in specific humidity for a given case, divided by the change in specific humidity that would result if all the entrained moisture were removed.

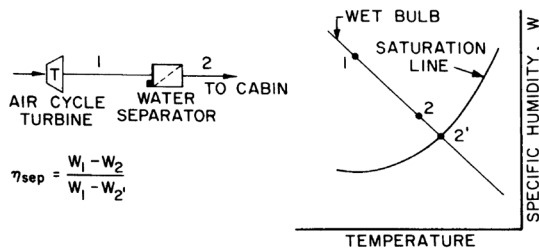


Figure 3B-18 - Psychrometric Diagram of Mechanical Water Separation Process

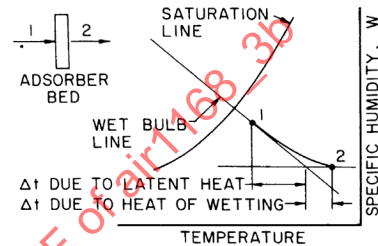


Figure 3B-19 - Psychrometric Diagram of Chemical Moisture Removal Process

2.6.1.2 Water Separator (Kinetic Separation)

A centrifugal device (such as a turbine rotor or a form of swirl tube) imparts kinetic energy to the suspended water which, at a given speed of rotation, is much greater than that of the air which carries the water. Therefore, it is possible to trap a portion of the water at the periphery of a centrifugal separator and allow for the air to pass on through the system at reduced moisture content.

The efficiency of the water separation depends upon the difference between the kinetic energy imparted to the water particles and that imparted to the suspending air. Since the kinetic energy of the water particles depends upon the particle mass, extremely fine vapor arising from the refrigeration process upstream of the separator results in fine droplets of low mass with corresponding low kinetic energy values. Thus, specific devices are necessary to increase the mass of the water particles upstream of the centrifugal action.

2.6.1.3 Dehumidification with Vapor Cycle Refrigeration

The use of vapor cycle refrigeration systems simplifies the problem of moisture removal, since the surface temperature of the evaporator is usually below the dew point temperature of the air; that is, the air is cooled to its dew point temperature as it flows through the evaporator. The excess moisture condenses and collects on the heat transfer surfaces of the evaporator. By providing a simple water trap immediately downstream from the evaporator the water droplets, blown from the evaporator by the air stream, are collected and drained away.

2.6.1.4 Moisture Removal by Chemical Means

Moisture removal by chemical means is a simultaneous heating and dehumidification process. Solid adsorbents, such as gel or activated alumina, or solutions in water of calcium chloride or lithium chloride may be utilized. When the air flows through any of these materials, moisture is condensed from the air, and the latent heat surrendered by the condensing vapor, plus the heat of adsorption (or heat of wetting), raises the temperature of the air. Solid adsorbents can hold approximately 40% of their initial dry weight of water. Fig. 3B-19 shows a psychrometric diagram of the chemical moisture removal process.

Molecular sieves, a group of crystalline adsorbents, may also be used for moisture removal. When they are reactivated by heating, to remove the water of crystallization, they become highly porous materials with a great affinity for water in addition to other gaseous and liquid materials. The major advantages of molecular sieves are:

1. Perform better than other adsorbents.
2. Can be used at elevated temperatures (approximately 200°F).
3. Can be designed with high face velocities.
4. Can be designed for selective removal of other impurities together with water.

Fig. 3B-20 compares the performance of adsorbent materials.

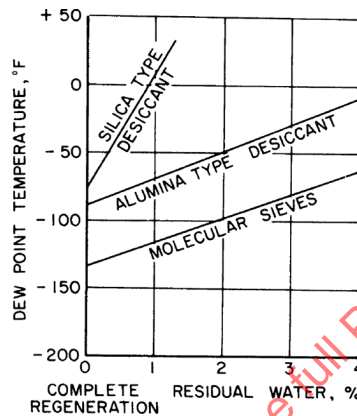


Figure 3B-20 - Comparison of Desiccants (adsorbents)

2.6.1.5 Summary

The choice of the refrigeration system usually dictates the method of moisture removal; for example:

1. For air cycle refrigeration, water separators (mechanical separation of moisture).
2. For vapor cycle refrigeration, condensation of moisture on cold surfaces; that is, the evaporator of a vapor cycle, or a heat exchanger that cools air by utilizing a cold mixture of water and glycol.

Chemical methods of moisture removal have not been utilized in aircraft except in specialized moisture removal applications for electronic and other equipment.

2.6.2 Humidification

Humidification is not as complicated as dehumidification. The various types of humidifiers are:

1. Electric boilers, using the "steam kettle" principle. Water is boiled by the heat from the electric resistance heaters and the resulting steam or water vapor is passed into the air.
2. Fine sprays, using high pressure pumps to force water through jet orifices located in the air stream.
3. Venturi humidifiers, using a venturi, a water storage tank, and a solenoid valve to cut off the water supply, provide means for increasing the moisture content of the air when operating for long periods at high altitudes. These units are efficient, simple, light, and reliable.

When humidification is required, the control valve is opened so that water is free to pass to the inlet ports located in the restricted portion of the venturi throat, causing the water to be drawn from the inlets and absorbed by the passing air.

A natural turbulence caused by the shape of the humidifier assists the process of absorption, and free water in the air stream is retained by a series of inclined porous louvers at the exit. The louvers are maintained in a wet condition and, acting as wicks, further assist the process of evaporation. If the exit louver elements become choked (iced), air can still pass between the louvers without undue restriction.

3. VAPOR CYCLE SYSTEMS

Note: The refrigerants used in this section are no longer in use due to high ozone depletion potential. The replacement refrigerants are now in question due to high global warming potential. When performing tradeoff studies, the refrigerants currently in use should be analyzed. Properties of the refrigerants are typically available on line.

3.1 Basic Considerations and Cycle Components

The vapor cycle refrigeration system is, in effect, a heat pump, since it transfers heat from a low temperature environment to one at a higher temperature.

Fig. 3B-22 traces the vapor cycle process. Evaporation of the liquid refrigerant in the evaporator absorbs heat from the heat source fluid. The refrigerant is in turn compressed to a higher pressure and temperature and then cooled in a condenser where the acquired heat is rejected to the heat sink. The refrigerant liquid leaving the condenser flows to the evaporator through a throttling (expansion) valve. The vapor cycle system is a closed circuit system.

The power required to operate the heat pump depends on the difference in temperature levels between the evaporator and condenser, and the amount of heat being absorbed in the evaporator. When the temperature difference is small, the heat equivalent of the work required may be only a third to a quarter of the amount of heat being extracted from the heat source. If the temperature difference is large, the work input may equal or exceed the equivalent of the heat extracted.

For any given refrigerant, there is a limiting temperature range over which it can be used. The critical temperature defines the maximum limit of the condenser temperature. In practice, however, the maximum temperature must be considerably below the critical because the refrigeration effect decreases and the work of compression increases rapidly when the temperature approaches the critical value.

Vapor cycle systems can be applied to all types of aerospace vehicles and are of particular interest in the case of large and high speed aircraft for the following reasons:

1. They have a high coefficient of performance.
2. They are flexible in that cooling may be directed accurately to required areas.
3. They solve the problem of dehumidification on the ground and at low altitudes.

It is important to note that the fluid in the evaporator must absorb both latent and sensible heat. Therefore, when the system is designed to cool and dehumidify the air, the system must produce sufficient refrigeration to supply the humidity control and cabin cooling requirements.

For additional information on the application of vapor cycle systems to aircraft, refer to Ref. 18.

3.1.1 Definition of Ton of Refrigeration

The unit of measure for refrigeration output is the ton:

$$\begin{aligned} 1 \text{ ton} &= 200 \text{ Btu / min} \\ &= 12,000 \text{ Btu / hr} \\ &= 288,000 \text{ Btu / day} \end{aligned}$$

One ton of refrigeration is equivalent to the heat required to melt 1 ton of ice in 24 hr (latent heat of fusion = 144 Btu/lb).

3.1.2 Typical Pressure-Enthalpy (P-H) Diagram

This type of schematic diagram is extremely useful in representing and directly solving vapor cycle problems (ref. Fig. 3B-22).

3.1.3 Ideal Refrigeration Cycle

This is the reversed Carnot cycle with a vapor as the refrigerant, as shown in Fig. 3B-21, where points are represented as:

- (1) 1-2: Isothermal vaporization (evaporation) process.
- (2) 2-3: Reversible adiabatic compression process.
- (3) 3-4: Isothermal condensation process.
- (4) 4-1: Reversible adiabatic process.

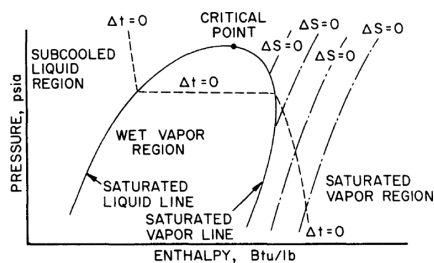


Figure 3B-21 - Typical Pressure-enthalpy (P-H) Diagram. Note: $\Delta t = 0 = \text{Constant temperature}$ and $\Delta S = 0 = \text{Constant entropy}$

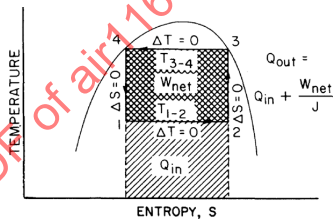


Figure 3B-22 - Ideal Refrigeration Cycle

The applicable equation is

$$\begin{aligned}
 \text{COP} &= \frac{\text{Refrigeration obtained}}{\text{Work done on system}} \\
 &= \frac{Q_{in}}{Q_{out} - Q_{in}} = \frac{JQ_{in}}{W_{net}} \\
 &= \frac{T_{1-2}}{T_{3-4} - T_{1-2}}
 \end{aligned} \tag{3B-31}$$

The reversed Carnot cycle is very useful as a standard of comparison, but it is not a practical cycle because:

1. Wet compression (point 2) tends to damage the compressor.
2. Isentropic expansion of a liquid (4-1) in a work-producing device (that is, a turbine) is not practical.

3.2 Analysis of Basic Vapor Cycle System

The nearest practical approach to the reversed Carnot cycle standard is the basic vapor cycle system. See Fig. 3B-23, where lines are represented as:

- (1) 1-2: Constant pressure process (evaporator); absorption of heat evaporates liquid refrigerant into vapor.
- (2) 2-3: Reversible adiabatic compression process (compressor).
- (3) 3-4: Constant pressure process (condenser); loss of heat to cooling medium (sink) condenses refrigerant vapor.
- (4) 4-1: Throttling process; pressure reduced in passing through expansion (needle) valve.

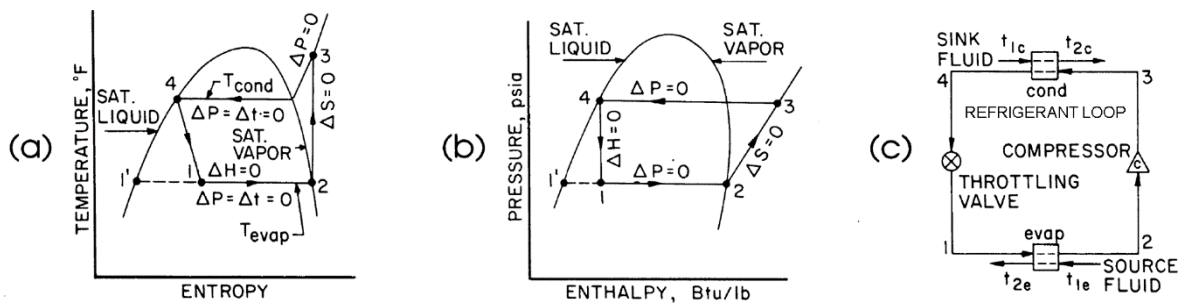


Figure 3B-23 - Basic Vapor Cycle System, (a) T-S diagram; (b) P-H diagram; (c) Basic simple cycle

Friction losses (pressure drops) of components and connecting lines have been neglected in the illustration. Line 1-1' is the portion of refrigerant liquid that flashes into vapor when passing through the throttling valve.

3.2.1 Evaporator Performance

Applicable equations are:

$$h_2 - h_1 = \text{Refrigeration effect (amount of heat absorbed in evaporator per pound of refrigerant)} \quad (3B-32)$$

$$q_{in} = q_{1-2} = \text{Amount of heat absorbed in evaporator by refrigerant} \quad (3B-33)$$

$$= \text{Amount of heat lost by fluid being cooled (the heat source)}$$

$$q_{1-2} = w_f(h_2 - h_1) \text{ Btu / min} \quad (3B-34)$$

$$= w_f Q_{evap}$$

$$= w_e c_{pe}(t_{1e} - t_{2e})$$

where

w_f = Refrigerant flow rate, lb/min

w_f = Refrigerant flow rate per ton of cooling

$$= \frac{200}{h_2 - h_1} \text{ lb / min-ton}$$

Q_{evap} = Evaporator capacity, tons

w_e = Source fluid flow rate, lb/min

3.2.2 Compressor Performance

The representative equation is

$$q_{3-2} = \text{Theoretical work of compression (reversible adiabatic); } \eta_{comp} = 100\% \quad (3B-35)$$

$$= w_f(h_3 - h_2) \text{ Btu / min}$$

$$= \frac{w_f(h_3 - h_2)}{42.4} \text{ hp}$$

3.2.3 Condenser Performance

This is expressed by

$$\begin{aligned}
 q_{out} &= q_{3-4} \\
 &= \text{Amount of heat rejected in condenser by refrigerant} \\
 &= w_f(h_3 - h_4) \text{ Btu/min} \\
 &= w_f(h_2 - h_1) + w_f(h_3 - h_2), \text{ which is the amount of heat absorbed in} \\
 &\quad \text{evaporator plus heat equivalent of compressor work} \\
 &= w_c c_{pc}(t_{2c} - t_{1c}), \text{ which is the amount of heat absorbed by the heat sink from the condensing refrigerant}
 \end{aligned}
 \tag{3B-36}$$

where w_c = Sink fluid flow rate, lb/min

3.2.4 System Performance

$$\begin{aligned}
 \text{COP} &= \frac{h_2 - h_1}{h_3 - h_2} = \frac{200(Q_{evap})}{42.4(W_c)} \\
 &= 4.715 \frac{Q_{evap}}{W_c} \\
 \frac{\text{hp}}{\text{ton}} &= \frac{4.715}{\text{COP}}
 \end{aligned}
 \tag{3B-37}$$

3.2.5 Major Deviations of Actual Basic Cycle from Theoretical Basic Cycle

Three areas are bounded by points in Fig. 3B-24 as follows:

1. Area 2'-2''-3'-3: Superheating from 2 to 2' in an evaporator is necessary to ensure that no liquid goes into the compressor. When vapor is superheated in the evaporator, then it is part of the refrigerating effect. If vapor is superheated outside of the evaporator, it cannot be credited to the refrigerating effect.
2. Area 2'-3''-3': An increase in entropy and enthalpy results from less than a 100% efficient compression process.
3. Area 1'-1-4-4': Subcooling from 4 to 4' is necessary to ensure that there is no flashing of liquid to vapor upstream of the expansion (throttling) valve; it also increases the refrigeration effect (useful cooling) of the evaporator.

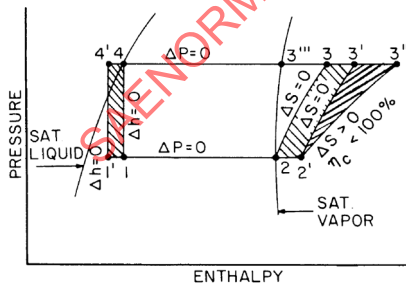


Figure 3B-24 - Comparison of Actual versus Theoretical Vapor Cycles. Pressure Drops have been Neglected

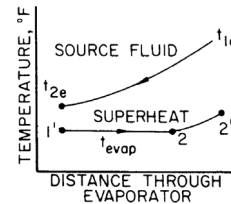


Figure 3B-25 - Evaporator Performance

3.2.5.1 Actual Evaporator Performance

A plot of the heat source and refrigerant temperatures in the evaporator is shown in Fig. 3B-25.

$$q_{in} = q_{1-2'} = w_f (h_{2'} - h_{1'})$$

$$\text{Refrigeration effect} = (h_{2'} - h_{1'})$$

$$w_f = w_{f'} Q_{evap} \text{ lb/min}$$

$$w_{f'} = \frac{200}{h_{2'} - h_{1'}} \text{ lb/min-ton} \quad (3B-38)$$

3.2.5.2 Actual Compressor Performance

The equations are (see Fig. 3B-24)

$$q_{3'-2'} = w_f (h_{3'} - h_{2'}) \quad (\eta_{comp} < 100\%)$$

$$(h_{3'} - h_{2'}) = \frac{h_{3''} - h_{2'}}{\eta_{comp}} \text{ Btu/min} \quad (3B-39)$$

3.2.5.3 Actual Condenser Performance

Fig. 3B-26 shows the temperature of the refrigerant and the heat sink as they pass through the condenser.

$$q_{out} = q_{3'-4'} = w_f (h_{3'} - h_{4'}) = w_f (h_{2'} - h_{1'}) + w_f (h_{3''} - h_{2'}) \quad (3B-40)$$

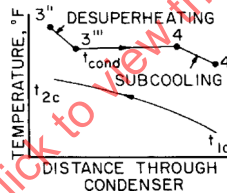


Figure 3B-26 - Condenser Performance

3.2.5.4 Actual System Performance

The COP for actual system performance is (Ref. Fig. 3B-24):

$$\text{COP} = \frac{h_{2'} - h_{1'}}{h_{3'} - h_{2'}} = \frac{4.715 Q_{evap}}{W_c} \quad (\text{Ref. Eq. 3B-37}) \quad (3B-41)$$

$$\text{where } W_c = \frac{(q_{3'-2'})}{42.4}$$

3.2.6 Frictional Effects on Vapor Cycle System Performance

The effects of friction losses may be summarized as follows (losses have been exaggerated for clarity; see Fig. 3B-27):

Δp_1 = Evaporator pressure drop; results in reduced evaporator mean temperature and a larger evaporator size

Δp_2 = Suction line pressure drop; results in increased compressor power requirements

Δp_3 = Discharge line pressure drop; results in increased power requirements for compressor

Δp_4 = Condenser pressure drop; usually negligible in actual operation

Δp_5 = Liquid line pressure drop; results in liquid flashing into vapor, which may reduce capacity of throttling valve

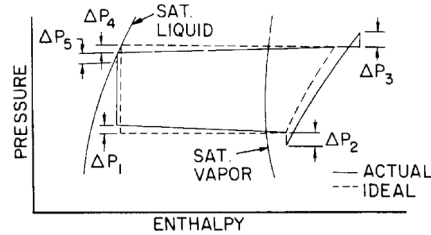


Figure 3B-27 - Vapor Cycle Showing Pressure Losses

All pressure losses reduce the COP of the actual cycle below that of the ideal vapor cycle. In the order of importance in the reduction of COP, these losses may be listed as follows:

1. Suction line pressure drop.
2. Compressor discharge line pressure drop.
3. Evaporator pressure drop.
4. Liquid line pressure drop.
5. Condenser pressure drop.

It may be noted that inefficiency of compression has a bigger effect on the COP than the pressure losses listed above.

3.3 Vapor Cycle Systems Variants

3.3.1 Multiple Evaporator Operation

For divided cooling loads (that is, aircraft occupied compartment cooling together with unoccupied electronic compartment cooling), multiple evaporators in parallel are necessary. (See Fig. 3B-28.) Individual back pressure valves are required when different temperature levels are to be maintained.

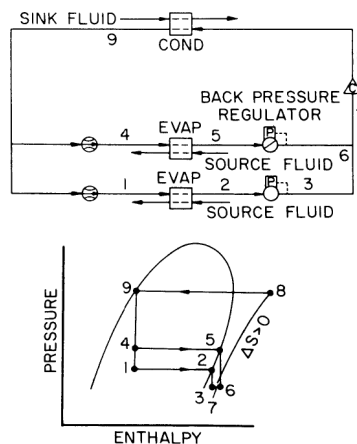


Figure 3B-28 - Multiple Evaporator Operation

Operation at different temperatures, with the suction pressure throttled to the lowest evaporator pressure, is inefficient unless the evaporator at the lowest temperature carries most of the heat load.

3.3.2 Addition of Subcooler-Superheater to Actual Basic Cycle

The system is shown in Fig. 3B-29. Applicable equations are

$$q_{evap} = w_f(h_2 - h_1)$$

$$q_{comp} = w_f(h_4 - h_3)$$

$$q_{cond} = w_f(h_4 - h_5)$$

$$\frac{(h_3 - h_2)}{(h_5 - h_6)} = 1$$

$$COP = \frac{h_2 - h_1}{h_4 - h_3}$$

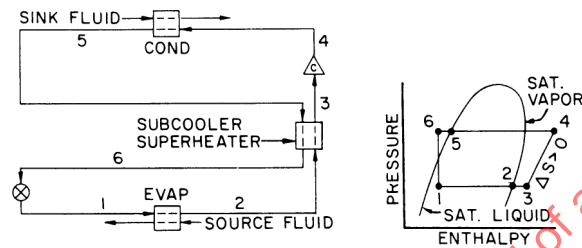


Figure 3B-29 - Subcooler-superheater Cycle

The benefits derived from its use are:

1. A heat exchanger between the compressor and evaporator supplies useful superheat and prevents liquid carryover to the compressor (especially with flooded evaporator applications) and also prevents vapor flashing upstream from the expansion valve.
2. The refrigeration effect of the evaporator is increased.
3. The cycle COP is increased.
4. Useful superheating (with no subcooling) may also be accomplished by extending the evaporator without the use of a separate heat exchanger. However, more benefits may be derived from the separate superheater (assuming air being cooled in the evaporator):
 - a. The mean Δt between condensed liquid and evaporator exit vapor is higher than the Δt between the evaporator air being cooled and the evaporator exit vapor.
 - b. The section of the evaporator being used as a superheater is a gas-to-gas heat exchanger, which is very inefficient when compared to the liquid-to-gas transfer of a separate superheater.

3.3.3 Compound Cycles

Figs. 3B-30 through 3B-35 depict several variations of the basic vapor cycle:

1. Simple compound cycle (Fig. 3B-30).
2. Two stage system with open type flash intercooler (Fig. 3B-31), for which

$$q_{7-6} = w_{f2}(h_6 - h_7)$$

$$q_{6-5} = w_{f2}(h_6 - h_5)$$

$$q_{3-2} = w_{f1}(h_3 - h_2)$$

$$q_{1-2} = w_{f1}(h_2 - h_1)$$

and

$$\frac{w_{f2}}{w_{f1}} = \frac{h_4 - h_9}{h_4 - h_8} = \frac{h_3 - h_9}{h_5 - h_8} = \frac{h_3 - h_5}{h_5 - h_4}$$

3. Compound cycle with expanded refrigerant intercooling (Fig. 3B-32).
4. Compound cycle with expanded refrigerant closed subcooler (Fig. 3B-33).
5. Compound cycle with superheater (Fig. 3B-34).
6. Compound cycle with subcooler and superheater (Fig. 3B-35).

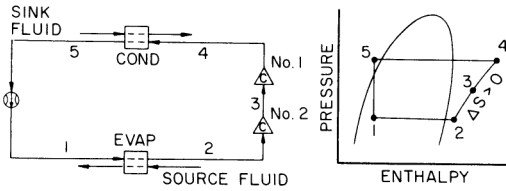


Figure 3B-30 - Simple Compound Cycle

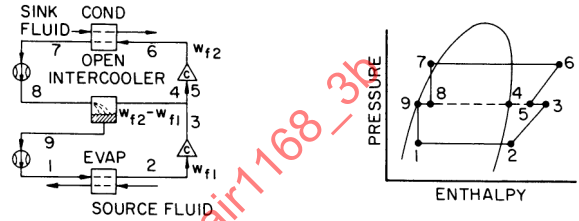


Figure 3B-31 - Two-stage System with Intercooler

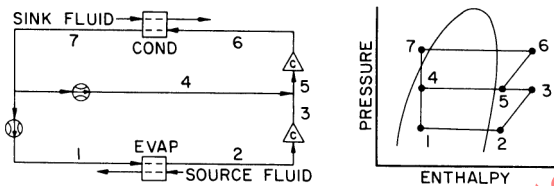


Figure 3B-32 - Compound Cycle with Intercooling

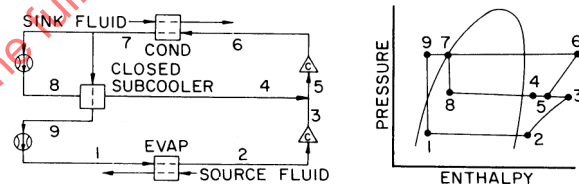


Figure 3B-33 - Compound Cycle with Subcooler

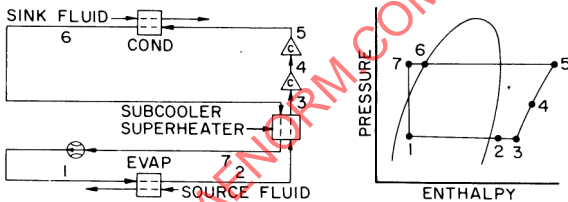


Figure 3B-34 - Compound Cycle with Superheater

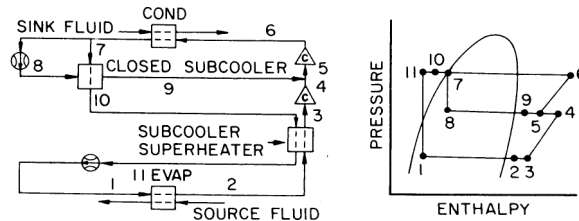


Figure 3B-35 - Compound Cycles with Subcooler and Superheater

3.3.3.1 Simple Compound Cycle (Fig. 3B-30)

This is the simplest method for accommodating what would otherwise be an excessive pressure ratio for a single stage. Two or more stages of compression may be in the same compressor housing, or separate compressors may be utilized. The method of analysis is identical to that of a simple cycle.

and

$(COP)_{cascade} < \text{COP of individual loops of system}$

$(COP)_{cascade} > \text{COP of single simple cycle operating between extreme temperatures}$

3.3.4.1 General Considerations for Cascade Systems

1. The increased mechanical complexity for multiple stage cascade systems favors the use of the least number of stages. However, the COP of the system decreases rapidly with each single cycle as the temperature spread between the evaporator and condenser increases because the proportion of irreversible to reversible processes in the cycle rises.
2. In addition to the irreversibilities present in the individual cycles, there is an additional irreversibility associated with the transfer of heat across the finite temperature difference between cycles. Temperature differences between cycles are usually small (approximately 10-20°F).
3. Different refrigerants may be used for each cycle. This does not markedly improve system COP and makes for a more complicated system, but it may result in definite saving in overall low stage compressor size and weight.
4. The COP of the cascade system is usually better than for the compound or simple cycles, especially when comparison is based on actual compressor efficiencies.
5. The cascade cycle is readily adaptable to two evaporators operating at different temperature levels, by the addition of an evaporator in parallel with the condenser-evaporator in loop 2. The system then becomes a simple cycle with respect to the high temperature evaporator and a cascade cycle with respect to the low temperature evaporator. This arrangement is recommended for applications where the high temperature evaporator carries most of the heat load.
6. There are less severe compressor requirements for the cascade system, since lower operating pressure differentials are used.
7. In determining the minimum possible number of cycles to be cascaded between widely separated temperatures, the maximum temperature spread for the application of each refrigerant must be evaluated. The cascading of refrigerant cycles requires a thorough study of the refrigerant characteristics applied to each cycle in order to arrive at the optimum compromise.

3.4 Expendable Refrigerant Vapor Cycle Systems

A simple open vapor cycle system is one in which the refrigerant (water, ammonia, or similar fluid) is evaporated directly to the atmosphere. The usual aircraft system consists of the liquid refrigerant in a liquid reservoir that feeds an evaporator (boiler) in which the cooling of the heat source fluid is accomplished. The saturated or superheated vapor is discharged overboard. A compressor (vacuum pump) may be located downstream from the evaporator in the vapor line to decrease the boiling temperature of the refrigerant below the temperature corresponding to the ambient pressure.

In systems for cooling ram air taken aboard, a fuel heat exchanger can be located upstream of the boiler and a cooling turbine may be located downstream of the boiler for additional cooling. Thus the boiler of an expendable refrigerant vapor cycle system is located between the primary heat exchanger and the turbine of a simple air cycle system.

The simplest combination of a vapor cycle cooling system with an expendable refrigerant vapor cycle system is made by using water as the ultimate heat sink for a closed system condenser. The condenser becomes a combination condenser-expendable fluid boiler. A vacuum pump and throttling valve are used for controlling the boiling pressure, which, in turn, sets the condensing pressure and temperature for the vapor cycle system.

3.5 Comparison of Vapor Cycle Systems

3.5.1 General Rules for Simple and Cascade Cycle Selection

To compare coefficients of performance when selecting optimum refrigerants for use over a particular temperature range, a series of graphs similar to Fig. 3B-37 may be prepared, one graph for each refrigerant. The COP may be read from the graph for any combination of evaporator and condenser temperatures and for a particular compressor efficiency.

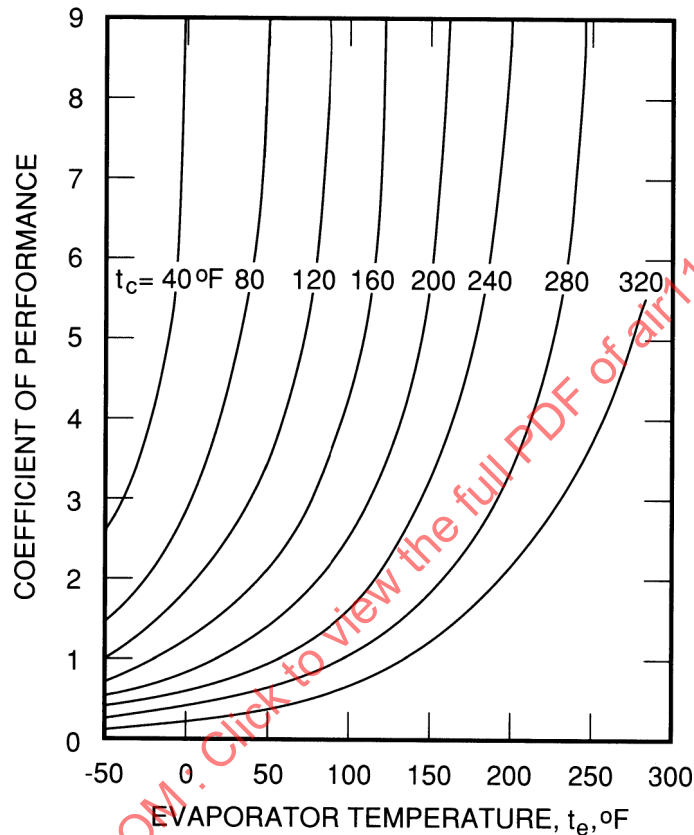


Figure 3B-37 - Vapor Cycle Performance Curves, R-11, t_c = condenser temperature, compressor efficiency = 60%

The comparison of the relative COP together on a single graph reveals which refrigerant would be thermodynamically best in each temperature range, see Fig. 3B-38. The actual COP for 13 different refrigerants as well as the corresponding Carnot standard COP have been plotted, each for simple cycles with condenser temperatures 100°F higher than the evaporator temperatures.

The following general rules may be summarized:

1. Actual cycle coefficients of performance are about half the ideal Carnot cycle COP over the entire temperature range considered:

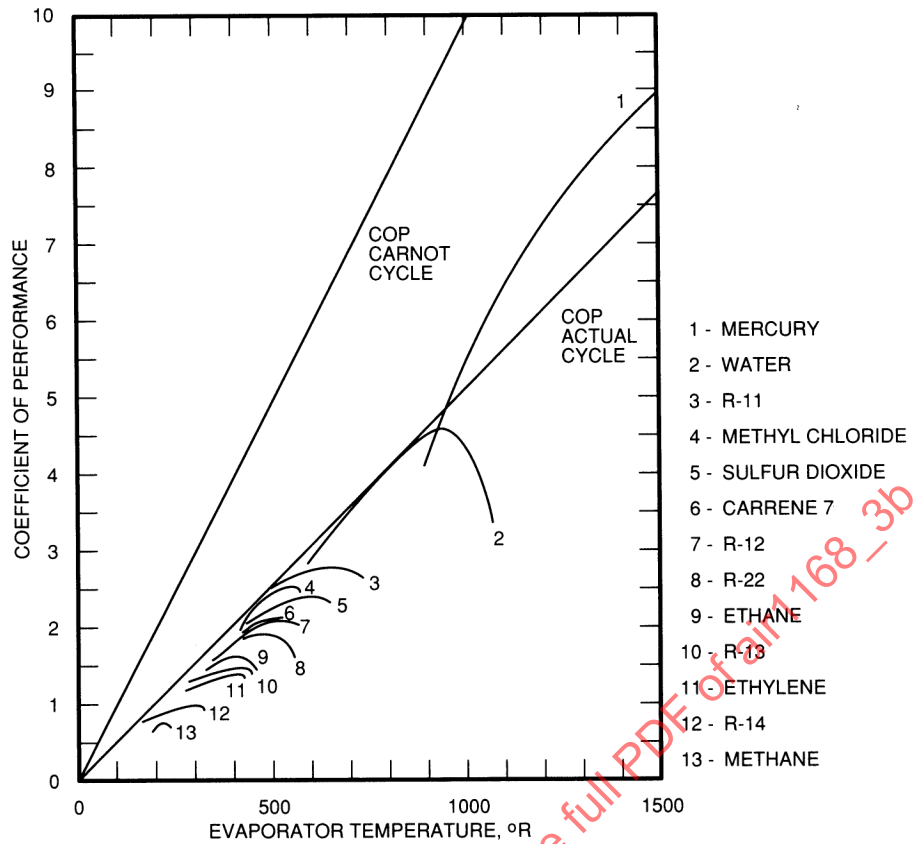


Figure 3B-38 - Comparison of Relative COP's for 13 Different Refrigerants

$$\begin{aligned}
 (\text{COP})_{\text{ideal Carnot}} &= \frac{T_{\text{evap}}}{T_{\text{cond}} - T_{\text{evap}}} \\
 &= \frac{T_{\text{evap}}}{100}
 \end{aligned}
 \tag{3B-44}$$

2. The useful temperature range of each refrigerant tends to decrease as the evaporator temperature level decreases.
3. Any refrigerant cycle has an optimum COP point, which decreases rapidly as the condenser temperature increases toward the refrigerant critical temperature.
4. All COP values tend to blend together on the same line as the difference between the refrigerant critical temperature and the cycle evaporator temperature increases for each refrigerant. However, this region for each refrigerant is accompanied by extremely small pressures and large specific volumes, precluding use in this range. The equation for the line is (in the operating region distant from the critical point):

$$\begin{aligned}
 \text{COP} &= 5.15 \times 10^{-3} T_{\text{evap}} \\
 &= \frac{T_{\text{evap}}}{194}
 \end{aligned}
 \tag{3B-45}$$

5. A refrigerant selected with its optimum COP point near the desired condensing temperature will continue to give thermodynamic performance equivalent to other refrigerants at lower temperatures as its evaporator temperature is lowered indefinitely. However, decreasing saturation pressure and increasing vapor specific volume simultaneously dictate a practical lower limit of application for a given refrigerant.

Cascading will become necessary as the temperature difference between condenser and evaporator becomes large. A series of refrigerants, each of optimum performance in its own temperature range, is selected to comprise a multiple cascade cycle.

6. Thermodynamic performance is not the sole criterion for selecting the optimum intermediate evaporator-condenser temperature between successive stages. Practical requirements limiting equipment size and pressure cause the addition of another refrigerant stage when the evaporator pressure is very low. On the other hand, the least mechanical complexity corresponds to the fewest subcycles in series between two widely-separated temperatures.
7. Complex cycles do not furnish a means of escaping from the low COP that is inevitable with a large temperature difference between the evaporator and the condenser.

Presented below are some general rules for selecting a thermodynamically optimum refrigerant in a particular temperature range, utilizing Fig. 3B-38:

1. The range where the refrigerant specific volume is lowest corresponds to the maximum COP part of each refrigerant curve. The absolute evaporating pressure exceeds sea level atmospheric pressure in this range.
2. For the specified evaporator temperature range, generally select the refrigerant that exhibits the highest COP.
3. Where two or more refrigerants are close in performance, further detailed cycle computations will reveal which refrigerant possesses the best characteristics.

So far only thermodynamic performance has been considered. Additional criteria for refrigerant selection are:

1. High density of liquid and vapor.
2. Low viscosity of liquid and vapor.
3. High thermal conductivity.
4. Low oil solubility.
5. Good chemical stability.
6. No toxicity and odor.
7. No reaction with water and oil.
8. No reaction with material used in cycle components and in aircraft structure.
9. Simple means of leak detection.
10. No special handling methods required.
11. Any other safety considerations.
12. Low cost.

3.5.2 Comparison of Subcooler-Superheater Performance in Basic Simple Cycle

The graphs in Fig. 3B-39 indicate the improvement resulting from superheating in a separate subcooler-superheater (see Par. 3.3.2). Varying magnitudes of increased performance are obtained depending upon the refrigerant used. In addition to the increase in COP, an accompanying decrease in cfm/ton is obtained, resulting from the increase in refrigeration effect through subcooling.

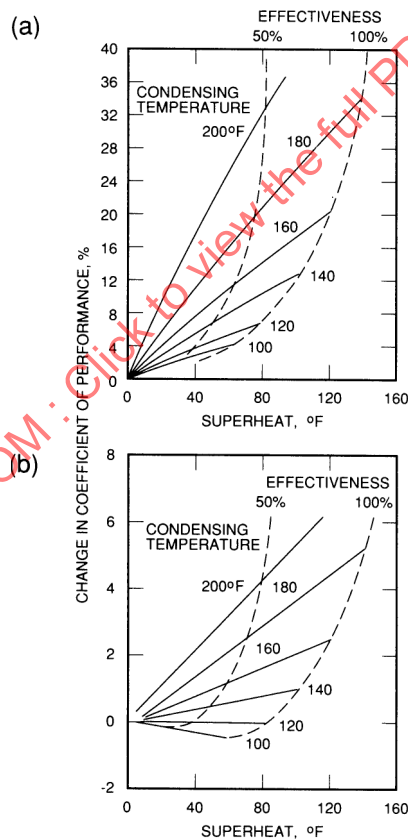
3.5.3 Comparison of Simple, Compound, and Cascade Cycles

Fig. 3B-40 compares the cascade cycle with the simple or compound cycle, on an ideal basis, operating between the same overall temperature limits. Curves 1 and 2 may be compared on an ideal basis for the cascade and compound or simple cycles, respectively.

To take into account the effect of irreversible compression and the finite temperature difference necessary in the intermediate heat exchanger of the cascade cycle, curves 1' and 2' may be compared. Comparison of the COP's reveals a definite advantage for the cascade system. A further comparison is made in Table 3B-1.

The data in Table 3B-1 indicate:

1. The superiority of the cascade cycle over the basic compound cycle, with this superiority usually increased by the use of different refrigerants in the cascade cycle.



**Figure 3B-39 - Effect of Superheat Gained in Performing Useful Cooling,
(a) Refrigerant 12, $t_{evap} = 40^\circ\text{F}$; (b) Refrigerant 11, $t_{evap} = 40^\circ\text{F}$**

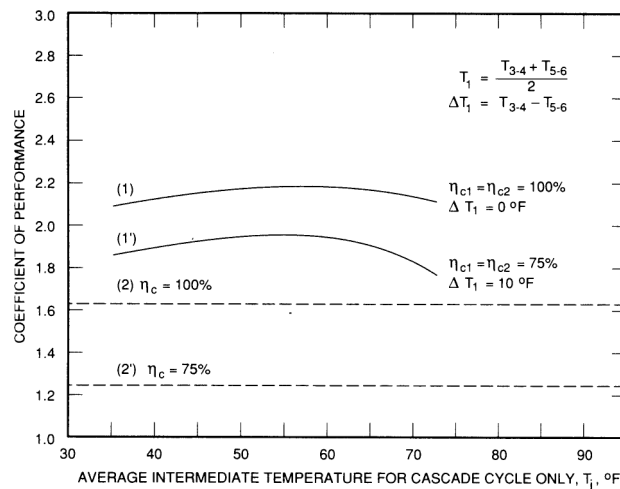


Figure 3B-40 - COP of Cascade Cycle for Refrigerant 12 in Both Stages

2. The advantage of the cascade cycle over the compound cycle holds for both ideal and actual cycles.
3. The cascade cycle possesses inherent disadvantages since additional components are required and a more complex control problem must be solved.
4. Item 3 usually outweighs items 1 and 2; therefore, the compound cycle usually should be used in applications where there is a single heat source and a large temperature difference between source and sink.

Table 3B-1 - Performance of Vapor Cycle Systems

System	Refrigerant	Overall COP	Low Press. Stage COP	High Press. Stage COP
Basic Vapor Cycle	R-11	2.02		
(Par. 3.2)	R-12	1.64		
Cascade Cycle	R-12:R-12	1.96	4.93	3.94
(Par. 3.3.4)	R-22:R-11	2.12	4.84	4.55
	R-22:R-12	1.95	4.84	3.94
Compound Cycle	R-11	2.02		
(Par.3.3.3)(Item 1)	R-12	1.64		
Compound Cycle	R-11	2.02		
(Par. 3.3.3)(Item 3)	R-12	1.64		
Compound Cycle	R-11	2.32		
(Par. 3.3.3)(Item 4)	R-12	2.09		
Compound Cycle	R-11	2.05		
(Par. 3.3.3)(Item 5)	R-12	1.82		
Compound Cycle	R-11	2.32		
(Par. 3.3.3)(Item 6)	R-12	2.15		

Notes: Condensing temperature = 140 °F

Evaporating temperature = - 20 °F

Intermediate temperature = 46 °F

Compressor efficiency = 100%

Intermediate heat exchanger temperature difference = 10 °F (cascade cycle)

4. COMBINED VAPOR CYCLE AND AIR CYCLE SYSTEMS

In general, since open air cycles are limited by a relatively small temperature spread between source and sink temperatures, the closed vapor cycle may be combined with the air cycle system to increase the effective temperature range of the cooling system. With moderate temperature differences, one vapor cycle system may suffice; with extremely large temperature differences, cascade vapor cycle systems may be required. Although many permutations are possible, several representative systems are listed in Table 3B-2. Other component arrangements may be used for specific applications.

Schematic diagrams are shown in Fig. 3B-41; the systems are compared in Fig. 3B-42. In Fig. 3B-41, one or more vapor cycles in series (cascaded) are represented by only one cycle, for simplicity.

Table 3B-2 - System Summary

Type Designation	Source of Cabin Air	Sink Air Condition
I	Bleed air	Ram air
II	Bleed air	Expanded ram air
III	Ram air	Ram air
IV	Ram air	Expanded ram air
V	Type IV with regeneration	

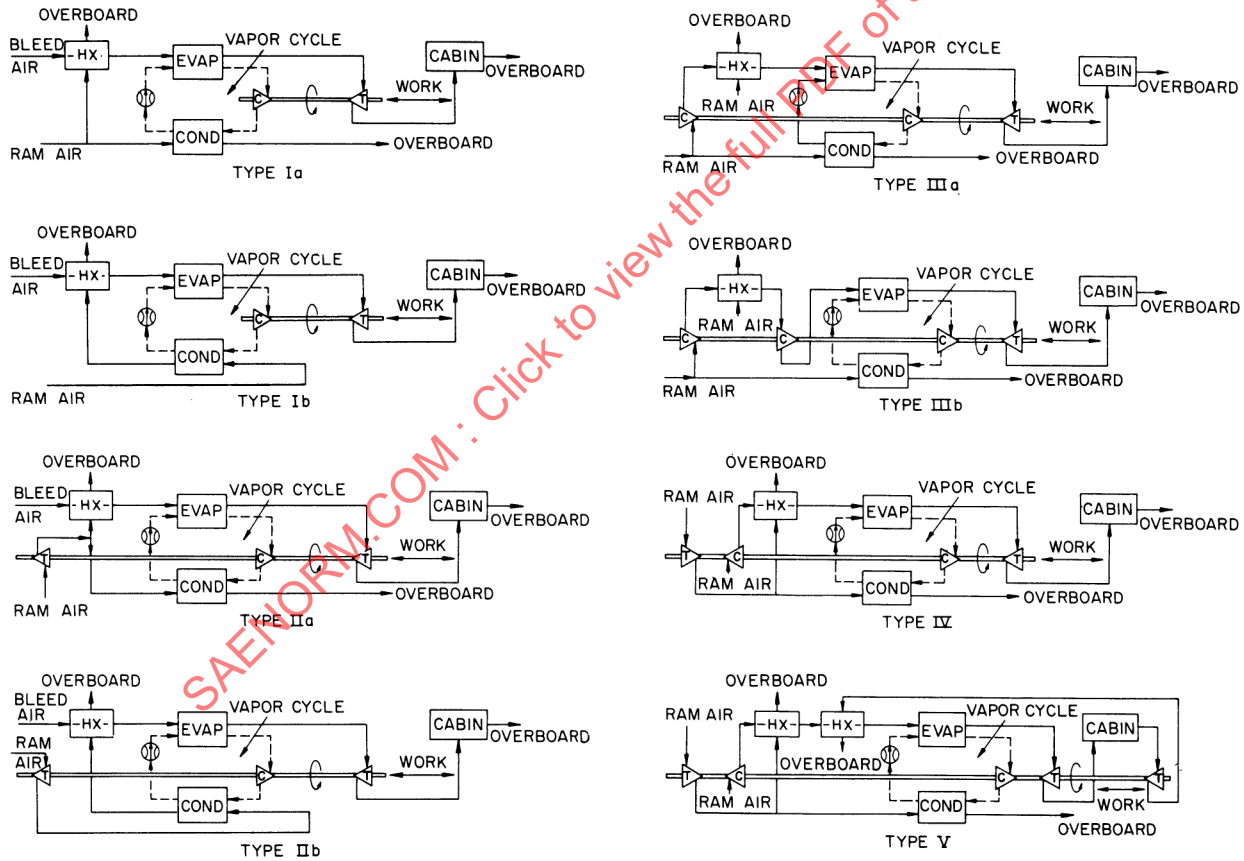


Figure 3B-41 - Representative Combined Air Cycle and Vapor Cycle Systems. Note: One or more vapor cycles in series (cascaded) are represented by only one cycle, for simplicity

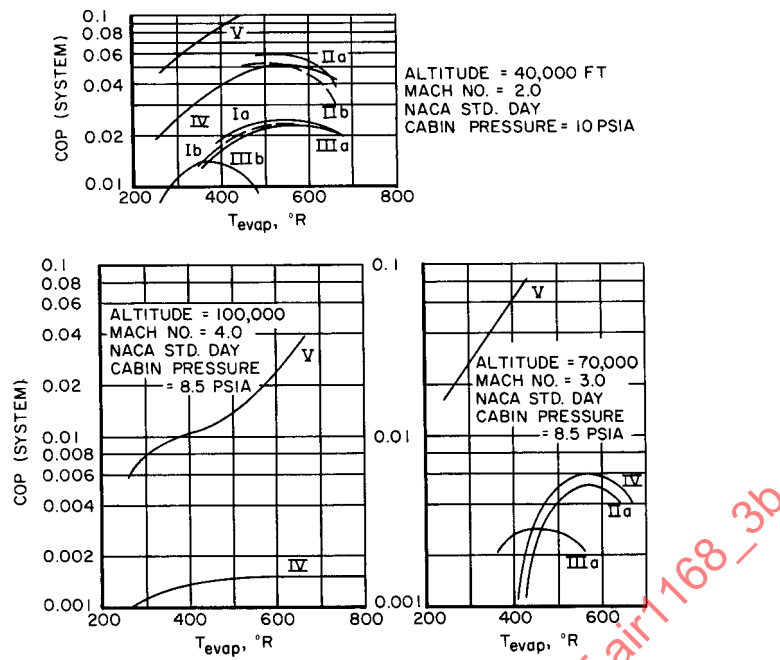


Figure 3B-42 - System Comparisons. Notes: Turbojet eff = 83% (comp); compressor eff = 60%; turbine eff = 70%; $T_{cab} = 510^{\circ}R$; HE effectiveness = 80%; pressure drops = 10% air side HE, 5% cabin supply line, and 15% bleed air line

The total system net work consists of the net engine compressor shaft work for compression of the bleed air, all of the ram air drag, and the auxiliary power necessary for the cooling system compressor.

$$(COP)_{system} = \frac{\text{Amount of cabin cooling}}{\text{Total system net work}}$$

The trend of cooling effect, system work, and COP obtained by varying each of several parameters is summarized in Fig. 3B-43 for a typical combined system (Type Ia). The optimized values are summarized in Table 3B-3.

5. THERMOELECTRIC COOLING

5.1 General Discussion

Although the theory of thermoelectric cooling has been known for many years, only in recent years has progress been made in the development of materials and equipment to pin point potential fields of application in the aerospace industries.

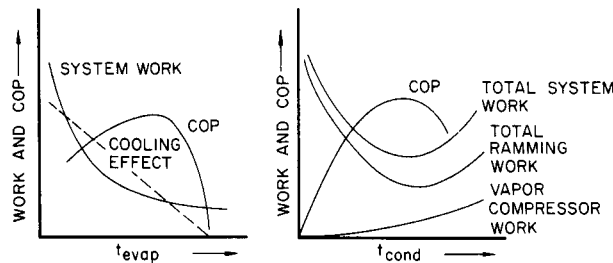


Figure 3B-43 - Parameter Variations for Combined System (Type Ia): Fixed condenser temperature; Fixed Mach number and altitude; Fixed cabin-air compression ratio

Table 3B-3 - Summary of System COP Values

System	Optimum Value of Parameters				Typical Refrig. Required			Number of Vapor Cycles
	Cooling Effect Btu/lb	Evap Temp °R	Cond Temp °R	System COP	Hg	H ₂ O	R-11	
Mach 2.0, 40,000 ft:								
Ia	30	590	1460	0.029	x	x	x	3
Ib	17	610	1460	0.025	x	x	x	3
IIa	27	560	660	0.057	—	—	x	1
IIb	33	540	660	0.050	—	—	x	1
IIIa	26	560	1460	0.023	x	x	x	3
IIIb	17	420	1460	0.015	x	x	x	3
IV	32	560	660	0.051	—	—	x	1
V	32	—	—	0.104	Optimizes with no vapor cycle			
Mach 3.0, 70,000 ft:								
IIa	18	560	780	0.005	—	—	x	1
IIIa	20	480	1860	0.003	x	x	x	3
IV	21	560	780	0.006	—	—	x	1
V	27	—	—	0.063	Optimizes with no vapor cycle			
Mach 4.0, 100,000 ft								
IV	19	420	1660	0.0015	x	x	x	3
V	15	—	—	0.033	Optimizes with no vapor cycle			

The thermoelectric cycle seems to be uniquely suited on the basis of size, simple construction, no moving parts, and ease of control (from 100% cooling to 100% heating). These factors bear consideration in analyzing space, weight, and reliability requirements. On the other hand, performance may not always compare favorably with other systems (air cycle or vapor cycle) at critical load requirements. However, the entire flight envelope at actual flight conditions must be evaluated in order to make a valid comparison of overall merit.

5.2 Present Application

In the aerospace field, thermoelectric cooling has been limited to specialized applications, mainly the cooling of local hot spots in electronic component cooling. In the commercial field, the thermoelectric cooling cycle is successfully being applied to laboratory equipment, water coolers, refrigerators, ice makers, and air conditioners. Present capacities range up to 4000 watts of cooling, depending on conditions and application.

5.3 Fundamental Theory

The thermoelectric cycle consists of two different semiconductor materials (much like a thermocouple) in series electrically and in parallel thermally. The connecting material at the junctions must be a good electrical and thermal conductor.

When a DC voltage is applied to the circuit, heat will be absorbed at one junction and rejected at the other. When the current is reversed, the junctions will also reverse their operation. The absorption and rejection of heat at the junctions is known as the Peltier effect.

In addition to the Peltier effect, heat is conducted from the hot side to the cold side through the semiconductor elements, and heat is also dissipated due to electrical resistance. Losses due to the Thompson effect can be assumed negligible, provided the Seebeck coefficient for each material remains relatively constant in the temperature range of operation for the hot and cold junctions.

The Thompson heating effect is defined as

$$Q_t = t(T_h - T_c)I \quad (3B-46)$$

where Q_t =Thompson heat, W
 t =Thompson coefficient, V/R
 $= d\alpha/dT$, the differential of Seebeck coefficient with respect to temperature
 I =Current, A
 R =Electrical resistance, Ω

and subscripts h and c are the hot and cold junctions, respectively.

The Seebeck effect is the electromotive force (emf) that exists in a circuit of two different materials (p, n, see Fig. 3B-44) when the junctions are maintained at different temperatures:

$$E = (\alpha_p - \alpha_n)(T_h - T_c) \quad (3B-47)$$

where E = emf, V

α = Seebeck coefficient, V/T

T = Temperature, °R

P = Electric power input, W

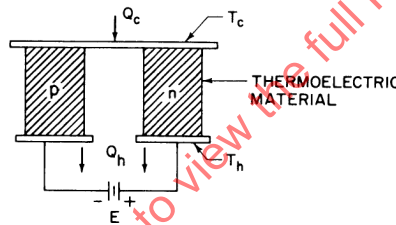


Figure 3B-44 - Basic Thermoelectric Couple or Module

If a DC voltage is applied to the circuit, the following equation defines the net Peltier cooling effect for the steady-state condition of a single module or thermoelectric couple, shown schematically in Fig. 3B-44:

$$Q_c = (\alpha_p - \alpha_n)IT_c - \frac{I^2R}{2} - \frac{K(T_h - T_c)}{3.415} \quad (3B-48)$$

where Q_c = Net cooling at cold junction, W

3.415 = Conversion factor, Btu/hr-W

$K = kA/L$

in which k = Thermal conductivity, Btu/hr-°F-in

A = Area cross section, in.²

L = Length of elements, in.

The net cooling effect equals the Peltier effect at the cold junction minus the losses due to electrical resistance and heat transfer by conduction from the hot to the cold side. From the equation, it can be seen that $(T_h - T_c)$ is a maximum when the net cooling effect approaches zero with the current held constant. If the cooling requirement is held constant and the maximum allowable current is supplied to the system, the required system ΔT can be calculated.

The electric power required to drive the thermoelectric device is made up of two factors: energy to overcome the Joule effect (electrical resistance) and energy to overcome the thermal emf of the circuit. Thus,

$$P = I^2 R + (\alpha_p - \alpha_n)(T_h - T_c)I \quad (3B-49)$$

The coefficient of performance is then defined as the ratio of the net cooling or heating effect to the power input:

$$COP = \frac{Q_c}{P} \quad (3B-50)$$

For any given thermoelectric device and temperature difference, the maximum coefficient of performance can be calculated as follows in terms of temperature and the thermoelectric material constants:

$$(COP)_{max} = \frac{T_c}{T_h - T_c} \frac{\left[1 + \frac{Z(T_h + T_c)}{2}\right]^{0.5} - \frac{T_h}{T_c}}{\left[1 + \frac{Z(T_h + T_c)}{2}\right]^{0.5} + 1} \quad (3B-51)$$

$$\text{where } Z = \frac{\alpha_p - \alpha_n}{RK}$$

The term Z, or figure of merit, under steady-state conditions, is the controlling factor for defining maximum performance of a thermoelectric device. When Z approaches infinity, the performance of the thermoelectric device approaches ideal Carnot efficiency:

$$(COP)_{ideal} = \frac{T_c}{T_h - T_c}$$

For several materials, a family of curves can be constructed for comparison purposes of COP versus temperature difference, with figure of merit as a parameter (see Fig. 3B-45 for example).

5.4 Application

For a successful application of a thermoelectric system to a cooling and heating design, it is necessary to evaluate full power consumption, weight, space requirements, auxiliary systems, reliability, and initial and long term costs. The curves illustrated in Figs. 3B-46 and 3B-47 show one method for evaluating the performance of 100 bismuth-telluride thermocouples, 0.125 in. long and 38.2 mm² cross section. Figs. 3B-46 and 3B-47 are used together to determine cooling capacity.

Fig. 3B-46 shows the absorbed heat when both junctions are at the same temperature. Fig. 3B-47 is a plot of the heat flow by conduction when the junctions are maintained at different temperatures. For example, if the cold junction is absorbing heat at 40°F, the current flow is 40 A and the hot junction is maintained at 100°F, the net cooling effect is 300 W (Fig. 3B-46) less 140 W (Fig. 3B-47) equals 160 W.

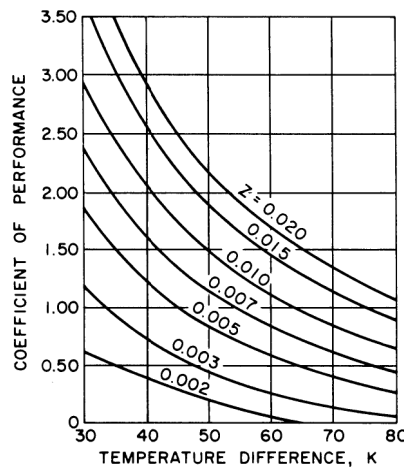


Figure 3B-45 - Optimum COP versus Temperature Difference for Various Figures of Merit. $T_h = 330\text{ K}$

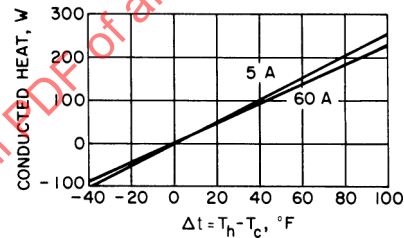
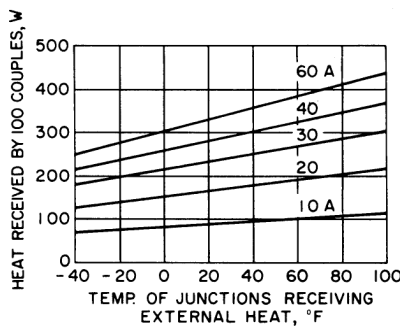


Figure 3B-46 - Cooling Capacity in Watts at $0^\circ\text{F } \Delta t$ (Ref. 22)

Figure 3B-47 - Cooling Capacity in Watts versus Δt Correction; applies to Fig. 3B-46 (Ref. 22)

If more or less cooling is required for this condition, the number of thermocouples can be varied in direct proportion to the net cooling effect desired. After the size and number of thermocouples is established at a critical cooling or heating requirement, additional performance points at other loads and temperatures can be analyzed.

Fig. 3B-48 shows the maximum voltage required for a known current at $\Delta t = 0^\circ\text{F}$, and Fig. 3B-49 shows the emf or opposing voltage that must be overcome and is generated as a result of a temperature difference in the circuit. Therefore, in the first example, where the cold junction is at 40°F and the current is 40 A, Fig. 3B-48 shows a DC voltage of 5.7 V. To this is added 2.5 V (Fig. 3B-49) in order to overcome the opposing voltage due to a temperature difference of 60°F , for a total of 8.2 V.

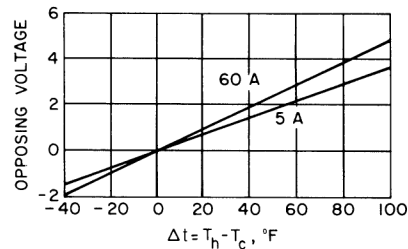
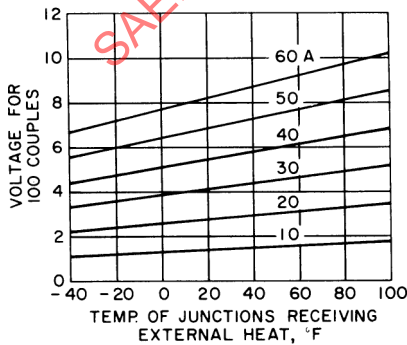


Figure 3B-48 - Voltage Requirements at $0^\circ\text{F } \Delta t$ (Ref. 22)

Figure 3B-49 - Voltage Correction versus Δt ; applies to Fig. 3B-48 (Ref. 22)

When the system goes on heating, a similar approach is used with Figs. 3B-50 and 3B-51. The power consumption is obtained from Figs. 3B-48 and 3B-49, just as in the case for cooling.

The power input will then equal the product of volts times amperes, or

$$P = EI$$

Then it follows that the coefficient of performance can be calculated by definition:

$$\text{COP} = \frac{Q_{\text{cool net}}}{\text{Total power input}} = \frac{Q_c}{P}$$

The COP can be improved by increasing the number of modules or the size of the elements. The preceding method can then be used to evaluate performance at other conditions.

5.4.1 Power Supply

Most available power supplies have 3-phase alternating current and therefore must be rectified to DC for the thermoelectric system. A major portion of the volume and weight of any thermoelectric system is required for the power supply equipment, which must be capable of operation up to maximum current and voltage as demanded by the control system. If the system is to operate for both heating and cooling, a reversing switch is required to reverse the polarity of the couples.

5.4.2 Cascade Systems

If temperature differentials are to be increased, modules can be stacked one upon another and thermally in series. The cold side of one module absorbs heat from the hot side of the next, and so on. Temperature differentials can approach 180°F in this system.

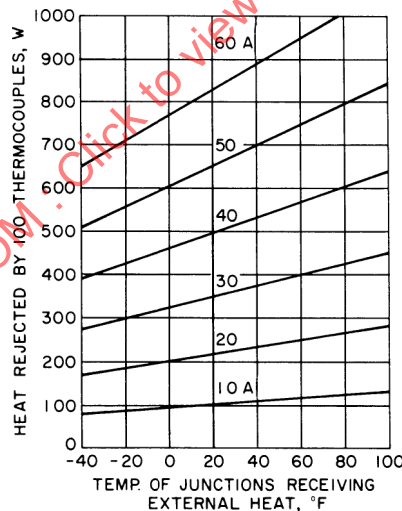


Figure 3B-50 - Heating Capacity in Watts at 0°F Δt (Ref. 22)

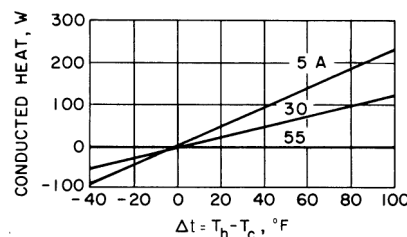


Figure 3B-51 - Heating Capacity versus Δt Correction in Watts; applies to Fig. 3B-50 (Ref. 22)

To provide maximum temperature differentials and to allow for system inefficiencies, each stage from top to bottom should have three to four times as many junctions as the preceding stage. Electrically, the stages are in series, and the junctions should have equal and constant cross-sectional areas.

5.4.3 System Evaluation

When the materials as well as the size of the elements for the modules are known, an estimate can be made of the size of the package. It may be advantageous to use a smaller power supply by making trade-offs such as increasing the number of thermoelements so as to reduce power requirements. Each application will have a unique requirement, depending on space, load, and current available. However, it should be noted that a package could be matched to requirements with controls from 100% cooling to 100% heating.

It is extremely difficult to compare thermoelectric cooling to conventional methods strictly on the basis of COP. The advantages of reliability and ease of control seem to outweigh added initial costs in applications where loads are suitable for thermoelectric cooling or heating. Large capacities are difficult to obtain, owing to the excessively large number of thermoelements and high power consumption at critical points where temperature differences are large. However, special applications are currently in use for electronic cooling and should spread as the state of the art advances.

5.4.4 Auxiliary Systems

For successful operation of a thermoelectric cooling system, the effectiveness of auxiliary systems for transferring heat at both the hot and cold junctions is important. Assume that heat will be absorbed and rejected by using fins to surrounding air (see Fig. 3B-52).

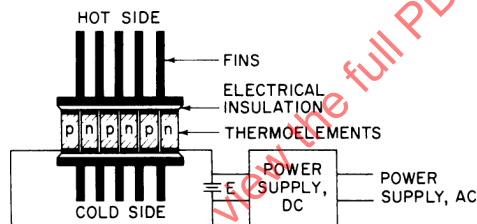


Figure 3B-52 - Thermoelectric System (Ref. 22)

An inspection of Eqs. 3B-48 and 3B-49 indicates that for a given cooling load, it is desirable to reject heat at the lowest possible junction temperature. Similarly, on the cold side, the effectiveness of absorbing heat should be as high as possible in order that the difference between the cold junction temperature and the cooled space temperature is a minimum. The less effective the heat transfer, the greater will be the temperature difference between the junctions. Power requirements will increase, as shown by a reduction in coefficient of performance. Conventional auxiliary systems such as blowers, ram air, or other fluids can effectively improve performance by forced convection at both the hot and cold junctions.

Guidelines to evaluate a thermoelectric cooling cycle are suggested as follows:

1. Determine the cooling and heating requirements and the range of temperatures expected for hot and cold junctions.
2. Determine the space and weight limitations.
3. Determine the methods for heat transfer at the hot and cold junction (free convection, radiation, or mass forced cooling).
4. Determine the size, number and arrangement of thermoelectric couples or modules.
5. Determine the current and voltage requirements.
6. Determine the heat rejection media and auxiliary equipment.

6. REFERENCES

1. J. W. Rizika, "The Thermal Problems of High Speed Flight and the General Electric Aircraft Cooling Program." ASME Paper 56-SA-24.
2. E. J. Gabbay, "Some Aspects of Refrigeration in Supersonic Aircraft," Journal of the Royal Aeronautical Society, Vol. 62, No. 575, November 1958.
3. E. W. Still, "Into Thin Air." A study of aircraft air conditioning systems, Normalair Ltd., Yeovil, England.
4. J. P. Barger, W. M. Rohsenow, and K. M. Treadwell, "A Comparison of Refrigerants When Used in Vapor Compression Cycles over an Extended Temperature Range." ASME Paper 56-SA-6.
5. E. F. Obert, Thermodynamics. The McGraw-Hill Book Co., Inc., 1948.
6. J. L. Mason, W. L. Burriss, and T. J. Connolly, "Vapor Cycle Cooling for Aircraft." WADC Technical Report 53-338.
7. "Preliminary Survey of Possible Cooling Methods for Hypersonic Aircraft." NACA RME57L19.
8. R. H. Zimmerman et al., "Equipment Cooling Systems for Aircraft," Parts 1, 2, and 3. WADC Technical Report 54-359.
9. J. L. Mason et al., "Study of Vapor Cycle Refrigerants for High Performance Aircraft." WADC Technical Report 56-93.
10. J. P. Barger, W. M. Rohsenow, and K. M. Treadwell, "Turboconditioning Systems with Vapor Compression Cycles." ASME Paper 56-SA-7.
11. E. W. Still, "Air Conditioning in Aircraft," Journal of the Royal Aeronautical Society, November 1957.
12. J. E. Coppage et al., "A Study of the Performance of Aircraft Air-Cycle Refrigeration Units with Internally Controlled Turbomachine Components." WADC Technical Report 56-584.
13. E. J. Gabbay, "Open Cycle Refrigeration, The Bootstrap Refrigerator," Aircraft Eng., Vol. XXX, No. 349, March 1958.
14. H. J. Wood, "Air Conditioning of Turbine-Propelled Military Aircraft." SAE Paper, Oct. 3, 1946.
15. J. VanWinkle, "A Survey of Refrigerants for High Temperature Applications." ASME Paper 56-SA-12.
16. L. R. Stevens, Jr., "A Systematic Study of Air Cycles for Aircraft Cooling Applications." ASME Paper 56-SA-11.
17. V. H. Larson, "Equipment Cooling Systems for Aircraft." WADC Technical Report 56-353.
18. "General Requirements for Application of Vapor Cycle Refrigeration Systems for Aircraft." SAE ARP 731.
19. A. F. Ioffe, Semiconductor Thermoelements and Thermoelectric Cooling. London: Infosearch Ltd., 1957.
20. P. Egli, Thermoelectricity. John Wiley & Sons, Inc., 1960.
21. H. G. Goldsmit, Applications of Thermoelectricity. John Wiley & Sons, Inc., 1960.
22. A. B. Newton and K. V. Schmittle, "Thermoelectric Heating and Cooling - Applications to Air Conditioning," National Engineer, Vol. 68, No. 2, February 1964.
23. R. Crump, "Design in Your Thermoelectric Cooling," Product Engineering, Sept. 16, 1963.

SECTION 3C - HEATING SYSTEM DESIGN

1. INTRODUCTION

1.1 Scope

At subsonic airspeeds, heating systems are of major importance, because large capacity heating systems are necessary to make up for heat losses to the cold outside air. With the advent of supersonic speeds for both missiles and aircraft, heating has assumed a minor role, although it is usually required for certain regimes of flight and the rapid warmup of cold-soaked aircraft on the ground.

The advanced performance of modern aircraft requires an increase in the amount of specialized equipment that must be regarded as essential for maintaining performance. Foremost of these specialized functions are air conditioning and pressurization systems. It is important to treat the area of air conditioning (cooling, heating, humidification, dehumidification, ventilation, and pressurization) as a complete entity, and not as separate and uncoordinated design activities, so that satisfactory operation with the simplest and lightest configuration is obtained.

1.2 Common Abbreviations

°F — Degrees Fahrenheit

ft — Feet

Ref. — Reference

2. HEATING METHODS

2.1 Bypass Systems

Heating may be supplied to the occupied areas of an aircraft by bypassing the cooling turbine or the ram air heat exchanger of an air cycle refrigeration system, or both. This method is applicable to both bleed air supply or supply from engine driven compressors. Thus the heat of compression from the pressurization compressor or the main engine compressor is usually adequate for most requirements.

A valve is used occasionally to increase the back pressure on the engine-driven compressor, thus increasing the temperature rise across the compressors. For proper operation, fairly high cabin differential pressures are necessary, and sufficient pressure must be available from the engine driven compressors to ensure an adequate flow to the cabin against the back pressure of the valve.

If additional heating is required beyond what is available from the heat of compression, a supplementary electric or combustion heater can be used as described below.

Circumstances that would preclude this system from being fully effective are operation at low cabin differential pressures and a low compressor output.

2.2 Electric Heaters

Electric heaters normally consist of resistor elements that heat the air passing through the heater. Recently, extended surface (plate fin) heat exchanger elements with applied ceramic-coated electrical conducting material on each side of the elements have been developed. An epoxy-resin insulating film is added for protection, and heating is modulated in finite steps.

Units have been built that withstand surface temperatures of 500°F, but normal operating surface temperatures are in the order of 200-250°F. These units are characterized by their compact, lightweight configuration, and provide an efficient mode of heating aircraft or missiles. (See Ref. 1.)

2.3 Radiant Panels

Cold wall and floor surfaces close to seated passengers can be eliminated by the use of electrically heated radiant panels. Surface temperatures are limited to temperatures slightly higher than the prevailing cabin air, thus walls contribute only a small amount of heat into the cabin. In essence, they operate as a barrier and greatly decrease the heat loss from the cabin.

A typical configuration consists of aluminum honeycomb filler, sandwiched between two aluminum plates, and having aluminum braided resistance wire buried in the honeycomb inside the outer sheet. The wire, similar to that used in domestic electric blankets, is spirally wound on a thread of dielectric material to prevent breakage due to deflection of the panels.

Typical power dissipation values vary from 10 to 400 watts/ft². Resistance temperature sensors are also embedded in the honeycomb for modulated thermal control. These panels permit an installation of little additional weight, since the honeycomb panels are still needed for trimming. (See Ref. 1.)

2.4 Combustion Heaters

Self-contained combustion heaters can be used to provide the required amount of heating, or be used to supplement other forms of heating. Such heaters are comprised of an internal burner operating in a combustion chamber around which the cabin air supply is directed. Provisions are made to prevent the cabin supply air from coming into contact with the air used for combustion and thus becoming contaminated by the products of combustion.

The cabin air passes between the main heater casing and the exterior of the combustion chamber, its temperature being increased by the transfer of heat from the double wall of the combustion chamber. The hot air then passes into the cabin to maintain the required cabin temperature. Precautions must be taken to prevent an uncontrolled flow of fuel in case of fuel line rupture or flame-out of the internal burner.

The combustion air is usually obtained from a forward facing scoop, adequately protected against ice formation. Combustion heaters are large and heavy, thus posing a number of installation problems, not the least of which is the need to ensure that the fire risk is eliminated completely. For ground operation, a combustion air blower is required. (See Ref. 2.)

2.5 Exhaust Heating

Two methods are available for applying exhaust air heating:

1. A muff, or air duct, can be built around the hottest parts of the engine exhaust system, and ram air can be directed through the muff to be heated by the heat transferred from the hot surfaces.
2. A portion of the exhaust gases can be fed to a heat exchanger to heat the ram or recirculated air or both, which can then be directed to areas requiring heating.

The products of combustion must not leak into the muff or through the structure of the heat exchanger and contaminate the air supply. For this reason, and also because of the difficulty in obtaining sufficient air flow and heat for cabin heating, this method lends itself more specifically to de-icing and similar applications.

3. SUMMARY AND RECOMMENDATIONS

The selection and comparison of various heater methods depend almost entirely on the specific application. The simplest and lightest method for heating is obtained by using the heat of compression from the engine-driven pressurization compressor or the main engine bleed. The bleed heating method has been used primarily for military applications because of possible contamination of the bleed air. Commercial jet aircraft can use engine-bleed air for heating, with considerable savings in weight and complication because the design of oil systems and seals in jet engines takes into consideration the importance of clean engine-bleed air.

For aircraft equipped with pressurization compressors, discharge air is readily available for heating. Supplementary heat is then supplied by a lightweight electric duct heater, which is sized to provide sufficient heating for rapid warmup of a cold-soaked aircraft on the ground.